HZB Helmholtz Zentrum Berlin

NINTH JOINT BER II AND BESSY II USER MEETING

Dec. 13-15, 2017

- Synchrotron Instrumentation Day
- Young Scientists Sessions
- Science Day
- Vendor Exhibition
- Poster Session
- Neutron Instrumentation Day

Keynote Lecture:
Roel van de Krol (HZB)

Public Lecture:
George Malliaras (University of Cambridge)

Invited Talks:
Anna Palau *(ICMAB-CSIC)*
Niels Bech Christensen *(DTU)*
Peter Strasser *(TU Berlin)*
Christian Papp *(Uni Erlangen-Nürnberg)*
Denis Vyalikh *(CSIC-UPV/EHU)*
Benjamin Palmer *(Weizmann Institute of Science)*
Quentin Berrod *(CEA)*
Yves Muller *(Uni Erlangen-Nürnberg)*
Justin Wells *(Norwegian University of Science and Technology)*
Stephan Hofmann *(University of Cambridge)*

Satellite Workshop:
Diffraction Data Processing using DIALS - a practical workshop. The workshop will take place on Friday, December 15th at the Wilhelm-Conrad-Röntgen-Campus in Adlershof.

Wilhelm-Conrad-Röntgen Campus (Berlin-Adlershof), WISTA and Lise-Meitner-Campus (Berlin-Wannsee)

http://hz-b.de/um2017

Helmholtz-Zentrum Berlin

für Materialien und Energie GmbH

Wilhelm-Conrad-Röntgen-Campus:

BESSY II

Albert-Einstein-Str. 15
12489 Berlin
tel +49 (0)30 8062-14666/12931
fax +49 (0)30 8062-14746
photons@helmholtz-berlin.de

Lise-Meitner-Campus:

BER II

Hahn-Meitner-Platz 1
14109 Berlin
tel +49 (0)30 8062-42304
fax +49 (0)30 8062-42523
neutrons@helmholtz-berlin.de

http://www.helmholtz-berlin.de

Dear friends and users,

Welcome to the 9th Joint BER II and BESSY II User Meeting of HZB, which brings together users from the neutron and synchrotron sources at our sites in Berlin Wannsee and Adlershof.

In 2017 the synchrotron source BESSY II extended its portfolio of state-of-the-art beamlines and enhanced its performance in both user service as well as novel and established infrastructures.

Tailored filling pattern of the storage ring and specific bunch characteristics were further developed and implemented - motivated by user needs. The successful operation of the few bunch mode on the Sundays of the single bunch weeks, offering an increased repetition rate from 1.25 MHz to 5MHz, was enthusiastically welcomed by our users. To increase the flexibility of our storage ring even beyond the current status, a "twin orbit operation" with two independent filling patterns stored simultaneously on two independent orbits will be tested in a dedicated user week early next year. Both developments are accompanying important innovations on our way to BESSY VSR.

In September the first soft X-rays from the new undulator UE48 were successfully guided to the CAT and SISSY experiments in the EMIL@BESSY II laboratory. The parameters important for later experimental operation, such as beam diameter (108 x 56 μm^2), photon flux (approx. 1012 s^{-1}) and resolution (50 meV at 400 eV), meet all expectations and calculated values. The installation of the tender X-ray undulator CPMU17, however, experienced some delay and is expected to be carried out during the up-coming shutdown in summer 2018.

The X-ray microscope TXM is back in full user operation offering significantly better quality images compared to the former X-ray microscopy station. It is located at the new TXM beamline on the common insertion device U41 shared with the combined RIXS and XPS station PEAXIS. PEAXIS is currently in friendly user operation and will be available to all users from the next semester onwards.

Several other projects like ENERGIZE, a beamline dedicated to research on hybrid materials and energy efficient technologies, as well as METRIXS, a high-resolution state-of-the-art spectrometer for resonant inelastic X-ray scattering, have started this year.

In May 2017 CALIPSOplus, an integrated activity for advanced communities within Horizon2020 had its kick-off meeting. The aim of CALIPSOplus is to lower barriers to entry to world-class accelerator-based light sources in Europe and the Middle East, and to promote and support international exchange and transnational access with an emphasis on European integration. In this scope HZB manages the work package "Dissemination and Training" and is involved in the research project MOONPICS (Metrology On One Nanometre Precise Optics).

HZB has established a comprehensive quality management system for its User Service at BESSY II, to further improve user support and to optimize the full process chain of user beamtime projects. In an extensive audit process, TÜV Süd put this system through intensive

testing and, on 21st of November 2017, awarded the ISO 9001:2015 certificate. BESSY II is thus the first European synchrotron radiation source to have its user service approved under these strict quality criteria.

At BER II ten internationally competitive instruments at highest possible standards are operated for users until end of 2019, amongst them, the HFM/EXED instrument, which enables experiments in the strongest continuous magnetic field for neutron scattering worldwide. The upgraded time-of-flight spectrometer NEAT entered into regular user operation in 2017. Some instruments were transferred to other reactors, like for example the reflectometer BioRef. It will be set up again at the OPAL neutron source, which is part of the Australian Nuclear Science and Technology Organisation (ANSTO) in Sydney. It is expected to be available to the international scientific community in 2018 under the name "Spatz".

Complementing the large scale facilities, HZB provides state-of-the-art laboratories as well as unique equipment (CoreLabs) for the scientific community by offering services and infrastructure to external academic and industrial users. Besides EMIL@BESSY II this new multi-user platform hosts the X-ray CoreLab providing a variety of diffraction methods focusing on in-situ studies of phase transitions and texture analysis. The microscopy CoreLab (participating in the ZEISS labs@location program with the most modern ZEISS electron microscopes available), HySPRINT (for Hybrid Silicon Perovskite Research), the Competence Centre Thin-Film and Nanotechnology for Photovoltaics Berlin PVcomB, and the CoreLab Quantum Materials (accommodating instruments and methods for the synthesis and the investigation of new materials) round off the suite of infrastructures.

This year's Joint User Meeting is highlighted by the public lecture by George Malliaras from the University of Cambridge, UK, with the title "Interfacing the brain using organic electronics" and the Innovation Award and the Ernst-Eckhard-Koch Prize bestowed by the "Freundeskreis Helmholtz-Zentrum Berlin e.V.". The Science Day on Thursday concludes with a poster session accompanied by the traditional "Berliner Buffet", kindly sponsored by the companies represented in the industrial exhibition. The Synchrotron Day and the Neutron Day each have a special highlight with a young scientists session. A satellite workshop "Diffraction Data Processing using DIALS" completes the meeting.

We look forward to inspiring and fruitful discussions during the User Meeting and to exciting new experiments and collaborations beyond it. Thank you all for joining us and enjoy the meeting.

Sincerely,

Prof. Dr. Bernd Rech
Acting Scientific Director

Contents

Wednesday, December 13th, 2017:
Young Scientists and Synchrotron Day

Wilhelm-Conrad-Roentgen Campus
Albert-Einstein-Str. 15
Rudower Chaussee 17
12489 Berlin

13:30 – 18:00	**Registration and Vendor Exhibition**	WISTA Centre
14:00 – 15:50	**Synchrotron Session** *(Chair: Christian Jung)*	Bunsen Auditorium
14:00	*Bernd Rech (HZB)* **Welcome**	
14:10	*Andreas Jankowiak (HZB)* **Accelerator operation and projects @ HZB**	
14:30	*Alexander Föhlisch (HZB)* **BESSY II: Photon science**	
14:50	*Paul Goslawski (HZB)* **BESSY II: few bunch mode, island buckets and twin orbit test week**	
15:10	*Ieva Bidermane (HZB)* **Electron-electron coincidence station at BESSY II**	
15:30	*Gerd Schneider (HZB)* **Developments in X-ray microscopy**	
15:50 – 16:05	**General Discussion**	Bunsen Auditorium
16:05 – 16:30	**Coffee Break**	WISTA Centre
16:30 – 17:45	**Young Scientists Session** *(Chair: Carolin Schmitz-Antoniak)*	Bunsen Auditorium
16:30	*Kateryna Medjanik (Johannes Gutenberg Universität Mainz)* **New way of performing ARPES by time-of-flight momentum microscopy**	
16:45	*Rebecka Lindblad (Lund University)* **X-ray absorption and XMCD of cationic molecules studied in gas-phase**	
17:00	*Tobias Bock (Max Delbrück)* **Crystal structures and beyond – the alternative myxobacterial isovaleryl CoA biosynthesis and its regulation**	
17:15	*Miriam Weller (Johann Wolfgang Goethe-Universität Frankfurt am Main)* **Imaging the temporal evolution of molecular orbitals during ultrafast dissociation**	
17:30	*Soohyung Park (Humbold Universität Berlin)* **Direct determination of monolayer MoS_2 and WSe_2 exciton binding energies on insulating and metallic substrates**	
18:00-20:00	**Traditional curried sausage with “Schrippen” and beer**	Bunsen Auditorium

Thursday, December 14th, 2017:
Science Day

Wilhelm-Conrad-Roentgen Campus
Albert-Einstein-Str. 15
Rudower Chaussee 17
12489 Berlin

9:00 – 16:00	**Vendor Exhibition**	WISTA Centre
8:30 – 17:00	**Registration and Poster Set-up**	WISTA Centre BESSY II
9:30 – 9:40	**Opening** *Bernd Rech (HZB)*	Bunsen Auditorium
9:40 – 10:10	**Keynote Lecture** *(Chair: Christian Papp)* *Roel van de Krol (HZB)* **New infrastructures at HZB for energy materials research**	
10:10 – 10:40	**Coffee Break and Vendor Exhibition**	WISTA Centre
10:40 – 12:20	**Oral Presentations I** *(Chair: Catherine Dubourdieu)*	Bunsen Auditorium
10:40	*Anna Palau (ICMAB-CSIC)* **Encoding magnetic states in monopole-like configurations using superconducting dots**	
11:00	*Niels Bech Christensen (DTU)* **Magnetic phase diagram of strongly magnetoelectric $LiCoPO_4$**	
11:20	*Peter Strasser (TU Berlin)* **In situ electrocatalysis – watching the dark side of solar fuels at work**	
11:40	*Christian Papp (Universität Erlangen-Nürnberg)* **Liquid organic hydrogen carriers (LOHCs) - Towards a hydrogen-free hydrogen economy**	
12:00	*Denis Vyalikh (CSIC-UPV/EHU)* **Exotic magnetism and electron-correlation phenomena in rare-earth based antiferromagnets**	
12:20 – 13:30	**Lunch Break**	(Canteens on site)
13:30 – 15:10	**Oral Presentations II** *(Chair: Svante Svensson)*	Bunsen Auditorium
13:30	*Benjamin Palmer (Weizmann Institute of Science)* **Crystal-eyes: biogenic crystals used for vision**	
13:50	*Quentin Berrod (CEA)* **Transport properties of ionic liquids under 1D nanometric confinement**	
14:10	*Yves Muller (Uni Erlangen-Nürnberg)* **Insight into herpesvirus replication from structural studies at the HZB-MX beamlines**	

14:30	*Justin Wells (Norwegian University of Science and Technology)* **In situ patterning of ultrasharp dopant profiles in silicon**	
14:50	*Stephan Hofmann (University of Cambridge)* **Integrated crystal growth of advanced nanomaterials: from model systems to integrated manufacturing**	
15:10 – 15:40	**Coffee Break and Vendor Exhibition**	WISTA Centre
15:40 – 15:50	*Christian Papp (Universität Erlangen-Nürnberg)* **Report from the user committee**	Bunsen Auditorium
15:50 – 17:00	**Bestowal of Prizes: Friends of Helmholtz-Zentrum Berlin e.V.** *(Chair: Mathias Richter)*	Bunsen Auditorium
17:00 – 18:00	**Public Lecture** *(Chair: Emil List-Kratochvil)* *George Malliaras (University of Camebridge)* **Interfacing with the brain using organic electronics**	Bunsen Auditorium
18:00 – 20:00	**Poster Session**	(BESSY II Experimental Hall)
20:00	**Berliner Buffet and Poster Prize** (sponsored by the companies participating in the vendor exhibition)	(BESSY II Foyer)

Friday, December 15th, 2017:
Young Scientists and Neutron Day

Lise-Meitner Campus
Hahn-Meitner-Platz 1
14109 Berlin

8:30 - 9:00	**Registration**	(LMC-Foyer)
9:00 – 9:50	**Neutron Session** *(Chair: Klaus Habicht)*	(Lecture Hall)
9:00	*Bernd Rech (HZB)* **Opening**	
9:10	*Siqin Meng (CIAE/HZB Guest)* **MultiFLEXX: the multi-energy array analyzer at FLEXX**	
9:30	*Eneli Härk (HZB)* **Chasing electrons with neutrons – Investigation of the microstructure of RP-20 carbon electrode**	
9:50	*Michael Tovar (HZB)* **Experimental opportunities of the X-ray CoreLab: Crystal structure, stress, texture**	
10:10	*Markus Wollgarten (HZB)* **The CoreLab correlative spectroscopy and microscopy at HZB at a glance**	
10:30 – 11:00	**Coffee Break**	(Café Jahn)
11:00 – 12:30	**Young Scientist Session** *(Chair: Susan Schorr)*	(Lecture Hall)
11:00	*Miriam Steinhauer (DLR)* **In situ investigations of the solid electrolyte interphase's long-term growth on amorphous graphite during prolonged cycling**	
11:15	*Leonie Heinze (TU Braunschweig)* **Magnetism of atacamite, $Cu_2Cl(OH)_3$**	
11:30	*Pavlo Portnichenko (TU Dresden)* **Magnetic-field dependence of the ferromagnetic excitation in the heavy-fermion metal CeB_6**	
11:45	*Rasmus Palm (University of Tartu)* **Small angle neutron scattering for determination of porous structure of molybdenum carbide-derived carbons**	
12:00	*Anton Werwein (Universität Leipzig)* **Zintl phase hydrides $LaGaD_x$, $TmGaD_x$ and $NdSiD_x$**	
12:15	*Jooseop Lee (Cornell University)* **Study on high magnetic field phase of UPt_2Si_2**	
12:30 – 14:00	**Poster Session and Lunch**	(Café Jahn)

Abstracts of the Young Scientists Session - Synchrotron Day

Wednesday, 13th of December

K. Medjanik 13.12.17, 16:30

New way of performing ARPES by time-of-flight momentum microscopy

K. Medjanik[1]

1 Institut für Physik, Johannes Gutenberg-Universität, Germany

The electronic structure of solids is a key element in materials research and design. The most common types of angular-resolved photoemission (ARPES) instruments, which allow to perform such investigations are dispersive electron energy analyzers. Newly discovered materials very often demand high momentum- and energy resolution, along with fast and efficient measurements, including the spin degree of freedom. As the performance of conventional analyzers has reached principal limits, alternative methods are needed, which can further improve the detection efficiency.
In this contribution I will present a new way of performing ARPES employing time-of-flight k-space microscopy in three different timing regimes of BESSY II: single-bunch, 8-bunch and hybrid/multi-bunch modes. The presentation will be focused on the performance of the k-microscope in the VUV regime at beamline U-125 (RGBL and 10m NIM).
The electronic surface states on Mo(110) [1] and W(110) [2] have been studied in single-bunch mode. The k-microscope yields a simultaneous acquisition of the E-vs-$\boldsymbol{k}$ spectral function in the full surface Brillouin zone and several eV energy interval. We find bands with linear dispersion along $\overline{H}-\overline{\Gamma}-\overline{H}$ that exhibit the spin texture of a Dirac state. For graphene on Ir(111) [3] we find an unprecedented wealth of information, exploiting the enhanced acquisition speed of the newly-established 8-bunch mode. Finally, first data have been obtained in multi-bunch mode selecting the camshaft pulse via an electronic chopper.

References:
[1] Ultramicroscopy 159, 453 (2015).
[2] Nat. Materials 16, 615 (2017).
[3] Appl. Phys. Lett. 108, 261602 (2016).

R. Lindblad 13.12.17, 16:45

X-ray absorption and XMCD of cationic molecules studied in gas-phase

R. Lindblad[1,2], V. Zamudio-Bayer[2,3], C. Bülow[2], M. Timm[2,3], B. von Issendorf[3], T. Lau[2]

1 Department of Physics, Lund University, Sweden
2 Institut für Methoden und Instrumentierung der Forschung mit Synchrotronstrahlung, Helmholtz-Zentrum Berlin, Deutschland
3 Physikalisches Institut, Universität Freiburg, Deutschland

An ion trap coupled to a soft x-ray beamline enables spectroscopic studies of mass-selected charged molecules and clusters in gas-phase. In the present work we have studied the molecular cations FeO_{1-4}^+ at the NanoClusterTrap end-station at BESSY II [1,2]. The molecular cations are produced in a magnetron sputter source, mass-selected in a quadrupole mass filter and stored in a linear ion trap directed along the x-ray beam. X-ray absorption in ion yield has been used to study the electronic structure near the oxygen K-edge and the iron $L_{2,3}$-edges for each molecule separately. In addition the magnetic properties has been followed via x-ray magnetic circular dichroism (XMCD) at the iron $L_{2,3}$-edges.

Based on the experimental results we propose geometrical structures of the iron oxide cations and we discuss the formal oxidation states that can be associated with each molecular cation. This information is valuable for understanding chemical reactions related to oxygen transport in biological systems as well as reactions between iron and ozone in the atmosphere.

References:
[1] J. Phys. B: At. Mol. Opt. Phys. 42, 154029 (2009)
[2] Phys. Rev. B 90, 184420 (2014)

T. Bock 13.12.17, 17:00

Crystal structures and beyond – the alternative myxobacterial isovaleryl CoA biosynthesis and its regulation

T. Bock[1,2], J. Kasten[1], J. Reichelt[1], C. Volz[3], V. Hering[1], A. Scrima[1], E. Luxenburger[3], J. Hoffmann[3], V. Schütza[4], C. Feiler[5], R. Müller[3], W. Blankenfeldt[1]

1 Structure and Function of Proteins, Helmholtz Centre for Infection Research, Germany
2 Structure and Membrane Interaction of G-Proteins, Max-Delbrueck-Center for Molecular Medicine, Germany
3 Microbial Natural Products, Helmholtz Institute for Pharmaceutical Research Saarland, Germany
4 Institute of Reconstructive Neurobiology, University Hospital Bonn, Germany
5 Macromolecular Crystallography, Helmholtz-Zentrum Berlin, Germany

Isovaleryl coenzyme A (IV-CoA) is a crucial building block for iso fatty acids and lipids that are essential during development in myxobacteria [1]. In general, IV-CoA is produced according to textbook biochemistry by the branched chain α-keto acid dehydrogenase complex (Bkd) during leucine degradation. In addition, a second, *de novo* and acetyl-coenzyme-A-utilizing route that is activated under leucine-limiting conditions has been discovered and partially characterized in the past. This pathway, assigned as alternative isovaleryl coenzyme A biosynthesis (AIB), includes four chemical steps catalyzed by five different proteins and is of particular interest, since AIB has been proposed to be useful for the renewable and green generation of isobutene, a precursor applied in the production of fuel additives and chemicals [2]. The entire pathway including the 3-hydroxy-3-methylglutaryl coenzyme A synthase MvaS [3], the 3-hydroxy-3-methylglutaryl dehydratase LiuC [4], the decarboxylase AibA/AibB [5] and the reductase AibC [6] could be characterized on the structural level. Additional complexes with coenzyme A derivatives led to the identification of important residues involved in substrate binding and catalysis and enabled the formulation of reaction mechanisms of almost all enzymes involved in AIB.
In addition to enzymes responsible for *de novo* IV-CoA production, the AIB regulatory system comprising the TetR-like transcriptional regulator AibR and IV-CoA could be characterized in atomic detail, which not only unveiled the mode of transcriptional regulation *in vitro*, but also allowed the identification of a potential additional player in AIB [7].

References:
[1] J. Bacteriol 188, 6524 (2006)
[2] Angew. Chem. Int. Ed 52, 1304 (2013)
[3] ChemBioChem 17, 1257 (2016)
[4] ChemBioChem 17, 1658 (2016)
[5] Angew. Chem. Int. Ed 56, 9986 (2017)
[6] Acta Crystallographica F72, 652 (2016)
[7] Nucleic Acid Research 45, 2166 (2017)

M. Weller 13.12.17, 17:15

Imaging the Temporal Evolution of Molecular Orbitals during Ultrafast Dissociation

M. Weller[1], H. Sann[1], T. Havermeier[1], C. Müller[1], H.-K. Kim[1], F. Trinter[1], M. Waitz[1], J. Voigtsberger[1], F. Sturm[1], T. Bauer[1], R. Wallauer[2], D. Schneider[1], C. Goihl[1], J. Tross[1], K. Cole[1], J. Wu[1], M.S. Schöffler[1], H. Schmidt-Böcking[1], T. Jahnke[1], M. Simon[3], R. Dörner[1]

1 Institut für Kernphysik, Universität Frankfurt, Germany
2 Fachbereich Physik, Philipps-Universität Marburg, Germany
3 Sorbonne Universités, UPMC Université Paris, France

We investigate the breaking of chemical bonds and thus the transition of a molecular orbital to an atomic orbital. To realize this, we coincidently measure the fragment momenta of the molecular decay of HCl through Ultrafast Dissociation with a COLTRIMS system.
Ultrafast Dissociation proceeds as follows: Using narrow-bandwidth synchrotron radiation, an inner shell electron is resonantly excited to an antibonding molecular $6\sigma^*$-orbital in the pump step. The molecule now rapidly dissociates in the timescale of a few femtoseconds along the steeply repulsive potential energy surface. Competing with the molecular dissociation, Auger decay takes place. The Auger electron can be emitted either within the molecular Franck-Condon region, during bond breakage or when the molecule is already fragmented into two atoms. The Auger decay can thereby be used as a probe of the state of the decaying system. By coincidently measuring the ionic fragment and the emitted electron, we gain information about internuclear distance and hence the timespan from excitation to the point when each decay took place. The internuclear distance is encoded in the kinetic energy of the fragments as well as in the energy of the emitted Auger electron. For different time steps we can now investigate the Auger electron angular distribution in the molecular frame. These distributions are a fingerprint of the systems orbital structure.
In reality, the situation is considerably more complicated because many initial and final states are involved. In the analysis, these states as well as the two possible fragment channels could be separated by restricting to the channels of interest via coincident energy maps.
Finally, we can image the transition of the molecular σ-type orbital via bond breakage to the atomic p-orbital mapped in the Auger electron emission pattern.

Reference:
[1] Phys. Rev. Lett 117, 243002 (2016)

S. Park 13.12.17, 17:30

Deciphering magnetic properties of bacteria produced nanoparticles by PEEM

S. Park,[1,2] N. Mutz,[3] T. Schultz,[1] S. Blumstengel,[3] A. Han,[4,5] A. Aljarb,[4,5] L.-J. Li,[4,5] E. J. W. List-Kratochvil,[3] P. Amsalem,[1] N. Koch,[1,2]

1. Institut für Physik & IRIS Adlershof, Humboldt-Universität zu Berlin, Germany
2. Bereich Solarenergieforschung, Helmholtz-Zentrum Berlin, Germany
3. Institut für Physik, Institut für Chemie & IRIS Adlershof, Humboldt-Universität zu Berlin, Germany
4. Academia Sinica, Research Center for Applied Sciences, Taiwan
5. Physical Sciences and Engineering, King Abdullah University of Science and Technology, Saudi Arabia

Two-dimensional transition-metal dichalcogenides (2D TMDCs) are attractive candidates for next-generation optoelectronic devices due to their unique electronic and optical properties that originate from their low dimensionality and high-symmetry structure [1,2]. To employ 2D TMDCs in optoelectronic devices, understanding the fundamental physical properties is necessary. In this regard, one key parameter is the exciton binding energy [3]. It is the energy difference between the lowest-energy optical absorption and the charge transport energy gap. In this talk, we will present an experimental study combining angle-resolved direct and inverse photoelectron spectroscopy in order to measure the transport band gap, and reflectance measurements for a determination of the optical gap. In this manner we are able to determine the exciton binding energy for two common 2D TMDCs, MoS_2 and WSe_2, on two fundamentally different substrates consisting of an insulator and a metal. In addition, we will show that the dielectric environment of 2D TMDCs strongly impacts the transport gap while the energy necessary to form a bound electron-hole pair (exciton) is barely affected, indicating large exciton binding energy change. Therefore, a proper dielectric surrounding design for such 2D semiconductors can be used to optimize the optoelectronic properties of future device.

References:
[1] Nat. Nanotechnol. 7, 699 (2012)
[2] Nat. Chem. 5, 263 (2013)
[3] Quantum Theory of the Optical and Electronic Properties of Semiconductors, 5th ed. (Singapore, 2009)

Abstracts of the Keynote and Public Lecture - Science Day

Thursday, 14th of December

R. van de Krol 14.12.17, 9:40

New Infrastructures at HZB for Energy Materials Research

R. van de Krol[1]

1 Institut Solare Brennstoffe, Helmholtz-Zentrum Berlin, Germany

An important part of the research activities at HZB is the development of new materials for energy conversion and storage applications. Specific areas of interest are photovoltaic solar cells, the storage of solar energy in chemical fuels, electrochemical storage of electricity, and thermoelectrics. To complement its strong expertise on the analysis of materials properties, HZB is in the process of building up the Helmholtz Energy Materials Foundry, a new distributed infrastructure that aims to strengthen its materials synthesis capabilities. In this presentation I will give an overview of the planned investments, all of which will also be accessible to national and international users from both industry and academia.

Interfacing with the Brain Using Organic Electronics

G. Malliaras[1]

1 Department of Engineering, University of Cambridge, UK

One of the most important scientific and technological frontiers of our time lies in the interface between electronics and the human brain. Interfacing the most advanced human engineering endeavor with nature's most refined creation promises to help elucidate aspects of the brain's working mechanism and deliver new tools for diagnosis and treatment of a host of pathologies including epilepsy and Parkinson's disease. Current solutions, however, are limited by the materials that are brought in contact with the tissue and transduce signals across the biotic/abiotic interface. Recent advances in organic electronics have made available materials with a unique combination of attractive properties, including mechanical flexibility, mixed ionic/electronic conduction, enhanced biocompatibility, and capability for drug delivery [1]. I will present examples of novel devices for recording and stimulation of brain activity that go beyond the current state-of-the-art in terms of performance, compatibility with the brain, and form factor. I will show that organic electronic materials offer tremendous opportunities to design devices that improve our understanding of brain physiology and pathology, and can be used to deliver new therapies. I will finish the talk with a discussion of the fundamental materials work that needs to be done to move the field forward, highlighting work that could be done at BER II and BESSY II.

References:
[1] Nature 540, 379 (2016)

Abstracts of the Oral Presentations - Science Day

Thursday, 14th of December

A. Palau 14.12.17, 10:40

Encoding Magnetic States in Monopole-Like Configurations Using Superconducting Dots

A. Palau[1], S. Valencia[2], F. Kronast[2], M. Cialone[2], A. Arora[2], N. Del-Valle[3], C. Navau[3], A. Sanchez[3], D.A. Tennant[4], X. Obradors[1], T. Puig[1]

1 Institut de Ciència de Materials de Barcelona ICMAB-CSIC, Spain
2 Abteilung Materialien für grüne Spintronik, Helmholtz-Zentrum Berlin, Germany
3 Grup d'Electromagnetisme, Departament de Fisica, UAB, Spain
4 Neutron Sciences Directorate, Oak Ridge National Laboratory, USA

The capability to prepare and manipulate non-uniform spin configurations at the nano- and micro-scale, in the form of magnetic domain walls, vortices, monopoles, or skyrmions, represent nowadays a hot topic in physics and material science. Geometrical frustration has been the main strategy to generate nontrivial, monopolar-like defects and other exotic states in magnetic materials such as spin ice systems or magnetic nanowires. However, these strategies often involve complex procedures and are sometimes restricted to confined regions of the phase diagram. It is thus essential to explore new approaches which incorporate versatility and freedom in encoding stable modifiable nanometric magnetic structures.
In this work we introduce a completely new and flexible approach, based on the use of an artificial hybrid material, to encode a large manifold of non-trivial magnetic states in ferromagnetic thin films. Multifunctional hybrid materials have been widely explored as an efficient route to design materials, displaying unprecedented combination of desirable physical properties. Here we use the hybrid approach, combining high temperature $YBa_2Cu_3O_{7-\delta}$ superconducting dots (patterned with different shapes) with a continuous thin ferromagnetic Permalloy (Py) layer, in a hitherto unexplored way to design and generate multiple exotic magnetic states on demand. Robust, stable, and easily controllable non-trivial spin structures, including 2D monopole-like fields, are encoded, modified and annihilated in the Py film by defining a variety of magnetic states in superconducting dots.

References:
[1] Advanced Science 3, 1600207 (2016).

N.B. Christensen 14.12.17, 11:00

Magnetic phase diagram of strongly magnetoelectric $LiCoPO_4$

E. Fogh[1], R. Toft-Petersen[1], E. Ressouche[2], C. Niedermayer[3], S.L. Holm[3,4], M. Bartkowiak[5], O. Prokhnenko[5], S. Sloth[1], F.W. Isaksen[1], D. Vaknin[6], N.B. Christensen[1]

1 Department of Physics, Technical University of Denmark, Denmark
2 INAC-SPSMS, CEA & Université Grenoble Alpes, France
3 Laboratory for Neutron Scattering and Imaging, Paul Scherrer Institute, Switzerland
4 Nano-Science Center, Niels Bohr Institute, University of Copenhagen, Denmark
5 Abteilung Hochfeldmagnet, Helmholtz-Zentrum Berlin, Germany
6 Ames Laboratory and Department of Physics and Astronomy, Iowa State University, USA

Magnetoelectricity is the ability of certain magnetically ordered materials to respond to an externally applied magnetic field by developing an electrical polarization, and to respond to an applied electric field by changing magnetization (See e.g. Refs. [1, 2]). To linear order, these effects are described by a magnetoelectric tensor α defined by the twin equations $\boldsymbol{P}_k = \alpha_{ki} H_i$, and $\mu_0 \boldsymbol{M}_k = \alpha_{ik} \boldsymbol{E}_i$. Because it is the symmetry of the magnetic order that governs the allowed components of the tensor α neutron diffraction studies at high fields are essential to understand the interrelationship between charge and magnetic degrees of freedom.

In this talk, I will present the results of our neutron diffraction studies of the magnetic order and phase diagram of $LiCoPO_4$ [3], which displays one of the largest symmetry-allowed components (α_{xy}) of the tensor α among transition metal compounds [2]. We combined diffraction results obtained at ILL, Grenoble for fields up to $\mu_0 H$ =12T, with data taken at the truly unique-in-the-world high magnetic field facility at BER-II (HZB) [4, 5]. The latter data allowed us to reach much higher fields, $\mu_0 H_{max}$ =25.9T, whereby the magnetic phase diagram of $LiCoPO_4$ could be completed, and the observed magnetoelectric effect [6] correlated with the magnetic structures deduced from the neutron diffraction data.

References:
[1] Nature 442, 759 (2006).
[2] Introduction to complex mediums for optics and electromagnetics, SPIE Publications (2003).
[3] Phys. Rev. B 94, 104420 (2017).
[4] Rev. Sci. Instrum. 86, 033102 (2015).
[5] IEEE Trans. Appl. Superconduc. 26, 4301606 (2016).
[6] Low Temperature Physics 42, 280 (2016).

In situ electrocatalysis – watching the dark side of solar fuels at work

P. Strasser[1]

1 Department of Chemistry, Chemical Engineering Division, Technical University Berlin, Germany

Electrocatalysis plays a prominent role in the science of chemical storage and conversion of electricity in electrolyzers, photoelectrochemical cells, or fuel cells. There, storage and conversion is put into effect via molecular bond making and breaking, catalyzed at electrified interfaces of an ion conductor and an electrocatalyst material. For these reactions to occur with the smallest possible energy losses and the utmost atom efficiency, nanostructured multi-component electrode materials have proven indispensable, because they offer substantial advantages in atomic dispersion, often resulting in energy efficiency and performance benefits. Deeper insight into the chemical state of working electrocatalysts requires in-situ analytical techniques.

In this talk, I will share a few recent examples where *in situ* analytical techniques have advanced our understanding of structure-activity relationships of electrocatalysts and electrocatalytic reactions.

C. Papp 14.12.17, 11:40

Liquid Organic Hydrogen Carriers (LOHCs) - Towards a Hydrogen-free Hydrogen Economy

C. Papp[1], H.-P. Steinrück[1], J. Libuda[1], P. Wasserscheid[2]

1 Lehrstuhl für Physikalische Chemie, Friedrich-Alexander-Universität Erlangen-Nürnberg, Germany
2 Lehrstuhl für Chemische Reaktionstechnik, Friedrich-Alexander-Universität Erlangen-Nürnberg, Germany

The need to drastically reduce CO_2 emissions will lead to the transformation of our current, carbon-based energy system to a more sustainable, renewable-based one. In this process, hydrogen will gain increasing importance as secondary energy vector. Energy storage requirements on the TWh scale (to bridge extended times of low wind and sun harvest) and global logistics of renewable energy equivalents will create additional driving forces toward a future hydrogen economy. However, the nature of hydrogen requires dedicated infrastructures, and this has prevented so far the introduction of elemental hydrogen into the energy sector to a large extent.
Recent scientific and technological progress in handling hydrogen in chemically bound form as liquid organic hydrogen carrier (LOHC) supports the vision that a future hydrogen economy may work without handling large amounts of elemental hydrogen. LOHC systems are composed of pairs of hydrogen-lean and hydrogen-rich organic compounds that store hydrogen by repeated catalytic hydrogenation and dehydrogenation cycles.
This talk highlights the current state-of-the-art in hydrogen storage using LOHC systems. It introduces fundamental aspects of a future hydrogen economy and discusses some interesting new directions in the catalysis of LOHCs.

References:
[1] Chem. Rec. 14, 879 (2014).
[2] Acc. Chem. Res. 50, 74 (2017).
[3] ChemSusChem 6, 974 (2013).

D. Vyalikh 14.12.17, 12:00

Exotic magnetism and electron-correlation phenomena in rare-earth based antiferromagnets

D. Vyalikh[1,2]

1 Departamento de Fisica de Materiales and CFM-MPC UPV/EHU, Donostia International Physics Center (DIPC), Spain
2 IKERBASQUE, Basque Foundation for Science, Spain

For a long time, rare-earth (RE) intermetallic materials have attracted considerable interest because of their exotic properties at low temperatures, which include complex magnetic phases, valence fluctuations, heavy-fermion states, Kondo behavior and many others. It is widely believed that all of these properties stem from the delicate interplay between almost localized 4*f* electrons and itinerant valence band states.

Our experiments aim to disclose details of this interaction, and reveal the fine electronic structure of such materials near the Fermi level. To this end, we apply Angle-Resolved Photoemission Spectroscopy (ARPES) technique, which in spite of its surface sensitivity when working in UV mode, indeed, allows to gain deep insight not only into surface electron structure, but to probe the bulk derived states, too. In that regard, the particular point of our experiments is the proper discrimination of (sub-) surface and bulk related phenomena.

In the past years we performed extensive ARPES studies on the $RERh_2Si_2$ (RE = Yb, Ce, Eu, Gd and Ho) series of compound as well as in $REIr_2Si_2$. With our approach we were able to address the essential topics at the core of strongly correlated 4*f* electron systems: (i) observation of the crystal-electric field (CEF) splitted 4*f* states and their fine dispersion induced by *f-d* hybridization near the Fermi level; (ii) insight into the Fermi surface and manifestation of its strong 4*f* character in Kondo lattices. Disclosing its topology and features reflecting *f-d* coupling at the surface and bulk of the material as well as gaining insight into its temperature dependent properties; (iii) clear evidence of the interplay of Dirac fermions and heavy quasi-particles; (iv) manifestation of unusual and strong ferromagnetic properties of the Si-terminated surface in antiferromagnets $EuRh_2Si_2$, $GdRh_2Si_2$ and $HoRh_2Si_2$. The latter are caused by the exchange interaction of itinerant surface states with the ordered 4*f* magnetic moments lying four layers below Si-surface, and v) observation of tunable heavy-fermion properties of strongly spin-polarized surface state.

References:
[1] Nano Letters 17, 811 (2017).
[2] Nature Comm. 7, 11029 (2016).
[3] Sci. Reports 6, 24254 (2016).
[4] Phys. Rev. X 5, 011028 (2015).
[5] Nature Comm. 5, 3171 (2014).
[6] Nature Comm. 4, 1646 (2013).

B.A. Palmer 14.12.17, 13:30

Crystal-Eyes: Biogenic Crystals used for Vision

B.A. Palmer[1], A. Hirsch,[2] V. Brumfeld,[3] L. Kronik,[2] D. Oron,[4] L. Leiserowitz,[2] S. Weiner,[1] L. Addadi.[1]

1 Department of Structural Biology, Weizmann Institute of Science, Israel
2 Materials and Interfaces, Weizmann Institute of Science, Israel
3 Chemical Research Support, Weizmann Institute of Science, Israel
4 Physics of Complex Systems, Weizmann Institute of Science, Israel

Many optical systems in nature utilize crystals of organic molecules to manipulate light. These crystals, housed in specialized iridophore cells[1] are used produce an extraordinary array of optical phenomena in animals including diffuse scattering, broadband and narrowband reflectivity.[2] Perhaps the most 'sophisticated' function of these crystals in nature is in vision. Using a range of physical characterization techniques, including *in situ* microspot diffraction at BESSY, we describe the materials properties and hierarchical organization of two eyes which use mirrors made of organic crystals to form images.

Scallops possess a spectacular visual system comprising up to 200 eyes, each containing a concave mirror, rather than a lens to focus light, much like a reflecting telescope.[3] The hierarchical organization of this multilayered mirror, is exquisitely controlled for image formation from the component guanine crystals at the nanoscale to its complex 3D morphology at the millimeter level. The layered structure of the mirror is tuned to reflect the wavelengths of light penetrating the scallop's habitat and is tiled with a mosaic of square guanine crystals,[4] which reduces optical diffraction aberrations. The mirror forms images on a double-layered retina, used for imaging the peripheral and central fields of view, separately.

Shrimp, crayfish and lobsters possess a compound eye, which operates by reflective rather than refractive optics and is ideally suited to vision in dim-light. The eyes contain two sets of mirrors; one to focus light and the other to increase the amount of light being captured by the retina. Using *in situ* microspot diffraction we show that these mirrors are made of a previously unknown biogenic crystal – isoxanthopterin. We determine the crystal structure and refractive index of this highly reflective material using DFT calculations and use this information, in conjunction with measurements of the ultrastructural properties of the mirrors to rationalize the optical performance of the eye.

References:
[1] ChemPlusChem 82, 914 (2017).
[2] Adv. Func. Mater. 1603514 (2017).
[3] Science, in press.
[4] Angew. Chem. Int. Ed. 56, 9420 (2017).

Q. Berrod 14.12.17, 13:50

Transport properties of ionic liquids under 1D nanometric confinement

Q. Berrod [1], F. Ferdeghini [1], P. Judeinstein [1], J. Dijon [2] , M. Russina [3], J.-M. Zanotti [1]

1 Laboratoire Léon Brillouin, CEA, CNRS, Université Paris-Saclay, France
2 CEA, LITEN, DTNM, France
3 Institut Weiche Materie und Funktionale Materialien, Helmholtz Zentrum Berlin, Germany

Ionic liquids (ILs) are pure solutions of charged organic molecules with no solvent. These molecular electrolytes show a property original for a pure liquid: they self-organize in nanometric fluctuating aggregates [1]. When probed at the molecular scale, ILs behave as highly dissociated (i.e. strong) electrolytes [2] while, at the macroscopic scale, they show clear characteristics of weak ionic solutions [3]. Here, we report a multi-scale analysis to tackle these apparently at odd behaviors.
We investigate by Quasi-Elastic Neutron Scattering (QENS) and Neutron Spin-Echo (NSE), the nanometer/nanosecond dynamics of Bmim-TFSI and Omim-BF_4, two imidazolium based ILs showing low and strong nanostructuration, respectively. We also probe the same ILs on the microscopic (µm and ms) scales by Pulsed Field Gradient NMR. To interpret the neutron data, we introduce a new physical appealing model to account for the dynamics of the side-chains and for the diffusion of the whole molecule.[4] We reach a coherent and unified structural/dynamical description of the local cation dynamics: a localized motion within the ILs nanometric domains is combined with a genuine long-range translational motion. The QENS-NSE and NMR experiments describe a same long-range translational process, but probed at different scales. Depending on the ILs level of nanostructuration, the associated diffusion coefficients can be up to one order of magnitude different [5].
Due to their remarkable chemical and electrochemical stability, ILs-based electrolytes are prime candidates for the development of safe energy storage systems. We show that confinement of ILs in 1D Carbon NanoTube (CNT) membranes can be used to enhance their transport properties and hence to boost the power of batteries [6,7] (QENS data measured on NEAT at HZB will be shown).

References:
[1] Chem. Rev. vol. 115, 13, 6357 (2015).
[2] J. Phys. Chem. Lett. 6, 1, 159 (2015).
[3] Proc. Natl. Acad. Sci. 110, 24, 9674 (2013).
[4] Nanoscale 9, 5, 1901 (2017).
[5] Sci. Rep. 7, 1 (2017).
[6] Nanoscale 8, 15, 7845 (2016).
[7] ArXiv171006020 Cond-Mat (2017).

Y. Muller 14.12.17, 14:10

Insight into herpesvirus replication from structural studies at the HZB-MX beamlines

Y.A. Muller[1]

1 Division of Biotechnology, Department of Biology, Friedrich-Alexander Universität Erlangen-Nürnberg, Germany

Herpesviral infections cause a variety of often life-threatening human diseases. Despite existing antiviral treatments, the repertoire of therapy options and approved antiviral drugs is largely underserved so that novel targeting strategies are urgently needed. In collaboration with various groups from the virology department at FAU my group studies two prototypical β- and γ-herpesviruses, namely human cytomegalovirus (HCMV) and Epstein-Barr virus (EBV).
During the last years we investigated different structural biology aspects of the herpesviral replication mechanism, namely (i) the initial attachment of the virus to the host cell [1], (ii) the function of the first viral protein expressed in the host cell (immediate early protein 1, IE1) [2], and (iii) the nuclear egress mechanism that is required for the release of the preassembled viral capsids from the nucleus of the host cell [3,4].
During my talk, I will discuss how the results from our structural studies performed at the HZB-MX beamlines helped us to understand the action but also the limitations of an antiherpesviral immune therapy [1], how structural insight into IE1 enabled us to propose a functional mechanism for its action that proved later valid [2, 5] and how the core nuclear egress complex formed between HCMV pUL50 and pUL53 offers new opportunities for drug discovery [3,4].

References:
[1] PLoS Pathogens 10: e1004377 (2014) (PMC4192593)
[2] PLoS Pathogens 10: e1004512 (2014) (PMC4239116)
[3] J. Biol. Chem. 290: 27452-27458 (2015) (PMID26432641)
[4] Rev. Med. Virol. 27, doi: 10.1002/rmv.1934 (2017) (PMID28664574)
[5] Journal of Virology 91: e02049-16. (2016) (PMID27903803)

J. Wells 14.12.17, 14:30

In Situ Patterning of Ultrasharp Dopant Profiles in Silicon

J. Wells[1]

1 Department of Physics, Norwegian University of Science and Technology, Norway

Traditional electronics rely on the statistical properties of large numbers of dopants in semiconductors. On the other hand, recent developments have opened the possibility to place dopants with unprecedented precision to form atomically thin 2D sheets, 1D wires and 0D quantum dots. This ability to precisely place dopants within a semiconducting host offers an exciting “test bench” for building a wide range of novel quantum devices, which are fully integrated with existing traditional semiconductor technology.

In this talk, I will first present “delta doping”, a growth technique in which an atomically thin 2D sheet of phosphorus dopants is created within a 3D silicon wafer. I will discuss the electronic properties of such a structure, and the challenges (and successes) associated with measuring and fine tuning the band structure of such a structure. I will also discuss the possibility of patterning this layer on a wide variety of length scales, and describe the relevance for quantum devices, including quantum computation.

S. Hofmann 14.12.17, 14:50

Integrated Crystal Growth of Advanced Nanomaterials: from model systems to integrated manufacturing

S. Hofmann[1]

1 Department of Engineering, University of Cambridge, United Kingdom

With a focus on diverse applications in the electronics and display industry, we aim at developing integrated process technology for nanomaterials, like semiconducting nanowires, 2D materials and their heterostructures [1]. In order to go beyond empirical process calibrations, we systematically use in-situ metrology to reveal the mechanisms that govern the growth, interfaces and device behaviour of these nanomaterials in realistic process environments. I will review our recent progress in scalable CVD [1] and device integration approaches of highly crystalline graphene and hexagonal boron nitride (h-BN) films [2,3]. The growth mode thereby is catalytic and I will focus on our investigations of the interfacial chemistry during growth as well as subsequent transfer and device integration of these 2D materials [4,5].

References:
[1] J. Phys. Chem. Lett. 6, 2714 (2015)
[2] Nano Lett. 16, 6196 (2016)
[3] Nano Lett. 16, 1250 (2016)
[4] ACS Appl. Mater. Inter. 9, 29973 (2017)
[5] JACS 137, 14358 (2015)

Abstracts of the Young Scientists Session - Neutron Day

Friday, 15th of December

M. Steinhauer 15.12.17, 11:00

In situ Studies of Solid Electrolyte Interphase (SEI) Formation on Carbon Surfaces by Neutron Reflectometry

M. Steinhauer[1], M. Stich[2], B. Seidlhofer[3], M. Trapp[3], N. Wagner[1], K.A. Friedrich[1,4]

1 Institute of Engineering Thermodynamics, German Aerospace Center, Germany
2 Electrochemistry and Electroplating, Technische Universität Ilmenau, Germany
3 Soft Matter and Functional Materials, Helmholtz-Zentrum Berlin, Germany
4 Institute for Energy Storage, University of Stuttgart, Germany

During the first discharge of a lithium-ion battery a solid film forms on the anode surface in contact with the electrolyte. It mainly consists of decomposition products of the electrolyte and is therefore called solid electrolyte interphase (SEI). The SEI plays an ambiguous role in a lithium-ion battery as it on the one hand passivates the anode, preventing delamination of the anode material by co-intercalation of solvent molecules and slows down further electrolyte decomposition. On the other hand, the formation of the SEI invariably goes along with irreversible capacity losses. Furthermore the SEI plays an important role in critical degradation mechanisms that may lead to thermal runaway [1]. Although many studies have been performed the exact nature of the SEI is yet not fully understood [2]. We used Neutron reflectometry to observe SEI formation *in situ*. Therefore a thin layer of carbon was sputtered onto a silicon substrate. Lithium metal was used as counter electrode and the electrolyte was EC:DEC 3:7 v/v, 1M $LiPF_6$. The neutron reflectometry measurements show a maximum SEI thickness of 192 Å at the lower cut-off voltage. At open cell voltage (OCV) a lithium rich layer could be observed on the electrode surface. The most rapid changes of the SEI thickness and scattering length density were observed between 0.8 V and 0.6 V vs. Li/Li^+. The SEI thickness slightly increases during charging.

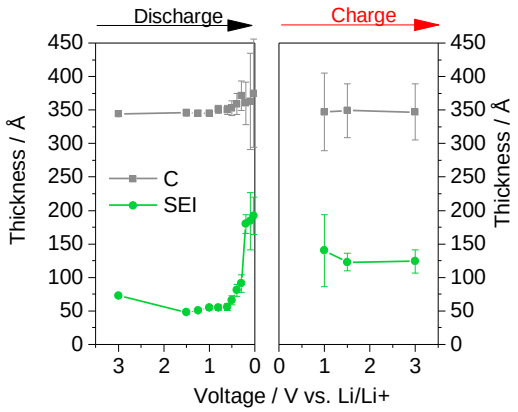

Figure 1: Thickness of the carbon and SEI layer during discharging and charging. The carbon layer slightly decreases with ongoing lithiation. The main thickness increase of the SEI can be observed between 0.8 V and 0.6 V vs. Li/Li^+

References:
[1] Solid State Ionics 148, 405 (2002).
[2] Z. Phys. Chem. 223, 1395 (2009).

L. Heinze 15.12.17, 11:15

Magnetism of atacamite, $Cu_2Cl(OH)_3$

L. Heinze[1], R. Beltran-Rodriguez[2], G. Bastien[2], A.U.B. Wolter[2], M. Reehuis[3], J.-U. Hoffmann[3], K.C. Rule[4], S. Süllow[1]

1 Institut für Physik der Kondensierten Materie, TU Braunschweig, Germany
2 Leibniz-Institut für Festkörper- und Werkstoffforschung IFW Dresden, Germany
3 Institut Quantenphänomene in neuen Materialien, Helmholtz-Zentrum Berlin, Germany
4 Australian Centre for Neutron Scattering, ANSTO, Australia

Atacamite, $Cu_2Cl(OH)_3$, has been reported to exhibit magnetic behavior characteristic of a frustrated quantum magnet. Notably, an antiferromagnetic transition at T_N = 9.0 K has been observed and, further, susceptibility measurements previously carried out indicate a Curie-Weiss temperature $|\Theta_{CW}| >> T_N$ [1,2]. So far, attempts have been undertaken to determine the symmetry of the magnetic ground state of this material by means of μSR and NMR measurements on polycrystalline material [2,3]. The conclusions drawn from these studies, however, are contradictory: From the μSR measurement, a disordered state was suggested [2] whereas from the proton NMR spectra it was assumed an “all-in all-out” alignment of the Cu magnetic moments on crystallographic inequivalent sites (μ_I = 1.12 μ_B and μ_{II} = 0.25 μ_B), similar to the magnetic structure of an antiferromagnetic pyrochlore lattice [3].
Starting from this given situation, we have reinvestigated the magnetic properties of atacamite. Single-crystalline, mineral samples were studied by means of susceptibility and magnetization measurements as function of temperature and field along the three principal crystallographic axes as well as by means of elastic neutron scattering. This way, we have established the symmetry of the long-range ordered magnetic ground state, and present the new insights into the unusual magnetic properties of atacamite.

References:
[1] Solid State Commun. 130, 107 (2004).
[2] Phys. Rev. B 71, 174404 (2005).
[3] J. Phys. Soc. Jpn. 82, 084707 (2013).

P. Portnichenko 15.12.17, 11:30

Magnetic-field dependence of the ferromagnetic excitation in the heavy-fermion metal CeB_6

P.Y. Portnichenko[1], S.E. Nikitin[1,2], S.V. Demishev[3], N.Y. Shitsevalova[4], Z. Huesges[5], Z. Lu[5], A. Schneidewind[6], J. Ollivier[7], A. Podlesnyak[8], D.S. Inosov[1]

1 Institut für Festkörperphysik, TU Dresden, Germany
2 Max Planck Institute for Chemical Physics of Solids, Germany
3 A. M. Prokhorov General Physics Institute of RAS, Russia
4 I. M. Frantsevich Institute for Problems of Material Sciences of NAS, Ukraine
5 Abteilung Methoden zur Charakterisierung von Transportphänomenen in Energiematerialien, Helmholtz-Zentrum Berlin, Germany
6 Jülich Center for Neutron Science, Outstation at MLZ, Germany
7 Institut Laue-Langevin, France
8 Quantum Condensed Matter Division, ORNL, USA

CeB_6 is a heavy-fermion metal with a simple cubic crystal structure, characterized by the rich magnetic-field – temperature phase diagram. In zero field, it exhibits a high-temperature paramagnetic phase I; an antiferroquadrupolar (AFQ) phase II at intermediate temperatures between T_N=2.3 K and T_Q=3.2 K [2]; and an AFM ground-state phase III below T_N. In addition, an external magnetic field B enhances T_Q and rapidly suppresses T_N. The AFQ state in CeB_6 has been extensively studied as it represents an example of a magnetically hidden order, most commonly associated with the ordering of magnetic quadrupolar moments [2–4]. In our earlier inelastic neutron scattering experiments, we have discovered an intense ferromagnetic low-energy collective mode that dominates the magnetic excitation spectrum of CeB_6 in the AFM phase [5]. Recently, ESR measurements revealed a significant anisotropy of the g-factor as a function of the applied field direction [6]. The g-factor remains temperature independent and isotropic for generic field directions like [110] or [111], but shows a noticeable anomaly for B // [100], where is decreases by ~20 % between 1.8 K and 3.4 K. Knowing that the energy of the ESR resonance matches perfectly with that of the field-induced INS excitation [7], we expected a corresponding softening of the zone-center mode in field parallel to [100]. However our results show absolutely no temperature effect on the g-factor at high fields, however we observe significant difference of the resonance energy upon change of the field direction. Observed difference of the resonance energy can be explained either by anisotropy or by redistribution of the spectral weight between inner branches, which we perceive as a change of the resonance energy.

References:
[1] J. Phys. Soc. Jpn. 64, 3941 (1995).
[2] Phys. Rev. Lett. 103, 017203 (2009).
[3] J. Phys. Soc. Jpn. 66, 1741 (1997).
[4] J. Phys. Soc. Jpn. 70, 1751 (2001).
[5] Nature Mater. 13, 682 (2014).
[6] Sci. Rep. 6, 39196 (2016).
[7] Phys. Rev. B. 94, 035114 (2016).

R. Palm 15.12.17, 11:45

Small angle neutron scattering for determination of porous structure of molybdenum carbide-derived carbons

R. Palm[1], H. Kurig[1], R. Härmas[1], M. Russina[2], I. Tallo[1], B. Kent[2], T. Romann[1], E. Härk[2], E. Lust[1]

1 Institute of Chemistry, University of Tartu, Estonia
2 Institut Weiche Materie und Funktionale Materialien, Helmholtz Zentrum Berlin, Germany

The structure of amorphous carbon materials has an important role in many applications from energy storage to gas separation [1]. The material pore size distribution and the pore shape have a large impact on the applicative performance of carbon, therefore the correct pore size and shape assumption for investigated carbon materials are of outmost importance. Gas sorption techniques are widely used to characterize the structure (specific surface area, pore volume, pore size distribution) of carbon materials using various models. A definite pore shape is presumed, usually a slit shape pore, to calculate the pore size distribution using density functional theory [2].
In addition to gas sorption measurement techniques, Small Angle Neutron Scattering gives vital information about carbon structure and allows determination of pore shape and size. Applying contrast variation techniques of Small Angle Neutron Scattering to the investigation of the microporous carbide derived carbon (CDC) materials, we have recently observed pores that differ from the standard presumed slit shape, with even bimodal distribution depending on the condition of the synthesis [3]. Based on the results an optimum carbon material structures could be found for different applications and new carbon materials with improved structures could be designed and synthesized.
We have extended this approach to the investigation of mesoporous Mo_2C derived carbons synthesized at different chlorination temperatures. With an increase in the temperature of halogenation we observe an increase of the ratio of graphitization and average pore size in the synthesized CDC [4]. For the contrast variation we have used deuterated toluene to match the scattering signal of the pores to the CDC materials. Applying Guinier-Porod and pore geometry based models to the intensity vs q-vector data obtained from small angle neutron scattering gives additional information about the pore structure. The change of pore shape and size information at different halogenation temperatures gives a deeper insight into the carbon structure formation during synthesis in addition to information about the structure of pores in carbon materials.

References:
[1] Nanomaterials Handbook, CRC Press (2006)
[2] Carbon 55, 70 (2013)
[3] Carbon 100, 617 (2016)
[4] Carbon 47, 23 (2009)

A. Werwein 15.12.17, 12:00

Zintl phase hydrides $LaGaD_x$, $TmGaD_x$ and $NdSiD_x$

A. Werwein[1], H. Kohlmann[1]

1 Faculty of Chemistry and Mineralogy, Department of Inorganic Chemistry, Universität Leipzig, Germany

Zintl phases are polar intermetallics composed of group one or two metal or a lanthanide and a group 13 to 16 element. They often follow a simple electron counting scheme (Zintl- Klemm rules) and feature polyanions with covalent bonds. Zintl phases react in various ways with hydrogen. The fundamental concept is the oxidation of the polyanion. Hydrogen can be incorporated in voids of the crystal structure (interstitial hydride) or bonded covalently to the polyanion (polyanionic hydride) [1].The intermetallic precursor of the title compounds are *Ln*Ga (*Ln* = La, Tm) and NdSi [2,3]. Considering structural and physical properties they may be described by ionic formulae $Nd^{3+}\,Tt^{2-}e^-$ and $Ln^{3+}Ga^{3-}$ where the polyanions form infinite zig- zag chains. The compounds were prepared by arc melting of the elements and studied during the hydrogenation by *in situ* thermal analysis under hydrogen pressures of from 1 to 5 MPa and temperatures up to 450°C. The compounds react with hydrogen at temperatures between 200 and 300 oC. Neutron diffraction (E9, HZB Berlin) studies on the deuterides revealed that the hydrogen is incorporated into tetrahedral voids in all compounds. For NdSi no further hydrogen positions were observed. Due to the hydrogenation the Si-Si bond length decreases from 2.598(5) to 2.418(9) (Fig.1).The hydrides of the monogallides exhibit further structural features, as $LaGaD_{1.66}$ shows additional hydrogen positions between the chains. In TmGaD deuterium also occupies tetrahedral voids only, but features alternating interchain distances (2.98 Å and 3.98 Å) (Fig.1).

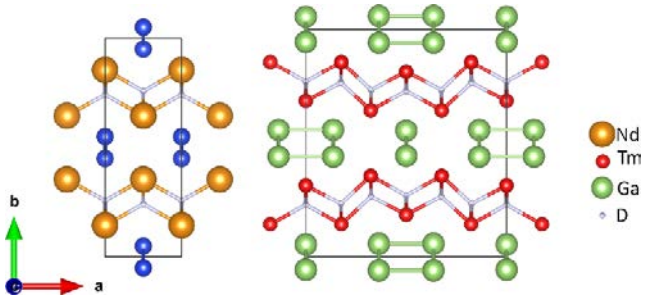

Fig 1. Left: crystal structure of $NdSiD_{0.9(1)}$; right: crystal structure of TmGaD

References:
[1] Struct. Bond. 139, 143 (2011)
[2] Acta Cryst. 23, 860 (1967)
[3] Acta Cryst, 20, 572 (1966)

J. Lee 15.12.17, 12:15

Study on high magnetic field phase of UPt_2Si_2

J. Lee[1], J. Mydosh[2], S. Dissanayake[3], O. Prokhnenko[4], M. Bartkowiak[4], K. Prokes[4], S. Süllow[5], F. Ye[3], J.P.R. Ruff[1], M. Matsuda[3], G.E. Granroth[3]

1 Cornell High Energy Synchrotron Source, Cornell University, USA
2 Institute of Lorentz, Leiden University, The Netherlands
3 Neutron Scattering Division, Oak Ridge National Laboratory, USA
4 Abteilung Hochfeldmagnet, Helmholtz-Zentrum Berlin, Germany
5 Institut für Physik der Kondensierten Materie,TU Braunschweig, Germany

The dual aspect of magnetism between localized and itinerant nature in 5f electron system has been a longstanding puzzle. UPt_2Si_2, on the other hand, has been considered as a rare example of uranium intermetallic with strongly localized moments. Here, we present high magnetic field neutron scattering studies, using both a pulsed and a continuous magnet, demonstrating that both itinerant and local moments of 5f -electrons are playing a major role in this system. We claim that very similar underlying physics exist both in UPt_2Si_2 and URu_2Si_2, the famous yet-to-be-understood hidden order system. Only a subtle perturbation onto nearly degenerate competing for energy scales leads to different ground states in these systems. Our high magnetic field scattering data find and charactierize rich magnetic phase diagram in high field, and suggest Lifshitz effect should be considered to fully understand this system.

Poster Abstracts – Science Day at BESSY II

Thursday, 14th of December

0a Quantum Material CoreLab

Siemensmeyer K, Islam N

Offers of the new Quantum Material CoreLab to BER II, BESSY II and external users: new material preparation in powder and single crystal form; material analysis: stoichiometry, phase purity, single crystallinity etc.; orientation, shaping and (multiple) mount of crystals for any experimental requirement; temperature, field and pressure dependence of magnetisation, resistivity, specific heat, thermal transport ...; a full user support which includes data analysis until publication ready.

0b Electronic structure of Hexacene and interface properties on Au(110)

Grüninger P, Balle D, Karstens R, Ovsyannikov R, Giangrisostomi E, Chassé T, Bettinger HF, Peisert H

Acenes are an important class of polycyclic aromatic hydrocarbons. However molecules larger than pentacene, a well-known material for organic electronics, are difficult to handle due to their low solubility and high reactivity. We successfully evaporated the six-ringed hexacene on Au(110) for the first time and studied the electronic properties as well as the molecular orientation using x-ray absorption and photoemission spectroscopy (XAS, PES).

0c Pump-probe two-photon photoemission study of tetracene-silicon interfaces for singlet fission solar cells

MacQueen RW, Borgwardt M, Friedrich D, Amsalem P, Mews M, Eichberger R, Lips K

Using pump-probe photoemission, we studied the exciton dynamics in thin films of the molecule, tetracene, evaporated on crystalline silicon. Tetracene performs singlet fission, an exciton multiplication process, which enables more efficient conversion of the solar spectrum to electricity in silicon solar cells. Understanding and controlling the organic-inorganic interface is key to achieving this.

0d Potentials and limitations of probe-before-destroy soft x-ray absorption spectroscopy on photosystem II and prototypical manganese complexes in solution

Kubin M, Kern J, Chatterjee R, Gul S, Fuller FD, Kroll T, Guo M, Lundberg M, Odelius M, Löchel H, Quevedo W, Erko A, Föhlisch A, Bergmann U, Mitzner R, Yachandra VK, Yano J, Wernet P

Here we discuss our recent progress on Mn L-edge x-ray absorption spectroscopy of Photosystem II and dilute Mn complexes in solution. Experimental limitations due to x-ray induced sample damage at synchrotrons and x-ray free electron lasers are discussed. Interpretation of the spectra with respect to the local electronic structure at the Mn is outlined within an ab-initio theoretical framework.

0e Hydrogen Bonding Structure of Aqueous Ammonia and Ammonium Probed with IR and X-ray Spectroscopy

Ekimova M, Quevedo W, Szyc L, Iannuzzi M, Wernet P, Odelius M, Nibbering ETJ

We determine and characterize the hydrogen bond (HB) structure of two amine model compounds aqueous ammonia and ammonium ion by combining local soft-x-ray and vibrational spectroscopies with ab initio MD simulations. The picture emerges of one strong accepting HB in case of NH_3, and four N-H donating HBs for NH^{4+} ion, providing a benchmark for further work.

0e-f Soft x-ray beam damage of a solid Mn(III) complex (determined with Mn L-edge absorption spectroscopy)

Ludwig J, Kubin M, Ekimova M, Mitzner R, Weniger C, Föhlisch A, Kern J, Yachandra V, Nibbering E, Yano J, Wernet P

Soft x-rays are widely used for L-edge spectroscopy on transition-metal compounds, but also cause beam damage due to photoreduction. For acquiring damage-free data it is necessary to determine the acceptable threshold of x-ray dose for spectroscopy. Here we compare the dose dependent photoreduction in L-edge absorption spectra of Mn(III) with Mn(II) compounds and discuss the underlying mechanisms.

0f Structure and magnetic properties of Y-Sr-Co-O layered complex cobalt oxides

Sikolenko V, Efimov V, Karpinsky D, Troyanchuk I, Levterova E, Többens D, Hoser A, Schorr S

The results on neutron and X-ray diffraction studies of magnetic and structurall properties of Y-Sr-Co-O, doped with Sr are presented. It was found, that the crystal structure of these compound family is orthorhombic rather than tetragonal as it was suggested before. The magnetic structure can be refined in the frame of the model with three independent Co moments.

1 Investigation of the detection limits of ZnSe and Cu_2SnSe_3 secondary phases in $Cu_2ZnSnSe_4$ by XANES

Ferreira R, Gurieva G, Schorr S

CZTSe is a promising semiconductor material for absorber layers in thin film solar cells, which often present a low open circuit voltage with respect to the band gap energy, a phenomenon that could be caused by compositional and phase inhomogeneities in the absorber layer. The sensitivity limits of XANES to the presence of two common secondary phases ZnSe and Cu_2SnSe_3 in $Cu_2ZnSnSe_4$ is examined.

2 Enhanced temperature and gas options at KMC-2

Többens DM, Schuck G, Wallacher D, Grimm N, Schorr S

A suit of newly developed sample environments is available for both end stations at KMC-2: CCR-XRD covers controlled atmospheres up to 150 kPa at 15 - 450 K. For small samples and precarious gases, capillary setups are available. Between the CRYO-GAS-JET, AROUND-AMBIENT, and HOT-AIR-JET systems, continuous flow or static atmospheres up to 10.000 kPa and 20 – 700 K are accessible.

3 Defining the phase diagram of hybrid perovskite $CH_3NH_3PbI_{3-x}Br_x$ solid solution

Lehmann F, Franz A, Többens DM, Schorr S

Recently, hybrid perovskite materials became attractive in photovoltaic applications, offering a broad range of properties, for instance a tunable wide-bandgap, which is directly related to their chemical composition. In this poster we analyzed the $MAPbI_{3-x}Br_x$ solid solution at complete temperature range by synchrotron X-ray diffraction. As a result of this study the phase diagram was established.

4 Structural and magnetic characterization of Pd-decorated cobalt ferrite multifunctional nanoparticles

Shams SF, Schmitz D, Smekhova A, Svechkina N, Siemensmeyer K, Tavabi AH, Dunin-Borkowski RE, Schmitz-Antoniak C

Pd-decorated cobalt-ferrite hybrid nanoparticles have been synthesized and elemental analyses used to confirm their successful decoration. Cations distributions, calculated from XANES and XRD measurements, show cation disorder for all samples with similar size-related trend. High-field XMCD and magnetometry reveal significantly enhanced magnetic moments after Pd decoration for both Fe and Co ions.

4a Evolution of Magnetism and Local environment in $Fe_{60}Al_{40}$ thin films under Ne^+ irradiation

Smekhova A, La Torre E, Szyjka T, Eggert B, Cöster B, Walecki D, Salamon S, Ollefs K, Bali R, Lindner J, Wilhelm F, Rogalev A, Weschke E, Többens D, Banerjee R, Sanyal B, Schmitz-Antoniak C, Wende H

EXAFS, SR-XRD, XANES, and XMCD techniques have been applied to probe consequential changes of local environment and related magnetic/electronic properties of Fe and Al atoms in $Fe_{60}Al_{40}$ thin films through the order-disorder phase transition induced by 20 keV Ne^+ ion irradiation. An interrelation between atomic local surrounding and continuous rise of Fe 3d spin polarization has been proven.

4b Properties of central d-metal ions in polyoxopalladates

Svechkina N, Izarova N, Schmitz D, Smekhova A, Schmitz-Antoniak C

3d and 4d metal ions in the centres of cuboid-shaped polyoxopalladates were studied element-specifically with XAS at low temperatures (4 K) in magnetic fields up to 6 T. Their crystal field parameters and valence states were quantified by comparing XANES, XMCD, and XMLD spectra with CTM4XAS simulations. Their magnetic spin and orbital moments were determined from XMCD spectra using sum rules.

5 X-ray Optics Research at MAXYMUS

Keskinbora K, Sanli UT, Baluktsian M, Weigand M, Bykova I, Schütz G

Diffractive optics have the highest resolutions in X-rays. We focus on developing novel optics and fabrication approaches based on Ion Beam Lithography and Atomic Layer Deposition methods. We will show innovative X-ray optics, including kinoforms with vaious topological charges, various binary FZPs and last but not least, ultra-high aspect ratio multilayer type FZPs and discuss their fabrication.

6 Capabilities of the MAXYMUS Beamline and Endstation

Weigand M, Bykova I, Bechtel M, Goering E, Stoll H, Schütz G

MAXYMUS, a scanning x-ray transmission microscope (STXM), is a permanent endstation at the UE46 undulator operated by the Max Planck Institute for Intelligent Systems. We will showcase recent highlights of reseach done at the instrument using advanced features as Ptychography for <10nm spatial resolution or pump and probe imaging with <20ps time resolution.

7 High-resolution Chemical and Magnetic Imaging with Ptychography at MAXYMUS X-ray Microscope

Bykova I, Weigand M, Keskinbora K, Sanli U, Gräfe J, Bechtel M, Goering E, Stoll H, Baylan S, Richter G, Schütz G

Ptychography is an X-ray imaging technique which can potentially achieve wave-length limited resolution. Implementation of a fast CCD camera (PNSensor) and in-house produced IBL FZPs at MAXYMUS microscope allowed drastic improvement of imaging resolution and contrast. We are going to present ptychographic imaging of samples with chemical and magnetic contrast obtained at MAXYMUS.

13 Redox processes at interfaces

Nemsak S, Hackl J, Mueller D, Duchon T

In-situ and operando advanced microscopies and spectroscopies are necessary to understand underlying chemical processes in operating devices. Instrumental developments at LEEM/PEEM facility of BESSY-II Berlin towards that aim.

14 Imaging laser induced magnetic domains in Co/Pt multilayers using photoemission electron microscopy

Parlak U, Adam R, Nemsak S, Gang S, Bürgler DE, Schneider CM

We investigated the effect of the number of pulses to achieve an efficient all-optical switching (AOS) in Co/Pt multilayers. The fs-laser induced magnetic domains were analyzed using an in-situ MOKE microscope. We employed PEEM with x-rays tuned to Co L3 absorption edge for a higher resolution of magnetic domains. Our results indicate that AOS scales with the number of pulses per illuminated area.

15 The growth mechanisms of ceria islands on copper (100)

Hackl J, Duchon T, Gottlob DM, Cramm S, Veltruska K, Matolin V, Nemsak S, Schneider CM

We present a microscopic study of the temperature dependent growth of nanometer-sized ceria islands on a Cu (100) substrate. X-PEEM, XAS, LEEM and micro-LEED are used to determine the morphology, shape, chemical state, and crystal structure of the islands. Utilizing real-time observation capabilities, we reveal a three-way interaction between ceria, substrate, and local oxygen chemical potential.

17 What can we learn using TOF spectrometer NEAT?

Russina M, Günther G, Grzimek V

The scientific demand for in-situ studies of dynamics in nanoscale and biological materials, materials under extreme conditions of magnetic field and pressure, and parametric studies dictate the nessesity for the instruments with higher power and new instrumental options.

18 The magnetic state of Dy_2AgIn_3

Kontopou VI, Kosmidou K, Siouris IM, Katsavounis S

The intermetallic Dy_2AgIn_3 adopts a $CaIn_2$-type structure. The magnetic behavior in the temperature range 2 K to 60 K, examined by ND shows neither magnetic nor increase intensity on nuclear peaks. This clearly confirms the formation of a spin glass state below Tf. Refinement of the structural parameters at 60 K, give (a=4.7565(2), c=7.2896 (6) and z= 0.5091).

19 The Effect of Carbon 1s Core Hole on the Polarization Spectra of Highly Oriented Pyrolitic Graphite (HOPG)

Legut D, Jansing C, Mertins H-C, Gaupp A, Oppeneer P, Timmers H, Wahab H

Our band structure calculation show a good agreement with experimental polarization spectra across the carbon 1s edge of HOPG. The change in rotation of polarization plane of up to 140° and the change to nearly fully circularly polarized light exhibit best agreement if half-core hole per excitation is taken into account.

20 In-situ XAFS characterization of PtPd nanoparticles synthesized by galvanic replacement

Tymen S, Scheinost AC

PtPd particles prepared by galvanic replacement with different times of synthesis are characterized by TEM, XAFS and in-situ XAFS at different potentials. Iterative transfer analysis and a metal-oxide model enable to follow the changes and the evolution of the relative concentration. The measurement of the catalytic activity reveals at dependence on the shape and composition of the particles.

22 In situ study of graphene patterning on SiC

Chellappan RK, Cooil S, Gotz A, Dahl O, Wells J

Graphene has been proposed as a promising candidate for the fabrication of radiation sensors due to its exceptional electronic properties. However, problems associated with the preparation of high quality graphene on a suitable substrate hinders the realization of the advantages of graphene. Therefore, this study focuses on patterned epitaxial iron mediated growth of graphene on silicon carbide.

24 Ultrafast XUV photoelectron spectroscopy study of solvent effect on photoinduced relaxation dynamics of $[Fe(CN)_6]^{3-}$ ion

Kuzkova N, Raheem A, Merschjann C, Kiyan IY

Relaxation dynamics of photoexcited ferricyanide is studied in ionic liquid and in aqueous solution by means of ultrafast photoemission spectroscopy. In both solutions, we confirm the double exponential decay of excited electron population, which is associated with a sequence of intersystem crossings in the molecular compound. However, the relaxation rates are different in two solvents.

25 Formation of a catalytic active surface layer on cu for the CO_2 reduction

Spodaryk M, Züttel A

The study is focused in electrochemical CO_2 reduction on new catalytic Cu-containing surfaces, such as nanorods and alloys. In case of $LaNi_{5-x}Cu_x$ intermetallic alloys enormous amount of H_2 prevents the CO_2 adsorption on the surface affecting the reduction process towards H_2 evolution. The amount of H_2 at the catalyst surface has to be much less than the CO_2.

26 Low Energy Electron Microscopy at Near Ambient Pressures

Breitschaft M, Hagen S, Kunze K, Schmidt D, Schaff O, Kampen T, Thissen A

We have built a near ambient pressure LEEM/PEEM based on the SPECS FE-LEEM P90. This new instrument allows studying dynamic surface processes from UHV to near ambient gas pressures. We present the design concept and first results with image resolutions < 30 nm in UHV and < 100 nm at 1 mbar.

29 Electron scattering resonances in graphene and their suppression by quantum dots

Krivenkov M, Marchenko D, Sánchez-Barriga J, Rader O, Varykhalov A

Transmission of low-energetic electrons through two-dimensional materials leads to unique scattering resonances. Using angle-resolved photoemission, we have systematically studied scattering resonances in epitaxial graphene grown on chemically differing substrates.

30 Topological quantum phase transition from mirror to time reversal symmetry protected topological insulator

Mandal PS, Springholz G, Volobuev VV, Caha O, Varykhalov A, Golias E, Bauer G, Rader O, Sánchez-Barriga J

The system Pb28%SnSe is a famous topological crystal insulator in which topological surface states are protected by mirror symmetry. By adding 2% Bi to Pb28%SnSe, we observe a topological quantum phase transition to a Z2 topological insulator where surface states are protected by time reversal symmetry.

31 Extremely Flat Band in Bilayer Graphene on Silicon Carbide

Marchenko D, Evtushinsky DV, Golias E, Varykhalov A, Seyller T, Rader O

We discover by ARPES that bilayer graphene on SiC shows an extremely at band with < 2 meV dispersion. We explain this band with a model hamiltonian and consider this flat band a candidate for explaining the reported superconductivity tendency of graphite interfaces at elevated temperatures.

32 Samarium hexaboride: a trivial surface conductor

Hlawenka P, Siemensmeyer K, Weschke E, Varykhalov A, Sánchez-Barriga J, Shitsevalova NY, Dukhnenko AV, Filipov VB, Gabáni S, Flachbart K, Rader O, Rienks EDL

SmB6 is predicted to be the first member of the intersection of topological insulators and Kondo insulators. We find instead the surface states to be of topologically trivial nature. Moreover we explain its famous surface conductivity also in a simple way, i.e., a surface shift of the f state. This will be important for the search for topological Kondo insulators.

32a Large magnetic Dirac gap in a novel class of Mn-induced Bi_2Te_3 heterostructures

Mandal PS, Wimmer S, Rienks EDL, Caha O, Volobuiev VV, Springholz G, Bauer G, Ney A, Minár J, Sánchez-Barriga J, Varykhalov A, Rader O

Magnetic topological insulators enable the quantum anomalous Hall effect but the necessary magnetic gap at the Dirac point has never been observed. Here, ARPES shows a magnetic gap at the Dirac point of Mn-doped Bi_2Te_3 which is 32 meV wide and thus twice as large as predicted by density functional theory. We discuss reasons for this.

33 Insight in catalytic mechanisms by (quasi) in-situ X-ray absorption spectroscopy at metal K-edges (at KMC-3): results on electrochemical water oxidation by freeze-quench experiments

Kubella P, Pasquini C, Chernev P, Dau H

Transition metal oxides are promising catalysts for electrochemical water oxidation in production of non-fossil fuels. Using a freeze-quench method, we investigated a set of (binary) oxides by X-ray absorption spectroscopy. Mechanistic insights and suggestions on the role of different metals (Co, Mn, Fe) are derived from metal oxidation-states (XANES) and structural changes (EXAFS).

34 Metal cofactors in enzymes studied by XAS at beamline KMC-3

Mebs S, Schuth N, Schrapers P, Kositzki R, Reschke S, Hemschemeier A, Schwalbe M, Dobbek H, Leimkühler S, Dau H, Haumann M

Metal cofactors in enzymes are involved in reactions with small molecules. The structures of the transition metal sites need to be determined. We used X-ray absorption spectroscopy at the new beamline KMC-3 at BESSY-II to collect XANES and EXAFS spectra at Fe and Co K-edges and the W L3-edge. This has provided insight in cofactor assembly, oxygen transport, and methane binding at the cofactors.

35 Insight in catalytic mechanisms by in-situ X-ray absorption spectroscopy at metal K-edges (at KMC-3): Electrochemical water oxidation for solar fuels

Chernev P, Loos S, González-Flores D, Zaharieva I, Pasquini C, Zizak I, Dau H

Electrocatalytic water oxidation is investigated by in operando XAS. The behavior of oxide films during cyclic voltammetry and potential stepping protocols was tracked by X-ray spectroscopy at the K-edges of Mn, Fe, Co, Ni. Mechanistic insights came from time-resolved oxidation state changes, revealing agreement between changes in metal oxidation state and electrochemical redox currents.

36 Self-supported $Ni(OH)_2/MnO_2$ on CFP as a Flexible Anode towards Urea Electrocatalytic Conversion

Liang Y, Chernev P, Dau H

We report a carbon fiber paper supported $Ni(OH)_2/MnO_2$ catalysts with various Mn contents used in electrocatalysis of the urea oxidation reaction. The catalysts which exhibit lower OER performance will present higher UOR activity.

36a Insight in catalytic mechanisms by in-situ X-ray absorption spectroscopy at metal K-edges (at KMC-3): Experimental approach, status and perspectives

Chernev P, Loos S, Zizak I, Zaharieva I, Dau H

The experimental setup for in situ (or operando) XAS at the KMC-3 beamline is described. The end station allows time-resolved XAS on catalyst materials containing transition metals, during electrocatalysis. Further extensions – including a fast energy-resolving 13-element Si-drift X-ray detector – are in progress and will improve the signal quality and effective time resolution significantly.

37 Crystallographic fragment-screening (CFS) at the Helmholtz-Zentrum Berlin and why CFS should be the first choice

Huschmann FU, Feiler C, Förster R, Gerlach M, Heine A, Hellmig M, Klebe G, Linnik J, Malecki PH, Metz A, Radeva N, Schiebel J, Röwer K, Steffien M, Ühlein M, Wilk P, Mueller U, Weiss MS

Fragment screening is a widely spread approach to identify compounds, which are able to bind to protein targets. Typically, binding fragments are identified by a cascade of biophysical methods and then further analyzed structurally by X-ray crystallography. We have put this pre-screening cascade on the spot and found that X-ray crystallography should be used as the primary screening method.

38 Human Prolidase and its pathological mutants - structural basis of Prolidase Deficiency

Wilk P, Ühlein M, Piwowarczyk R, Dobbek H, Mueller U, Weiss MS

In humans prolidase is the only metaloenzyme capable of hydrolysis of dipeptides containing Pro at its C-terminus. Several mutations were identified that lead to diminished Prolidase activity and in consequence to a severe clinical syndrom - Prolidase Deficiency. Here we characterized several of the pathological mutants of prolidase aiming at explanation of their influence on enzymes function.

39 The expert MX data processing system XDSAPP

Röwer K, Weiss MS

XDSAPP is an expert user interface for the fast and automated processing of X-ray diffraction images from single crystals with XDS. Additional software like SFCHECK, Pointless, XDSSTAT and phenix.xtriage are used for automatic decision making. We present the latest developments and features of the program.

40 The HZB MX-BioLab

Gless C, Feiler C, Foerster R, Gerlach M, Hellmig M, Huschmann F, Kastner A, Malecki P, Marbina S, Roewer K, Schmuckermaier L, Steffien M, Weiss M, Wilk P, Hauß T

The HZB MX-BioLab supports the whole workflow from gene to crystal: cell cultivation, protein purification, crystallization and sample preparation. In addition, samples for other biological investigations, e.g X-ray imaging and X-ray microscopy can be prepared. The Biolab is operated by the MX-group to support external and internal users for preparing their biological samples (safety level S1).

41 The SpectroLab for Macromolecular Crystallography

Hauß T, Gerlach M, Weiss MS

Next to the three beamlines for Macromolecular Crystallography (MX) the HZB-MX-group operates the SpectroLab. It is equipped with a micro-spectrophotometer which allows to measure the absorbance of tiny protein crystals in the UV-VIS spectral region.

42 A conserved structural element in the RNA helicase UPF1 regulates its catalytic activity in an isoform-specific manner

Gowravaram M, Bonneau F, Maciej VD, Fiorini F, Kanaan J, Raj S, Croquette V, Le Hir H, Chakrabarti S

The RNA helicase UPF1 exists as two splice isoforms in mammals, which differ only by 11 amino acids within a loop present in a regulatory domain. We show that the two isoforms of UPF1 exhibit differential catalytic activity and explain this by determining the Xray crystal structure of the yet unsolved isoform of UPF1, thereby linking alternative splicing to functional regulation.

43 Crystal structure of the heme-based oxygen sensor AfGcHK

Kolenko P, Skalova T, Stranava M, Man P, Martinek V, Martinkova M, Dohnálek J

The oxygen sensor AfGcHK from the soil bacterium Anaeromyxobacter sp. Fw109-5 consists of an N-terminal globin domain and a C-terminal histidine kinase domain. High-resolution crystal structures of the globin domain associated with the active and inactive state were determined using X-ray crystallography. Conformational changes observed in our crystal structures correspond to the HDX-MS results.

44 Crystal structure determination of porous Metal-Organic Frameworks

Bon V, Krause S, Senkovska I, Weiss M, Kaskel S

High quality datasets were collected on series of highly porous isoreticular MOFs. The solution and refinement of the crystal structures allow us to calculate textural properties such as geometrical surface area, total pore volume and pore size distribution. Moreover, the crystal structures serve as models for molecular dynamic simulation of the switchable properties of this material class.

45 Interaction of NKX2.1 with DNA

Bommer M, Heinemann U

NKX2.1 is a homeodomain transcription factor involved in the development of thyroid, brain and lung epithelium. We show the X-ray structure of the DNA binding domain of NKX2.1 binding to a DNA 12-mer containing the conserved CAAT sequence. Few direct protein side-chain to DNA-base interactions but many water molecules mediate sequence-specific interactions.

46 O_2-tolerant [NiFe] hydrogenase – a fine-tuned machinery

Schmidt A, Kalms J, Szczepek M, Frielingsdorf S, van der Linden P, von Stetten D, Carpentier P, Chatterjee R, Young I, Brewster A, Sauter N, Yachandra V, Orville A, Kern J, Lenz O, Scheerer P

Hydrogenases catalyze the interconversion of hydrogen and are of great interest in the field of renewable energy technologies. Crystal structures of membrane-bound [NiFe]-hydrogenase of R.eutropha wildtype or with multiple substitutions reveal a fine-tuned interplay between several pathways. Due to its high sensitivity towards X-rays, the free-electron laser has been used to gain further insights.

46a X-ray and cryo-EM structural studies of viral hijacking of the Cullin4-RING ligase ubiquitin-proteasome pathway

Banchenko S, Krupp F, Gotthold C, Spahn C, Schwefel D

Lentiviruses use the host's ubiquitination machinery to overcome the effect of cellular defense proteins that inhibit virus replication. In our current studies, we explore these mechanisms, focusing on the SIV Vpr/CRL4 complex by combining different methods, including X-ray crystallography, cryo-electron microscopy (cryo-EM), and proteomics.

47 Structural and Functional Characterization of the Spliceosomal Protein Prpf39

De Bortoli F, Loll B, Wahl M, Heyd F

Prpf39 is a spliceosomal protein associated with the U1 snRNP. It is an essential gene and is differentially alternatively spliced in murine naive and memory T-cells. Here we present the crystal structure of Prfp39 at 3.3 A resolution. The protein is organized as a dimer with three distinct subdomains. We are investigating the impact of dimerization on splicing with dimer disrupting point mutants.

48 Structural Characterization of Bacterial Phytochromes Using Free-Electron Laser and Synchrotron Radiation

Sauthof L, Schmidt A, Szczepek M, Qureshi B, Stevens T, Fernandez Lopez M, Velazquez Escobar F, Buhrke D, Michael N, Koch A, Chatterjee R, Fuller F, Gul S, Young I, Brewster A, Yachandra V, Butryn A, Aller P, Orville A, Kern JF, Krauss N, Lamparter T, Hildebrandt P, Scheerer P

Phytochromes are biliproteins of plants, bacteria and fungi that use light as a source of information to regulate fundamental physiological processes. We investigated structural dynamics of the far-red light absorbing bathy phytochrome as wild-type and mutated form of the bacterium A. tumefaciens. We obtained various crystal structures using the synchrotron radiation and the free electron laser.

49 Rhodopsin G-Protein Specificity –A Prototype for Gαi Binding GPCRs

Kwiatkowski D, Heyder N, Tiemann J, Speck D, Lê Công K, Kleinau G, Hildebrandt P, Szczepek M, Scheerer P

GPCRs transmit extracellular signals to activate intracellular G Proteins. Upon activation GPCRs undergo a conformational change, which allows G Proteins to bind. Structures of rhodopsin bound to G protein derived peptides and Gs bound to the adreno receptor provided structural insight in this interaction. Our studies give new insight into the common recognition mechanism of G proteins by GPCRs.

50 Structural characterization of complexes between of hydroxamate-based inhibitors and human glutamate carboxypeptidase II

Novakova Z, Barinkova J, Ptacek J, Skultetyove L, Pavlícek J, Slusher BS, Majer P, Barinka C

GCPII-specific inhibitors typically consist of a glutamate moiety linked to a zinc-binding group. Structural data describing GCPII interaction with hydroxamates are very limited. We show that complexes between GCPII and hydroxamates reveal unusual positioning of inhibitor in the internal GCPII pocket, markedly differing from the binding mode of prototypical GCPII inhibitors.

51 Electronic structure and surface chemistry of polymeric carbon nitride photocatalysts

Ren J, Petit T, Meng N, Choudhury S, Zhang B, Aziz EF

Since the pioneering work reported in 2009, polymeric carbon nitride (PCN) photocatalysts has drawn interdisciplinary attention. Here, the detailed characterization on surface chemistry and electronic structure, demonstrate that the formation of the oxygen-containing and $-NH_2$ groups in the atomically-thin mesoporous nanosheets is the origin of the enhanced photocatalytic performance.

52 Altering Mid-Gap Acceptor Levels by Morphology Tuning of Boron Doped Diamonds

Choudhury S, Kiendl B, Ren J, Gao F, Nebel C, Arnault J.-C, Girard H, Ekimov E.A, Vlasov I, Larsson K, Krueger A, Petit T

The use of deep UV illumination for photoexcitation of electrons in diamonds with a wide band gap of 5.5 eV presents a major challenge that can be overcome by doping diamond with boron. Boron atoms introduce surface states in the band gap which can be probed by X-ray absorption spectroscopy. Here we show how B induced surface states can be altered by tuning the morphology of the B doped diamonds.

53 X-Ray Absorption Spectroscopy of TiO_2 Nanoparticles in Water Using a Holey Membrane-Based Flow Cell

Petit T, Ren J, Choudhury S, Golnak R, Lalithambika S, Tesch M, Xiao J, Aziz EF

We introduce here the use of a flow cell with a holey membrane to probe nanoparticle in liquid using X-ray absorption spectroscopy with enhanced X-ray transmission in the water window. This method has been applied to TiO_2 nanoparticles in water, and the impact of solvation on both oxygen K-edge and titanium L-edge will be discussed.

54 Molecular species forming at the Fe_2O_3 Nanoparticle – Aqueous Solution Interface

Ali H, Seidel R, Pohl M, Winter B

Applying soft-X-ray photoelectron spectroscopy from a liquid-microjet, we investigate the electronic structure of Hematite nanoparticles in aqueous solution which is aimed at understanding the mechanism of water splitting.

55 Investigations on model intercalation cathodes for improved understanding of alkali ion batteries

Guhl C, Späth T, Fingerle M, Schulz N, Jaegermann W, Hausbrand R

With our research we want to understand and improve battery materials and their stability, which are both related to electronic structure. For this purpose, we measure SXPS and XAS on model systems such as pristine and coated cathodes as well as on solvents adsorbed on these electrodes.

56 Electronic structure of intercalated MXene: towards next generation supercapacitor

Al-Temimy A, Anasori B, Choudhury S, Ren J, Gogotsi Y, Petit T

MXenes are a new class of 2D materials consisting of transition metals carbides demonstrated extraordinary features for electrochemical energy storage. The impact of intercalation of urea between the MXene planes and the effect of aqueous dispersion on their electronic structure is studied. Correlation with the electrochemical properties of MXene-based supercapacitor has been investigated.

57 Electronic Structure Study of Manganese Oxide Nanoparticles Catalysts Probed by XAS and RIXS

Shaker MN

MnO_x nanoparticles (NPs), generated by laser ablation play the role of the catalyst in the water oxidation reaction. These NPs were characterized by DLS, EDX, and SEM and their catalytic activity was studied. To explore the influence of the quantum size effect on the electronic structure, XAS and RIXS at Mn L-edges and O K-edge were studied. This study will provide more insights into catalysis.

58 A novel electrochemistry flow cell for operando soft X-ray scattering experiments on 3d transition metal oxide based catalysts

Tesch MF, Bonke SA, Shaker MN, Jones TE, Xiao, J, Hocking, RK, Simonov AN

We present a novel flow cell design for soft X-ray scattering experiments optimized for electrochemistry. Operando soft X-ray scattering enables to obtain information about valence electronic processes like charge transfer in 3d transition metal oxides based catalysts. Experimental and theoretical soft X-ray spectroscopic results are presented for MnO_x and an outlook for future studies is given.

58a Introducing bulk-sensitive total-ion-yield detection for X-ray absorption spectroscopy in liquid cells

Schön D, Golnak R, Tesch MF, Winter B, Velasco-Velez J-J, Xiao J

During an electron yield process ions are a relaxation product too leading to ion yield for X-ray absorption detection. The measured currents in a liquid cell exhibit characteristic absorption edges as a function of excitation energy. The so termed total ion yield (TIY) also produces an undistorted Fe L-edge XA spectrum, indicating its promising role as detection method for XAS.

58b Detection of the electronic structure of iron-(III)-oxo oligomers forming in aqueous solutions

Seidel R, Kraffert K, Kabelitz A, Pohl M, Kraehnert R, Emmerling F, Winter B

We conducted systematic photoelectron-spectroscopy measurements from a liquid microjet to investigate the early stages of molecular frameworks of iron oxo complexes relevant in FeO_x nanoparticle formation in aqueous solutions. Different amounts of NaOH were added to a $FeCl_3$ precursor solution to alter the Fe/OH ratio to observe formation of molecular Fe-OH-complexes before precipitation occurs.

59 Hard and Soft X-Ray Spectroscopy Studies of Cobalt-Doped Anatase TiO_2:Co Nanopowders

Mesilov VV, Galakhov VR, Gubkin AF, Yermakov AY, Uimin MA, Zakharova GS, Kvashnina KO, Smirnov DA

Co-doped TiO_2 is one of the most extensively studied oxides for applying as dilute magnetic semiconductors due to its room temperature magnetism. We present results of the studies of TiO_2:Co nanopowders by means of soft X-ray absorption spectroscopy (Ti L2,3 and Co L2,3 spectra), hard X-ray absorption spectroscopy (Co K spectra), and 1s3p resonant inelastic X-ray scattering at the Co K edge.

60 Graphene synthesis via segregation of carbon atoms through metal films on HOPG

Pudikov D, Zhizhin E, Rybkin A, Shikin A

We present the study of graphene growth by segregation process on a cobalt film deposited on HOPG, when carbon atoms under temperature treatment float to the surface and arrange into graphene. It is shown that the mechanism of growth is the same with that observed on Ni and Gd films, but graphene growth starts at 350°C. Moreover, graphene on Co/HOPG has a better-ordered structure than on Ni/HOPG.

61 Measurements of the absorption cross section in the region of NEXAFS C1s-edge by the TEY method

Petrova O, Nekipelov S, Mingaleva A, Shomysv N, Sivkov V

The paper substantiates the applicability of the TEY method to study the distribution of oscillator strengths in the region NEXAFS C1s - absorption edge of nanostructure carbon materials. The results of the absorption cross section spectral dependences and the the oscillator strengths distribution of the fullerite C_{60}, MWCNT, and HOPG are discussed.

62 NEXAFS studies of the 3d-metal-doped bismuth titanate and bismuth niobate

Nekipelov S, Mingaleva A, Petrova O, Zhuk N, Sivkov V

Thermostable solid solutions Mn, Fe, Co, Ni, Cu- doped bismuth titanate and niobate have been investigated by NEXAFS- spectroscopy. Comparison of the obtained spectra with the spectra of the oxides of the 3d-metal allows us to conclude that the atoms of manganese, cobalt, nickel and copper presents mainly in the oxidation state +2, iron - in the +3, and titanium - in the +4.

63 IR Retarders for a Mueller-matrix Ellipsometer at the IRIS Beamline

Schade U, Ritter E, Puskar L, Borondic F, Garcia-Caureld E

The ellipsometer will augment the portfolio of analytical methods at the HZB for the development and evaluation of material systems important to solar cells and solar fuels, to thermoelectric applications and to energy-efficient information technologies such as spintronics.

64 Spectroscopic Ellipsometry on Liquids in the Far Infrared

Schade U, Ritter E, Puskar L, Beckmann J

The ATR ellipsometry technique is for several reasons more attractive than transmittance measurements when optical properties of liquids are studied. We demonstrate in the far infrared that the ellipsometric evaluation of ATR measurements on liquids yield reliable sets of Kramer-Kronig consistent optical constants.

65 Origin of the alpha transition for high-performance ionic polymers

da Silva J, Matos, B, Cao D, Schade U, Puskar L, Fonseca F

Ionic polymers such as Nafion are among the best solid conductors. However, above the alpha transition there is a dramatic drop of the proton conductivity. Better understanding of the alpha transition is necessary for advancing the performance of Polymer Electrolyte Fuel Cells. Infrared spectroscopy is used to investigate the interactions underlying this transition in Nafion.

66 A Synchrotron based Single-Shot Mid-infrared Spectrometer for the Microsecond time regime

Ritter E, Puskar L, Hofmann KP, Hegemann P, Schade U

A novel mid-infrared spectrometer for ‚Single-shot' measurements in the microsecond time regime is currently set-up at the IRIS-Beamline of BESSY II. Its design is based on IR synchrotron light with a dispersive element and a focal plane array detector to investigate irreversible biophysical and biochemical processes. Here we present the setup along with the first commissioning results.

66a Nanoscale Mo/Be/Si Multilayer Structures for EUV Lithography application

Sertsu MG, Schäfers F, Sokolov A, Chkhalo N, Gusev SA, Nechay A, Pariev D, Polkovnikov VN, Salashchenko NN, Svechnikov MV, Tatarsky DA

We fabricate beryllium based multilayer structures for applications in the EUV and soft X rays. The reflectometer facility at the end station of the Optics beamline here at BESSY II offers at wavelength metrology analysis of the multilayers. A record high reflectivities are obtained in the EUV spectral regime for the beryllium based structures.

67 Characterization of bioinspired and biological mineral materials using small and wide angle X-ray scattering

Wagermaier W, Gjardy A, Li C, De Falco D, Schmidt I, Seidt B, Siegel S, Fratzl P

Combining microbeam scanning SAXS/WAXS together with XRF or RAMAN at the BESSY II µSpot beamline allows the characterization of structure and composition of (i) the osteocyte network of bone, (ii) changes in polymer-metalfluoride particle composites during in-situ tensile testing and of (iii) bioinspired crystal calcium carbonate microlens arrays.

68 Tissue structural variability in quantitative synchrotron X-ray fluorescence micro-imaging: the impact and correction schemes

Surowka AD, Töpperwien M, Wrobel P, Bernhardt M, Nicolas JD, Osterhoff M, Salditt T, Marzec M, Adamek D, Szczerbowska-Boruchowska M

To address tissue structural variability in quantitative synchrotron X-ray fluorescence micro-imaging (SRXRF), we proposed two distinct approaches utilizing either the intensity of incoherently scattered X-rays or the phase shift in a sample. We proposed either sole SRXRF (mySpot beamline, BESSY II, HZB) or the combined SRXRF and X-ray Phase Contrast imaging (P10 beamline, PETRA III, DESY).

69 Fish (Pike) have evolutionary advanced damage resistant bones with layered lamellae different from mammal bones

Sauer K, Shahar R, Zizak I, Rack A, Zaslansky P

Bones without osteocytes in evolutionary advanced teleosts such as the fresh water Pike (Esox Lucius), function without containing the classical (e.g. human) bone cells. These cells are considered essential for upkeep i.e. re/modelling and healing. Our material investigations reveal intricate collagen and mineral motifs appearing to circumvent damage, allowing these bones to be long lasting.

70 In situ PXRD monitoring of a mechanochemical cocrystal formation in milling jars of different material

Kulla H, Becker C, Casati N, Paulus B, Rademann K, Emmerling F

We present an in situ PXRD investigation of the mechanochemical cocrystal formation of pyrazinamide with pimelic acid in two milling jar materials. In the steel jar a polymorph transformation presenting an exception of Ostwald's rule of stages is observed.

71 In situ investigation of mechanochemical syntheses of transition metal phosphonates

Akhmetova I, Wilke M, Emmerling F, Rademann K

The mechanochemical synthesis of different manganese phosphonates was followed in situ by synchrotron XRD in order to gain insight in the reaction pathways. Nitrilotis(methylenephosphonic acid) and N,N-Bis(phosphonomethyl)glycine were chosen as ligands. The liquid-assisted grinding process can be divided into three steps, including an amorphous stage.

72 In situ monitoring of a mechanochemical Knoevenagel condensation

Haferkamp S, Fischer F, Krauß L, Emmerling F

We present in situ investigations on the mechanochemical Knoevenagel condensation by combined X-ray diffraction and Raman spectroscopy. The milling process was performed under solvent-less conditions.

73 S2XAFS: A new set-up for time and spatially-resolved X-ray Absorption spectroscopy in a single shot.

Kulow A, Guilherme Buzanich A, Radtke M, Reinholz U, Riesemeier H, Streli C

With this new setup both time- and spatially resolved X-ray absorption information is obtained simultaneously. A primary broadband beam passes through the sample and is diffracted by a convexly bent Si (111) crystal. The divergent beam is collected by an area sensitive detector, in a θ-2θ-geometry. The bending behavior of the crystal surface was investigated experimentally and via computer simulations.

74 The core of things: A 3D imaging study of internal defects in post & core restorations of root-canal treated teeth

Prates Soares A, Ote P, Bitter K, Zaslansky P

Extensive dental restorations may present structural defects that lead to treatment failures. High quality PCE-CT 3D images (BAMline, BESSY) from post and core restorations in ex-vivo treated teeth showed us a large amount of voids and delaminations. Such information is vital to be able to use materials-engineering physical methods to improve both materials and clinical treatment procedures.

74a Distinguishing characteristic defect in additively manufactured Ti-Al6-V4 with synchrotron X-ray refraction radiography

Laquai R, Müller BR, Kasperovich G, Haubrich J, Requena G, Bruno G

Synchrotron X-ray refraction radiography (SXRR) is proven to identify different kinds of defects in Ti-Al6-V4 samples produces by selective laser melting. Namely, these defect types are empty pores and unprocessed powder, which are characteristic to the regions above and below the optimal laser energy density, respectively. Furthermore, SXRR detects small defects below the spatial resolution.

75 In-operando Synchrotron X-Ray and Neutron Radiography Studies of Polymer Electrolyte Membrane Water Electrolyzers

Arlt T, Höh M A, Kardjilov N, Manke I, Fritz D L, Ehlert J, Lüke W, Müller M, Lehnert W, Banhart J

PEM water electrolysis cells were studied using in-operando radiography, revealing insights into the gas-water distribution. The gas amount was quantified, revealing that the ratio of gas to water inside the channels decreases for an increasing water flow rate on the anode side. It is demonstrated that imaging is suitable to study gas/water two-phase flow in running electrolysis cells.

76 Synchrotron-based absorption edge tomography for 3D characterization of the microstructure of Mg-Y-Zn alloys

Gollwitzer C, Cabeza S, Garces G

Absorption edge tomography exploits the sudden change of the attenuation coefficient across the absorption edge of an element. Here, a non-destructive, three-dimensional characterization of the microstructure of a high strength Mg-Y-Zn alloy containing long period stacking ordered (LPSO) phases is performed at the synchrotron beamline BAMline at BESSY II with the microtomograpy setup of BAM.

77 Effects of Compression on Water Distribution in Gas Diffusion Layer Materials of PEMFC in a Point Injection Device by means of Synchrotron X-Ray Imaging

Ince UU, Markötter H, George MG, Liu H, Ge N, Lee J, Alrwashdeh SS, Zeis R, Messerschmidt M, Scholta J, Bazylak A, Manke I

This study investigates water distribution in gas diffusion layer (GDL) materials used for PEM fuel cells based on ex-situ measurements with a point injection device. By synchrotron X-Ray imaging, radial displacement of water agglomerations respective to the injection point, thereby through plane water transport in similar GDL samples compressed to different thicknesses are revealed.

78 Absorption edge sensitive radiography and tomography of Egyptian papyri

Arlt T, Manke I, Baum D, Hege H-C, Lindow N, Lepper V, Menei E, Siopi T, Mahnke H-E

To get access to one of the best sources of knowledge about our cultural origin, we aim at uncovering the text in folded ancient papyri. While the majority, especially the old scripts, have been written with carbon ink, for which a tomographic approach is still under investigation, even in papyri written with “metal ink”, e.g., iron gall, the contrast may not be sufficient for text reconstruction. We utilized the absorption edge to successfully increase the sensitivity.

79 Optical constants in the VUV spectral range by angle-dependent reflectometry and ellipsometry

Wiese K, Gottwald A, Siefke T, Kroker S, Esser N

For the vacuum-ultraviolet spectral range the existing data base for optical constants is rather short and/or were not generated in a metrological manner and thus it is also not possible to reasonably compare different data sets. We use reflectometry (change of amplitude) and ellipsometry (change in phase) to determine and validate optical constants provided with a sound uncertainty budget.

80 Nano jewelry: hybrid systems made of diamondoids and noble metals

Bischoff T, Röhr MIS, Knecht A, Merli A, Petersen J, Mitric R, Lau T, von Issendorff B, Möller T, Rander T

We synthesized hybrid systems consisting of small cationic gold and silver clusters and adamantanethiol using a collision cell. The hybrid clusters were stored in a linear ion trap and their absorption was studied via both photodissociation and ion yield spectroscopy. This approach utilizes a combination of synchrotron (U125/2 10M NIM beamline) and laser radiation (in-house OPO laser system).

81 Optical properties of small cationic aluminium clusters and (Al_7)-(1-adamantanethiol) hybrid systems

Knecht A, Lisinetskaya P, Bischoff T, Stolz M, Ußling F, Merli A, Möller T, Zamudio-Bayer V, Hirsch K, Lau JT, von Issendorff B, Röhr MIS, Mitric R, Rander T

Small aluminium clusters are interesting candidates for plasmon resonances on the molecular level. Al_n^+, n=6-10, and (Al_7)-(1-adamantanethiol)$^+$ hybrid clusters are generated and studied with partial ion yield spectroscopy at beamline U125-2 10m-NIM in the energy range 5-10eV.

87 2D growth mode and the crystal structure of homoepitaxial (100)-oriented beta-Ga_2O_3

Zongzhe C, Michael M, Zbigniew G, Achim T

Our work focuses on the analytics of (100)-oriented beta-Ga_2O_3 homoepitaxy as grown by MBE. It is revealed by the growth happens in a 2D mode accompanied by a (1x1) surface reconstruction. The crystal structure of the thin film shows a high quality and matches coherently with the substrate underneath. There is a high density of stacking faults and twin domains found in the layers by ex-situ TEM.

88 Ordered structure of Ge_2Fe arising during solid phase epitaxy

Jenichen B, Hanke M, Gaucher S, Herfort J, Kirmse H, Willinger E, Willinger M, Huang X, Heil T, Trampert A

Fe_3Si/(Ge,Si)Fe/Fe_3Si thin film stacks were grown by MBE and solid phase epitaxy. The (Ge,Si)Fe films have a well oriented, layered tetragonal Ge_2Fe P4mm structure. This kind of structure does not exist as a bulk material, it is stabilized by the solid phase epitaxy of Ge on Fe_3Si.

89 Industrial access and use at BESSY II

Boin M, Weiss M, Genzel C, Klaus M, Lörgen M, Manke I, Vollmer A

About 50 beamlines at BESSY II are available allowing for wavelength, polarization and energy adjustments such that spatial resolutions down to the nm-range and in-sights into the dynamics of ultrafast reactions are possible. Besides the scientists BESSY II attracts industrial users who appreciate the know-how of the beamline experts and the large-scale equipment for its exceptional reliability.

90 Early oxidation and sulfidation of high temperature alloys: An EDXRD in-situ study

Falk F, Menneken M, Stephan-Scherb C

P92 is an important steel for super heater tubes used in combustion plants. However, the formation of oxides and sulfides are challenging the material. To understand early corrosion mechanisms, important for process prediction, high temperature in-situ ageing experiments of Fe-Cr-Mn alloys in SO_2 and SO_2+H_2O atmosphere were performed, applying energy dispersive X-ray diffraction (EDXRD) analysis.

91 The Influence of the Support Structure on Residual Stress and Distortion in SLM Inconel 718 Parts

Mishurova T, Cabeza S, Thiede T, Nadammal N, Kromm A, Klaus M, Genzel C, Haberland C, Bruno G

The effect of support structure and of removal from the base plate on the residual stress state in SLM IN718 parts was studied by means of synchrotron X-ray diffraction. High tensile residual stress values were found, with pronounced stress gradient along the hatching direction. We conclude that the use of a support decreases stress values but stress relieving heat treatments are still needed.

92 A comprehensive study of the new transparent conductive oxide $MgGa_2O_4$ by Angle Resolved Photoemission Spectroscopy: electronic structure, band bending and ab initio modelling

Thielert B, Janowitz C, Titze F, Galazka Z, Mulazzi M

The electronic band dispersion of $MgGa_2O_4$, a wide band-gap transparent metal oxide was measured by ARPES, compared to ab initio calculations and an excellent agreement was found. Angle-dependent measurements of the Ga 3d core levels were done to determine the band bending depth dependence, the effective Debye length and the carrier concentration, very important information for device fabrication.

99 In situ studies of the reactivity of Bi_2Te_3 and Sb_2Te_3 single crystals towards molecular oxygen

Sirotina AP, Volykhov AA, Knop-Gericke A, Yashina LV

In situ studies of the reactivity of Bi_2Te_3 and Sb_2Te_3 single crystals towards molecular oxygen at partial pressures in the range 0.0275 mbar - 0.5 mbar. Bi_2Te_3 and Sb_2Te_3 oxidation mechanism was proposed. The influence of the excitation of oxygen molecules by X-ray radiation on the oxidation mechanism in in situ experiments, which leads to missing of induction period of reaction, was discovered.

100 Fundamentals of Electrochemical Interfaces: Operando-, Cryo- and Post-Operando PES

Fingerle M, Mayer T, Calvet W, Jaegermann W, Mom R, Knop-Gericke A, Starr D, Smykalla L, Favaro M, van de Krol R

BMBF InnoEMat “Fundamentals of Electrochemical Interfaces” joins German institutes. At the Institute of Materials Science TU Darmstadt, cryo- and post-operando PES on model systems reveals elemental charge-transfer processes at the semiconductor/electrolyte interface. At the Fritz-Haber-Institute operando-PES is conducted on metal/electrolyte interfaces. At HZB, operando studies on oxide/electrolyte interfaces are pursued by AP-HAXPES.

102a Electronic structure of $LiCoPO_4^-$ and $LiNiPO_4^-$ liquid electrolyte interfaces: the surface reactivity and the interface stability under charging potential.

Cherkashinin G, Eilhardt R, Jaegermann W

The chemical compatibility of carbon-free olivine-$LiCoPO_4$ and $LiNiPO_4$ thin film cathode materials towards $LiPF_6$/DMC/FEC liquid electrolyte was studied by using quasi in-situ SXPS, Co L-, Ni L-, O K-XANES. The materials are compatible with the electrolyte. However, the stability of the interfaces under a high charging potential depends strongly on the preparation conditions of $LiCoPO_4$ and $LiNiPO_4$.

102b KREIOS 150 - Next Generation ARPES Instrument for Advanced Materials Research: Graphene on TMDs

Wietstruk M, Böttcher S, Förschner F, Dedkov Y S, Fonin M

The SPECS KREIOS 150 is a next generation photoelectron spectrometer with unprecedented capabilities in combining spatial resolved PEEM with high resolution ARPES measurements. Here we show results from the first measurements with the KREIOS at UE56/2 of graphene on various substrates. On Gr/$NbSe_2$ we show the advantages of using a PEEM lens in combination with a hemispherical analyzer for μ-ARPES.

102c Electronic structure of the non-polar GaN(10-10) surface

Franz M, Appelfeller S, Eisele H, Ebert Ph, Dähne M

Using angle resolved photoelectron spectroscopy, we studied the electronic structure of GaN(10-10) cleavage surfaces and mapped the dispersion of the occupied, N derived surface state. It is found close to the valence band maximum, in contrast to the empty, Ga derived surface state, which is found 2.3 eV higher inside the fundamental band gap, as determined from the measured Fermi level position.

103 Photoactivity and Structural Study of Cu- or Fe-doped $BiVO_4$ Photoanodes

Xi L, Bian J, Xiao J, Tesch M, Drevon D, Schellenberger M, Ellmer K, van de Krol R, Lange KM

Solar water splitting is a potentially scalable method to store solar energy. $BiVO_4$ is a promising materials for the generation of H_2 gas from water. The performance can be improved by Cu-/Fe-doping. The photocatalytic performance can be further improved by electrodepositing a thin layer of MnPi or CoBi. The electronic structure of bare and doped films using ex/in-situ soft XAS is investigated.

104 Decoupling of graphene/substrate interaction by intercalation of gold investigated by polarization spectroscopy

Jansing C, Mertins H-C, Gilbert M, Krivenkov M, Rader O, Gaupp A, Sokolov A, Wahab H, Timmers H

We present polarization measurements at the C 1s edge of graphene on Co and Ni. Graphene/Co(Ni) shows a strong interaction with the substrate while by intercalating Au in the graphene/Co(Ni) system a clear reduction in the bonding strength is achieved. Polarization spectroscopy is the perfect tool for this task due to its high sensitivity to orientation of bonding between graphene and substrate.

105 SXPS studies of the interaction of aqueous electrolytes with $GaInP_2$(100) surfaces

Lebedev MV, Hajduk A, Kaiser B, Jaegermann W

$GaInP_2$ is important material for solar water-splitting devices. To understand related chemical processes, interaction of $GaInP_2$ surfaces with different aqueous solutions is studied. Interaction with pure water was considered in emersion and adsorption experiments. It was found that H_2O adsorbs dissociatively. In addition, the emersion from acidic (H_2SO_4) and alkaline (KOH) solutions was studied.

106 Reactivity of CO on Sulfur-Passivated Graphene-Supported Platinum Nanocluster Arrays

Düll F, Bauer U, Späth F, Bachmann P, Steinhauer J, Steinrück H-P, Papp C

Platinum nanocluster arrays grown on the graphene Moiré on Rh(111) are model systems for catalysis. Sulfur is a poison for many catalysts. We investigated the effects of sulfur on the adsorption and desorption of the probe molecule CO on graphene-supported Pt nanocluster arrays. We observed preferential blocking of step-like binding sites and a site exchange of CO and S during heating.

106a Tuning the Spin-Crossover Behavior of an Fe(II) Complex on a Graphite Surface by Methyl Groups

Bernien M, Ossinger S, Britton A. J, Arruda L. M, Nickel F, Naggert H, Luo C, Ryll H, Radu F, Tuczek F, Kuch W

To maintain the bistability of spin-crossover (SCO) molecules when adsorbed on surfaces is of interest in view of their potential application in molecular spintronics. We investigate the effect of methyl substitution on the thermal and light-induced SCO properties of $[Fe(H_2B(pz)_2)_2phen]$ on a highly oriented pyrolytic graphite surface using x-ray absorption spectroscopy.

106b Magnetic properties of ferrimagnetic $DyCo_5$ film

Luo C, Radu F, Ryll H

We report on XMCD and XMLD measurements of ferrimagnetic $DyCo_5$ single layer. Slightly above its compensation temperature, an exchange-bias-like effect is observed. Its origin is because the bulk magnetism is dominated by the Co while the surface magnetism is dominated by the Dy, which is proved by directly observing the out-of-plane domain wall between the surface and bulk via XMLD.

107 Resonant Soft X-Ray Scattering Ferromagnetic Resonance in the chiral magnet Cu_2OSeO_3

Pöllath S, Aisha A, Luo C, Ryll H, Radu F, Back CH

We report on X-ray Ferromagnetic Resonance (X-FMR) in scattering geometry in the skyrmion hosting chiral magnet Cu_2OSeO_3. Using a detector system which provides vertical and horizontal scanning capability mounted within the magnet bore[1], the diffraction patterns of the helical, conical and skyrmion phases are obtained. Through mapping of the magnetic scattering around the forbidden structural (001/2) Bragg peak, in resonant scattering at the Cu L3 edge, we can distinguish[2] and probe individually each of the helical, conical and skyrmion magnetic configurations. The system is excited via microwaves which at the resonant frequencies is directly as magnetic scattering contrast. The measurements were performed at the VEKMAG end station.

108 Enhanced Eu magnetism at the interface between Bi_2Se_3 and EuSe

Prokes K, Luo Ch, Ryll H, Marchenko D, Schierle E, Weschke E, Radu F, Abrudan R, Volobuiev V, Bauer G, Springholz G, Rader O

SQUID magnetometry suggests in the Bi_2Se_3/EuSe system for the field out of plane a small enhancement of the coercivity between TN = 4.8 K and 50 K. The remanent magnetization is very small and amounts to about 0.4 \% of the saturated magnetization. For the in plane configuration no enhancement is observed. XMCD on Eu M4,5 edges confirms a divalent configuration of the Eu but fails to identify unambiguously above TN a stable magnetic moment.

109 UNIFIT 2018 - the Improved Spectrum Processing, Analysis and Presentation Software for XPS, AES, XAS and RAMAN Spectroscopy

Hesse R, Denecke R

The improved software offers the data analysis of RAMAN spectra, too. In order to have more link-ing options for the fit parameters the fit procedures were improved. Two new 3D plots 'XY 3D 45° Colour Profile' and 'XY 3D -45° Colour Profile' were implemented in the batch processing subrou-tines. Now, all fit parameters, the position of the maximum and minimum can be selected.

110 PEAXIS, the new end-station at BESSY II for Q-dependent RIXS and XPS measurements on solids and liquids

Lieutenant K, Schulz C, Xiao J, Hofmann T, Habicht K

PEAXIS (Photo Electron Analysis and X-ray resonant Inelastic Spectroscopy) is a new end-station at BESSY II. In an energy range from 200 to 1200 eV, it combines resonant inelastic X-ray scattering with a continuous wave-vector resolution (Q-RIXS) and angular resolved photo electron spectroscopy (ARPES). PEAXIS is foreseen to foster energy material research at HZB with a focus on thermoelectrics.

111 Dissection of Hexacyanochromate's Electronic Structure Using Experimental and Simulated RIXS

Sreekantan NLS, Berg M, Atak K

The electronic structure of aqueous hexacyanochromate (III) has been investigated by employing RIXS technique at Chromium L-edge and Nitrogen K-edge resonances. The obtained experimental spectra are analyzed by simulating RIXS spectra, using DFT/ROCIS method. The signal integrated PFY-XA spectra are analyzed, revealing metal-ligand bonding, hybridization, and intramolecular charge transfer.

112 The U41-L06-PGM1 beamline for HZB X-ray microscopy at BESSY II

Guttmann P, Werner S, Siewert F, Sokolov A, Schmidt J-S, Mast M, Rehbein S, Häbel C, Jung C, Follath R, Schneider G

We present here the setup of the U41-L06-PGM1-XM beamline, results of metrology measurements of the optical elements installed in the beamline, as well as the higher performance with this new design compared to the old U41-L12-SGM beamline. An extension into the tender X-ray range with the UE32 under development will give access to two new important absorption edges, namely sulfur and phosphorus.

113 Nanoscale X-ray Linear Dichroism: Identifying Chemical Bond Modification upon Phase Transformation in TiO_2 Nanoribbons

Guttmann P, Krüger P, Sluban M, Umek P, Bittencourt C

Titanium dioxide in the TiO_2-B phase is a promising anode material for lithium ion batteries. Using nanoscale NEXAFS we studied the structural and electronic changes between nanoribbons in TiO_2-B and the thermodynamic stable anatase phase. Strong linear dichroism is observed in single nanoribbons, reflecting preferential O-2p to Ti-3d bond orientation in the low symmetry crystal structures.

114 3D nanoparticle organization in the cellular ultrastructure from cryo X-ray tomography

Drescher D, Büchner T, Živanović V, Szekeres GP, Zeise I, Guttmann P, Werner S, Schneider G, Kneipp J

By X-ray tomography, nanoparticles, used as optical probes, of different materials were localized in the cellular ultrastructure. The tomograms indicate that the aggregates differ in size, shape, and interaction inside endosomes. Their intracellular organization can be correlated with their surface using surface-enhanced Raman scattering.

119 Is there ultrafast proton migration in ice?

Richter C, Saak C, Mucke M, Geethanjali G, Lant C, Bidermane I, Leitner T, Björneholm O, Hergenhahn U

We will present experimental evidence for proton migration in competition with the time-scale of Auger decay, after O1s ionization of amorphous ice. To avoid radiation damage, the efficient time-of-flight spectrometers of the COESCA endstation were used.

120 Electronic Configuration and Charge Transfer of Terbium (I, II, III) Ions in Organometallic Ligand Complexes

Timm M, Bülow C, Zamudio-Bayer V, Lindblad R, von Issendorff B, Lau JT

The scope of this contribution is it, to highlight the electronic configuration in organometallic ligand complexes. Therefore, a central Terbium atom will be combined with different carbocyclic ligands in order to form magnetic molecules. By means of XAS and XMCD the electronic ground states will be assigned and it will be shown, that the magnetic moments are robust to the changes by the ligands.

121a In situ X-ray and neutron powder diffraction studies of gas adsorption induced phase transitions in series of flexible MOFs

Krause S, Bon V, Senkovska I, Többens DM, Franz A, Wallacher D, Grimm N, Kaskel S

Recently we discovered a new counterintuitive phenomenon of Negative Gas Adsorption (NGA) in the flexible Metal-Organic Framework (MOF) DUT-49 (DUT – Dresden University of Technology). In the present study, the structural dynamic in the series of flexible isoreticular MOFs with wide-ranging pore system was systematically investigated in the controlled gas atmosphere and temperature conditions.

121b Tuning the ferroelectric domain pattern in (K,Na)NbO_3 strained thin films

Schmidbauer M, Braun D, Kwasniewski A, Hanke M, Schwarzkopf J

Epitaxial growth of (K, Na)NbO_3 strained thin films on (110) $NdScO_3$ substrates leads to the formation of a complex ferroelectric domain pattern which is caused by coexistence of a1a2/MC monoclinic phases. The domain evolution can be controlled by variation of the K content and film thickness. The observed behavior yields a novel pathway for domain engineering and patterning of periodic structures.

122 Ultrafast Dynamics of Spin and Orbital Moments upon Demagnetization in GdFeCo alloys

Hennecke M, Radu I, Abrudan R, Kachel T, Holldack K, Mitzner R, Schüßler-Langeheine C, Tsukamoto A, Eisebitt S

We aim to investigate and reveal the path of angular momentum flow from and into the spin system during ultrafast laser-induced demagnetization and magnetization switching of a ferrimagnetic GdFeCo alloy. Therefore we employ time-resolved XMCD measurements at Femtoslicing facility and magneto-optical sum rules to disentangle the dynamics of elemental spin and orbital moments.

123 Fluence- and photon energy-dependent ultrafast magnetization dynamics in Gd and Tb films and TbGd bilayers

Gleich M, Bobowski K, Lawrenz D, Cagincan C, Pontius N, Schick D, Trabant C, Wietstruk M, Frietsch B, Schüßler-Langeheine C, Weinelt M

We studied the ultrafast magnetization dynamics in lanthanide thin films. In Gd the initial ultrafast demagnetization depends on the pump pulse photon energy ascribed to enhanced spin-flip scattering of non-equilibrated carriers. Due to strong spin-orbit-coupling Tb is more effectively demagnetized than Gd. In contrast we found a significantly reduced ultrafast Gd-demagnetization in TbGd bilayers.

136 Commissioning results of the soft EMIL beamline at BESSY-II

Hendel S, Gorgoi M, Schäfers F, Hävecker M, Lips K, Raoux S

Recently soft x-ray radiation from the UE48-undulator has reached the CAT- and the SISSY-experimental stations. The PGM-beamline has been commissioned and basic parameters such as energy resolution, photon flux and focus size have been determined in the last months. All results are well within expectation. We report on the beamline design, commissioning results and upcoming timelines.

137 Solution-based synthesis of amorphous germanium nano-particles from organogermanium halide precursors

Pescara B, Mazzio KA, Lips K, Raoux S

Germanium (Ge) nanoparticles (NPs) are of interest in many fields, particularly appealing is the size dependence of the NP properties. We investigate a synthetic scheme that combines sulfur with organometallic germanium precursors to form Ge NPs at relatively low temperatures, allowing for an efficient and inexpensive production of amorphous Ge NPs.

138 PINK: tender x-ray beamline for an x-ray emission spectroscopy at BESSY II

Peredkov S, Bauer J, Grotzsch, Pereira N, Wallacher D, Klemme B, Bürger M, Hendel S, Schäfers F, DeBeer S

The PINK beamline will be operated in the 2-10keV energy range that provides access to XAS/XES studies of transition metals ranging from Ti to Cu (Ka,Kb) and Zr to Ag (La,Lb), as well as light elements P, S, Cl, K, Ca. Taking advantage of a von Hamos analyzer to record the entire spectrum simultaneously, we will be able to provide very attractive time resolved 10ms-10s and two color XES measurements.

140 X-ray Crystallographic Screening of a 96-Fragment Library using Thermolysin as a Model for Metalloproteinases: PanDDA Analysis helps to Improve Density Maps and Increase Hit Rates

Magari F, Metz A, Heine A, Klebe G

TLN was used to validate our 96-entry library.Due to autoprotolysis of this enzyme, the active site always contains as cleavage product the Val-Lys dipeptide from the terminus.It was necessary to displace it from the crystals by incubating them with isopropanol. Then, fragments could be soaked using fragment concentrations of up to 100 mM. Autorefinement and PanDDA were used for hits identification.

141 Towards substrate and inhibitor binding studies of rat NTPDase1: establishment of a new crystal form

Richter PK, Stoppe S, Zebisch M, Sträter N

The previously reported structure of nucleoside triphosphate diphosphohydrolase (NTPDase) 1 from Rattus norvegicus was not suitable for substrate or inhibitor binding. The active site is blocked by a loop from a neighboring protein molecule. Hence, NTPDase 1 was engineered by surface entropy reduction. It crystallizes in space group P1 that allows for subsequent ligand binding studies.

142 Insights into the catalytic mechanism of CotB2

Driller R, Janke S, Fuchs M, Christmann M, Brück T, Loll B

Diterpenes are a versatile class of secondary metabolites predominantly derived from plants, fungi and some prokaryotes. Properties of these natural products include anti-tumor, anti-inflammatory, and antibiotic activities. Here we present both the open and closed crystal structure of the bacterial diterpene cyclase CotB2, giving insights into the catalytic mechanism of CotB2.

143 Presynaptic Spinophilin tunes Neurexin signaling to control active zone architecture and function

Driller JH, Muhammad KGH, Reddy S, Holton N, Lützkendorf J, Sigrist S J, Wahl M C, Loll B

Cytoplasmic active zone scaffolds, composed of several conserved multidomain proteins, decorate the presynaptic membrane. The mechanism to assemble and control the size of functional synapses remains to be characterized. Assembly and maturation of synapses depend on trans-synaptic Neurexin and Neuroligin signaling, which is promoted by the regulator Syd-1 at Drosophila neuromuscular synapses.

144 Structural basis of lambda N mediated processive transcription antitermination

Krupp F, Huang YH, Said N, Spahn CMT, Wahl MC

We combind a crystal structure of RNA-protein complex and a cryo-EM structure of Transcription Antitermination Complex to clarify the structural basis of lambda N mediated processive transcription antitermination which was unknown prior this work.

145 Competing out the enemy - efficient cryo-protection using deep eutectic solvents

Wator E, Feiler C, Gerlach M, Weiss M

X-ray crystallography is the major method used in structure determination of biological material. Fragile protein crystals, often difficult to obtain, require a special treatment with a cryo-protectant before they can be used in a diffraction experiment carried out at 100K. Here we show that a deep eutectic solvent mixture can be used as a powerful cryoprotectant in protein X-ray crystallography.

146 Structural studies on the substrate and cofactor binding mode of FAD-dependent monooxygenases

Kratky J, Weiße RW, Heine T, Tischler D, Sträter N

Styrene monooxygenases (SMOs) catalyse the enantioselective epoxidation of styrene and structurally related compounds. They are of interest for the development of new biocatalytical production processes for pharmaceuticals and fine chemicals. Our aim is to improve the substrate specificity and enantioselectivity of SMO for such applications.

147 Facilities for Macromolecular Crystallography at the HZB

Gerlach M, Feiler C, Förster R, Gless C, Hauß T, Hellmig M, Kastner A, Malecki P, Marbina S, Röwer K, Schmuckermaier L, Steffien M, Wilk P, Weiss MS

The MX-group at the HZB operates three beamlines. With more than 570 PDB depositions in 2016, they are currently among the most productive MX-stations in Europe. They feature state-of-the-art experimental stations and ancillary facilities, serving 100 research groups across Europe. BL14.1-2 are equipped with Pilatus detectors and sample changer robots, providing a high degree of automation.

148 Crystal structures of the D444V disease-causing mutant and the relevant wild type human dihydrolipoamide dehydrogenase

Szabo E, Mizsei R, Wilk P, Zambo Zs, Torocsik B, Weiss MS, Adam-Vizi V, Ambrus A

We report the crystal structures of the human (dihydro)lipoamide dehydrogenase (hLADH) and its disease-causing homodimer interface mutant D444V-hLADH at 2.27 and 1.84 Å resolution, respectively. Based on the structural information a novel molecular pathomechanism is proposed for the impaired catalytic activity and enhanced capacity for reactive oxygen species generation of the pathogenic mutant.

149 A case study of addressing bacterial virulence modulation - fragment screening on PA5507 from human pathogenic Pseudomonas aeruginosa

Marbina S, Feiler C, Gerlach M, Huschmann F, Weiss MS

Due to ineffective antibiotic treatments bacterial infections are the annually cause of multimillion deaths worldwide. A fragment screening campaign was carried out to identify drug-binding sites on a potential novel target protein involved in virulence factor production. Modulation of the proteins mode of action would help to combat multidrug resistant human pathogenic Pseudomonas aeruginosa.

150 MXCuBE2 - Next-generation experiment control for macromolecular crystallography experiments at the BESSY II photon source

Hellmig M, Kastner A, Weiss MS

The latest version of MXCuBE has been put into operation on both tunable HZB-MX beamlines. MXCuBE 2 now integrates the interface to the automatic sample changer and the sample-centring functionality into the main control software which strongly improved the reliabiltiy of the beamline operation. Furthermore it provides the basis for the implementation of more complex data-collection protocols.

151 Structure and function of a parasite chitinase with immunomodulatory activity

Balster K, Malecki P, Ebner F, Heuser A, Weiss MS, Hartmann S

The whipworm Trichuris suis produces and excretes a chitinase, which displays immunomodulation in murine airway hyperreactivity model. Structural analysis of the protein reveals a flexible dimer and a unique inter-molecular disulfide bond.

152 Structural and magnetic studies of tris(oxalato)ferrate and tris(oxalato)chromate complexes

Muziol TM, Tereba N, Podgajny R, Wrzeszcz G

We prepared new complexes: $[Cu_2(bpy)_4Fe(ox)_3]NO_3 \bullet H_2O$ (1), $[Fe(bpy)_3]_2[Fe(ox)_3]NO_3 \bullet 10H_2O$ (2), $[Cu(bpy)_3]_2[Fe(ox)_3]NO_3 \bullet 10H_2O$ (3), $[Cu_2(bpy)_4Cr(ox)_3][Cu(bpy)_2Cr(ox)_3] \bullet 7H_2O$ (4), $[Cu_2(phen)_4Cr(ox)_3][Cu(phen)_2Cr(ox)_3] \bullet 20H_2O$ (5), (bpy – 2,2'-bipyridine, phen – 1,10-phentanthroline). In (1), (4) and (5) we observed bridges between paramagnetic ions. Between (1) and (2) a structural conversion occurred.

164c Impact of alkali content on the CdS buffer layer / NaF/RbF post-deposition treated $Cu(In,Ga)Se_2$ absorber interface structure

Bombsch J, Avancini E, Carron R, Garcia-Diez R, Zhang Y, KunzeT, Handick E, Félix R, Buecheler S, Wilks R, Bär M

$Cu(In,Ga)Se_2$ (CIGSe) – based devices are considered to be high-efficient alternatives to silicon-wafer based solar cells. We used HAXPES (HiKE @ KMC-1) to study the impact of NaF/RbF post deposition treatments (PDT) on the chemical and electronic properties of CIGSe as a function of alkali content. Furthermore it was examined, how the formation of the CdS/CIGSe interface was influenced by the PDT.

164d In-situ photoelectron spectroscopy analysis of the impact of annealing on the Ag/In_2O_3:H interface properties

Xiao T, Erfurt D, Félix R, Handick E, Kunze T, Siebert A, Liao XX, Wilks RG, Schlatmann R, Bär M

The chemical and electronic properties of the Ag/In_2O_3:H interface and how they change upon in-situ annealing were investigated by HAXPES. We find a significant diffusion of Ag into the In_2O_3:H layer accompanied with Ag "oxidation". At the same time, the spectral intensity in proximity to the Fermi-level and the Schottky barrier disappears.

165 (De)-sodiation of carbon-coated TiO_2 nanoparticle based sodium-ion battery anodes

Siebert A, Dou X, Félix R, Handick E, Liu D, Garcia-Diez R, Zhang Y, Bombsch J, Kunze T, Wilks R, Buchholz D, Passerini S, Bär M

Carbon-coated anatase TiO_2 nanoparticles are a promising material for high-power sodium-ion battery anodes. During operation (i.e., charging and discharging), TiO_2 is expected to be sodiated and (partially) desodiated. The chemical composition and electronic structure at different states of sodium (de)-intercalation (i.e., at different charge/discharge states) was investigated with HAXPES and XAS.

166 Mechanisms of photoinduced magnetization in PCMO studied above and below charge-ordering transition temperature

Elovaara T, Tikkanen J, Granroth S, Majumdar S, Felix R, Huhtinen H, Paturi P

We report the effect of photonic field on the electronic and magnetic structure of a low bandwidth manganite PCMO. The study confirmed a mechanism how optical excitation directly activates the metamagnetic transition associated with the CMR of PCMO. It was found that producing optical phonons into the lattice could lower the free energy of the FM phase enough to significantly bias the CMR effect.

167 Engineering of anti-site disorder and oxygen vacancies in Sr_2FeMoO_6 thin films

Saloaro M, Angervo I, Granroth S, Liedke M O, Hoffmann M, Adeagbo W A, Palonen H, Huhtinen H, Laukkanen P, Hergert W, Ernst A, Paturi P

Anti-site disorder and oxygen vacancies have been proposed as a key factor improving the properties of SFMO films towards spintronic applications. To introduce a route to engineer these defects, the properties of post-annealed SFMO films has been studied with the HAXPES (HIKE, KMC-1), positron annihilation spectroscopy, magnetic measurements and theoretical calculations.

168 Solar illumination-induced changes in the chemical and electronic structure of perovskite thin-film solar cell absorbers

Liu D, Hartmann C, Rehermann C, Handick E, Félix R, Wilks R, Unger E, Bär M

The chemical and electronic structure of $CH_3NH_3Pb(Br_{0.75}I_{0.25})_3$, $CsPb(Br_{0.75}I_{0.25})_3$, and $CsPb(Br_{0.5}I_{0.5})_3$ perovskite films on FTO were studied using HAXPES before, during, and after solar illumination. We find significant changes in the film properties that seem to depend on cation types (organic vs inorganic) and halide ratio.

170 Investigation of Rechargeable Zn-MnO_2 Batteries with X-Ray Tomography

Osenberg M, Dimitrova I, Hilger A, Kardjilov N, Arlt T, Markötter H, Manke I, Banhart JT

We present in-operando X-ray tomographic investigations of the charge and discharge behaviour of rechargeable Zn-MnO_2 batteries. Changes in the three-dimensional structure of the zinc anode and the MnO_2 cathode material after several charge/discharge cycles were analysed. Results are compared to the behaviour of a conventional primary cell that was also charged and discharged several times.

171 In situ and operando Tracking of Microstructure Degradation of Silicon Anode using Synchrotron X-ray Imaging

Dong K, Markötter H, Sun F, Manke I, Hilger A, Kardjilov N, Banhart J

The internal morphology and structure changes of silicon electrodes during cycling were revealed by operando synchrotron radiography techniques. The combinations of the structure visualization and quantification analysis with electrochemical data are proposed herein, to deeply understand structural degradation mechanisms of silicon particles and improve the overall electrochemical performance.

172 Damage Analysis in Metal Matrix Composites by Synchrotron Radiation Computed Tomography

Evsevleev S, Cabeza S, Mishurova T, Bruno G

The damage evolution after compression tests of two types of MMC, consisting of eutectic $AlSi_{12}CuMgNi$ alloy and reinforced with 15vol% of Al_2O_3 fibers and with 7vol% of Al_2O_3 fibers+15vol% of SiC particles was studied by synchrotron CT. Internal damage at different pre-strain conditions in eutectic Si, intermetallic phases and Al_2O_3 fibers was observed, as well as debonding of SiC particles.

173 2D Nanomaterials With Switchable Pathogen Binding

Donskyi I, Lippitz A, Adeli M, Haag R, Unger WES

Graphene derivatives have shown great promise in the field of pathogen binding and sensing. Due to their diverse applications, they show a variety of activities that range from bacterial adhesion to bacterial resistance. Therefore, domination of the graphene-pathogen interactions is highly relevant for producing 2D platforms with the desired applications.

174 Deposition of a-C:H layers on biopolymer PLA – surface examination

Schlebrowski T, Rouabeh W, Fischer C B, Nefedov A, Weher S

Biodegradable polymers derived from renewable resources become increasingly important these days due to waste and resource problems. A promising candidate is the biopolymer polylactide (PLA). In order to customize this material for various applications it can be coated with amorphous hydrogenated carbon films (a-C:H). Here we show a surface study of differently thick a-C:H coatings on PLA foils.

175 NEXAFS and XPS investigations of a dual switchable rotaxane multilayer

Heinrich T, Hupatz H, Lippitz A, Schalley CA, Unger WES

A multilayer consisting of two different rotaxanes was investigated with different analytical methods. The rotaxanes can be switched with two different stimuli - chemical and photochemical. XPS indicates that our layer-by-layer approach worked and a layer growth with every deposition step is present. NEXAFS showed that both stimuli cause an increase of the multilayer's preferential orientation.

176 Fundamental insights upon the interaction of small molecules with well-defined iron oxide surfaces

Schöttner L, Ovcharenko R, Nefedov A, Wang Y, Voloshina E, Wöll C

The ideal surface of $Fe_2O_3(0001)$ is only consisted of one Fe^{3+}- species. However, after the exposure with atomic hydrogen this surface is composed by epitaxial $Fe_3O_4(111)$ facets as figured out by XPS/NEXAFS and LEED. Last experiments enhanced our generalunderstanding for iron oxide surfaces and confirmed previous results regarding model of water partial dissociation on hematite.

176a Surface Spectroscopic Investigations of Laterally Oriented Azobenzenes on Au(111)

Schlimm A, Strunskus T, Rusch T, Lautenschläger I, Magnussen O, Tuczek F

This project aims at the application of adsorbed photoswitchable molecules as light-driven molecular machines, particularly the controlled transport of nanoscaled objects on surfaces. Therefore we investigated the switching behavior of azobenzenes which are laterally oriented to the surface due to the used platform approach. For this purpose we employed XPS, angle-dependent NEXAFS and STM.

176b Photo-induced linkage of Ruthenium(II) bi-pyridyl complexes on amorphous hydrogenated carbon (a-C:H)

Rouabeh W, Schlebrowski T, Nefedov A, Wehner S, Imhof W, Fischer CB

This work addresses XPS-analysis carried out at HE-SGM-beamline to study a-C:H surface functionalization. The a-C:H film (500 nm) was previously deposited on Si via plasma enhanced chemical vapor deposition (PECVD) and afterwards UV-irradiated in the presence of differently substituted Ru-complexes. This produces mononuclear Ru-photosensitizers covalently linked on the surface.

177 Anomalous surface composition in thin films of a poly (vinyl methyl ether)/polystyrene (PVME/PS) blend

Radnik J, Madkour S, Lippitz A, Schönhals A, Unger W

Highly surface-sensitive X-ray photoelectron spectroscopy at HE-SGM beamline revealed in the outermost region (< 2nm) of thin films (15-65 nm) of PVME/PS blends a relative high amount of PS, whereas in slightly deeper regions PVME was enriched. Such enrichment of PVME in the whole near-surface region was proposed in former investigations based on conventional XPS studies.

178 Plasma polymerized conductive polymer thin films and nanoparticles

Kovacevic E, Pattyn C, Jagodar A, Dias A, Stefanovic I, Hussain S, Strunskus T, Nefedov A, Berndt J

Conducting polymers have a great variety of different applications: super capacitors, antistatic coatings, novel types of biosensors etc. Plasma polymerisation is very suitable for the production of pinhole free layers, strongly adhering to different substrates. This contribution deals with the NEXAFS analysis such ultra (thin) films and the correlation of the material with the plasma properties.

179 Angle oriented analysis of plasma produced free standing graphene and graphene nanowalls

Tatarova E, Dias A, Hussain S, Boulmer-Leborgne C, Pattyn C, Berndt J, Lecas T, Kovacevic E

Free standing graphene and vertically aligned graphene nanowalls were produced in PECVD and microwave plasma processes. This contribution deals with XPS and NEXAFS analysis of such structures (with special emphasis on the angle resolved measurements).

180 Quantitative Chemical Depth-Profiling by Synchrotron-Radiation-XPS: Investigation of SrF_2-CaF_2 Core-Shell Nanoparticles

Hermanns A, Ritter B, Dörfel I, Kemnitz E, Unger WES

SrF_2 nanoparticles can be doped with trivalent earth metal ions such as Eu^{3+} or Tb^{3+} to generate materials exhibiting an intensive red or green fluorescence. A CaF_2 shell increases intensity, fluorescence lifetime and quantum yield. The chemical composition of the nanoparticle core-shell region is investigated by XPS at different excitation energies corresponding to different information depths.

189 A compact and calibratable von Hamos X-Ray Spectrometer based on two full-cylinder HAPG mosaic crystals for high-resolution XES

Holfelder I, Fliegauf R, Kayser Y, Müller M, Wansleben M, Weser J, Beckhoff B

For high-resolution X-ray Emission Spectroscopy (XES), crystal-based Wavelength-Dispersive Spectrometers (WDS) can be applied to characterize nano materials. A novel calibratable von Hamos spectrometer based on two full-cylinder HAPG optics was realized at the PTB. It combines high efficiency with high spectral resolution in a compact arrangement for an energy range from 2.3 keV to 18 keV.

190 In-situ and operando near sulfur K-edge X-ray absorption spectrometry of Li-S battery coin cells

Zech C, Grätz O, Ivanov S, Hönicke P, Kayser Y, Grötzsch D, Stamm M, Bund A, Beckhoff B

Lithium Sulfur (Li-S) batteries are promising candidates for improved batteries offering up to 5 times higher capacity than conventional lithium ion batteries. By means of in-situ and operando near sulfur K-edge X-ray absorption spectrometry recorded during GCPL measurements we could determine the different sulfur species for 8 cycles of a Li-S battery and polysulfides formation could be revealed.

191 Study of selected thin layered samples to validate secondary excitation effects in X-ray fluorescence analysis

Wählisch A, Beckhoff B, Streeck C

This work aims to study the validity of well-known higher-order algorithms in X-Ray fluorescence analysis with selected thin layered samples, consisting of multiple transition metals. The calibrated instrumentation available in the PTB laboratory and the reference-free fundamental parameter approach allow for a direct validation of the computed theoretical intensities with measured intensities.

192 Reference-free X-ray spectrometry for 3D heterogeneous integration technology

Kayser Y, Hönicke P, Hou L, Oppermann H, Reinhardt F, de Wolf I, Beckhoff B

The 3D integration of circuits and devices is a key topics in today's microelectronic industry resulting in an increasing demand for metrology, e.g., reference-free X-ray spectrometry methodologies. Through Silicon Via and interfaces for metal to metal wafer bonding were investigated and the potential to contribute eventually to the metrology for in-line process control measurements demonstrated.

193 Characterization of a compact and calibratable von-Hamos X-Ray Spectrometer based on full-cylindrical HAPG mosaic crystals

Wansleben M, Kayser Y, Holfelder I, Beckhoff B

We present first results of a high-resolution wavelength-dispersive von Hamos spectrometer based on two full-cylindrical HAPG mosaic crystals. The spectral resolution and efficiency are identified as functions of different instrumental parameters and are discussed using different sample systems. A Monte Carlo ray-tracing simulation is used as a validation tool.

194 Quantitative in-depth characterization of nanolayer stacks using a combined reference-free GIXRF-XRR approach

Hönicke P, Beckhoff B

X-Ray Reflectometry is combined with PTB's reference-free Grazing Incidence X-ray Fluorescence, providing a direct access to the mass depositions of the present materials. This allows for a reduction of the degrees of freedom within the combined GIXRF-XRR modeling and thus improves the characterization reliability. This is demonstrated using the example of Al_2O_3-HfO_2 nanolaminate stacks.

195 In situ gas cell for the analysis of sorption behavior of volatile organic compounds on surfaces by using TXRF and XAS

Streeck C, Grötzsch D, Nutsch A, Malzer W, Kanngießer B, Beckhoff B

A novel measuring cell for in-situ metrology of volatile organic compounds and their sorption behavior on different surfaces was developed. The cell is designed for the soft X-ray range (especially C, N, and O) and is constructed for flow-through operation in a high-vacuum chamber. It allows for the analysis of the surface under total reflection geometry with TXRF and XAS.

196 Accurate experimental determination of Gallium K- and L3-shell XRF fundamental parameters

Unterumsberger R, Hönicke P, Colaux JL, Jeynes C, Wansleben M, Müller MS, Beckhoff B

The determination of fundamental parameters (FP) is an important part of the reliable, reference free quantitative X-ray fluorescence analysis (XRF). In order to reduce the uncertainties of the FP, transmission measurements of Ga samples and self-absorption correction have been experimentally determined. In this work, the fluorescence yield of Ga K and L3 was determined with low uncertainties.

CR1 Silica Bilayer Supported on Ru(0001): a Model System for Crystalline to Vitreous Transition and Chemistry in Confined Space

Prieto MJ, Klemm HW, Xiong F, Gottlob D, Menzel D, Schmidt T, Freund H-J

We will show results obtained with the SMART microscope, using in situ XPS, LEED and LEEM. Silica thin films are used as a model system to study crystalline to vitreous transformation. The obtained activation energy (Ea) for the process agrees with the Stone-Wales defect formation. Also, in the study of the effect of confinement on chemical reactions, a lower Ea for water formation is observed.

CR2 All-optical magnetization switching in FeTb alloys

Arora A, Mawass MA, Sandig O, Luo C, Ünal AA, Radu F, Valencia S, Kronast F

All optical helicity dependent switching (AO-HDS) has drawn attention for data storage applications by manipulating the magnetization via laser helicity without any external magnetic field.We spatially resolve the magnetization dynamics in TbFe by PEEM.We show that AO-HDS is a local phenomenon occurring in the vicinity of thermal demagnetization and depends on thermally induced domain wall motion.

PTBb EMPIR MetVBadBugs – Reference-free X-ray spectrometry depth profiling studies on the uptake of antibiotics in multi-resistant bacteria and biofilms

Seim C, Streeck C, Wansleben M, Hornemann A, Kjærvik M, Schwibbert K, Unger WES, Kästner B, Dietrich P, Thissen A, Vorng JL, Beckhoff B

EMPIR project Metrology vs. Bad Bugs aims to provide metrology to quantitatively measure penetration and localization of antibiotics and biocides in bacteria and biofilms. Ongoing reference-free X-ray spectrometry, near-ambient pressure X-ray photoelectron spectroscopy and Fourier-Transform infrared micro-spectroscopy studies on penetration of biocides/antibiotics into biofilms are presented.

PTBc Element sensitive reconstruction of nanostructured surfaces with finite-elements and grazing incidence soft X-ray fluorescence

Soltwisch V, Hönicke P, Kayser Y, Eilbracht J, Probst, Beckhoff B, Scholze F

A Si_3N_4 nanostructure was experimentally investigated with GIXRF and theoretical evaluated with the FE method. Maxwell solvers based on FE are ideally suited for modeling of field intensities for any arbitrary structure. This combined toolset of GIXRF and FE simulations paves the way for a versatile characterization of structured surfaces.

PTBd The fingerprint of the line roughness of gratings in the scattering pattern

Fernández Herrero A, Pflüger M, Scholze F, Soltwisch V

With the shrinking dimensions of the nanostructures the effect of roughness on their total performance has increased in importance. A rapid non-destructive method is needed for their characterization. EUV scatterometry is very sensitive to the imperfections and can be used for the identification of the roughnes contributions, which is essential for the unequivocal determination of the parameters.

Poster Abstracts - Neutron Day at BER II

Friday, 15th of December

1 Quantum Material Core Lab

Siemensmeyer K, Islam N

Offers of the new Quantum Material Core Lab to BER2, BESSY and external users: new material preparation in powder and single crystal form; material analysis, stoichiometry, phase purity, single crystallinity etc.; orientation, shaping and (multiple) mount of crystals for any experimental requirement; temperature, field and pressure dependence of magnetisation, resistivity, specific heat, thermal transport...; a full user support which includes data analysis until publication ready.

2 Influence of Deposition Hatch Length on Residual Stress in Selective Laser Melted Inconel 718

Thiede T, Cabeza S, Mishurova T, Nadammal N, Bode J, Kromm A, Haberland C, Bruno G

The residual stress distribution in IN718 parts produced by Selective Laser Melting was studied by means of neutron diffraction. Two deposition hatch lengths were considered. Neutron diffraction shows bulk stress gradients for all principal components. We correlate the observed stress patterns with the hatch length, i.e. with its effect on temperature gradients and heat flow.

3 Neutron diffraction study of deformation path of a 10M Ni-Mn-Ga magnetic shape-memory alloy single crystal

Chmielus M, Müllner P, Wimpory R

We magneto-mechanically deformed a Ni-Mn-Ga single crystal from one single domain state to another and back as well as 2 mixed domain states. hk0 diffraction pattern showed distinct differences according to deformation history, from single domain patterns to triple domain patterns. Comparing stress-strain and diffraction data a twinning stress increase due to multiple twinning domains.

4 The magnetic state of Dy_2AgIn_3

Kontopou VI, Kosmidou K, Siouris IM, Katsavounis S

The intermetallic Dy_2AgIn_3 adopts a CaIn2-type structure. The magnetic behavior in the temperature range 2 K to 60 K, examined by ND shows neither magnetic nor increase intensity on nuclear peaks. This clearly confirms the formation of a spin glass state below T_f. Refinement of the structural parameters at 60 K, give (a=4.7565(2), c=7.2896 (6) and z= 0.5091).

5 Effect of Mn doping on crystal and magnetic structure of $Bi_{0.85}La_{0.15}FeO_3$

Karpinsky DV, Troyanchuk IO, Sikolenko VV, Efimov V, Silibin MV

The composition $Bi_{0.85}La_{0.15}FeO_3$ is near the morphotropic phase boundary and doping in B- perovskite position with magnetically active Mn ions allows controlling both crystal and magnetic structures. Doping stabilizes the anti-polar orthorhombic structure, the crystal structure of the $Bi_{0.85}La_{0.15}Fe_{1-x}Mn_xO_3$ with $0 < x < 0.15$ contains both the rhombohedral and orthorhombic phases.

6 Neutron diffraction study of $(Ag_xCu_{1-x})ZnSnSe_4$ (ACZTSe)

Gurieva G, Franz A, Schorr S

ACZTSe is considered as potential candidate for photovoltaic applications. Powder samples (x=0, 0.2, 0.3, 0.5) were grown by solid state reaction of the elements. Neutron powder diffraction experiments were performed using fine resolution neutron powder diffractometer E9. The crystal structure of the room temperature modification was clarified as well as cationic point defects were deduced.

7 High Resolution Neutron Diffraction of Li-Isotope Adsorption in Structural and Interlayer Positions of Smectite Clays

Losa-Adams E, Gil-Lozano C, Hoser A, Fairen AG, Davila A, Gago-Duport L

We used neutron diffraction with both, H/D and $^6Li/^7Li$ isotopic mixtures to determine whether Li-isotopes remain at the interlayer positions of smectite clays or migrate to octahedral framework and to evaluate if there is a significant fractionation of the light isotopes. This behavior could make the use of Lithium isotopes useful to understand the extent of aqueous weathering in martian rocks.

8 Crystal structure of oxidized $Pr_{2-x}NiO_4^+$delta with A-site deficiency, explored by powder X-ray diffraction and neutron diffraction

Ning D, Song J, Scherb T, Ruhl R, Schumacher G, Bouwmeester H, Banhart J

We investigated the crystal structure of $Pr_{2-x}NiO_4^+$delta by powder neutron diffraction studies. The in-situ experiments have been carried out across the temperature range of phase transition under various oxygen partial pressure. Split-atom model and dynamic model of oxygen aoms are compared with Rietveld refinement. Both of the refined results are in good agreement with the value measured by TGA.

9 Helicoidal magnetic ordering in $NiMn_{1-x}Cr_xGe$ (x = 0, 0.04, 0.11, 0.18)

Penc B, Hoser A, Baran S, Szytula A

A helicoidal magnetic ordering has been determined for $NiMn_{1-x}Cr_xGe$ from neutron diffraction data (l=4.567 A) in the function of Cr content and temperature. The propagation vector has a form of k = [kx,0,0] where kx decreases from 2/11 (x=0), through 1/6 (0.04), 1/7 (0.11) down to 1/16 (0.18) at 2K. For x=0.18 a change of magnetic order at 150K from helicoidal one to ferromagnetic one is observed.

10 What can we learn using TOF spectrometer NEAT?

Russina M, Günther G, Grzimek V

The scientific demand for in-situ studies of dynamics in nanoscale and biological materials, materials under extreme conditions of magnetic field and pressure, and parametric studies dictate the nessesity for the instrumemnts with higher power and new instrumental options.

11 Lithiation of Silicon – operando investigations using reflectometry

Ronneburg A, Risse S, Trapp M, Cubitt R, Silvi L, Ballauff M

Silicon is a promisung material for energy storage due to its eleven times higher gravimetric charge capacity compared to conventional graphite electrodes. Up to now silicon electrodes suffer from strong capacity fading. Therefore more fundamental research needs to be done. The cycling behavior of a Li-Si-cell was investigated using NR and EIS. Also the Aging behavior of lithiated silicon electrodes in common electrolytes were investigated and a diffusion-like behavior and the formation of a SEI-layer was found.

12 Imaging of Water Distribution and Transport in Fuel Cells by Means of Neutron Imaging

Markötter H, Manke I, Arlt T, Kardjilov N, Kätzel J, Hilger A, Haußmann J, Klages M, Mohseninia A, Kartouzian D, Wippermann K, Schröder A, Sanders T, Banhart J

The water evolution and distribution in fuel cells are studied via neutron imaging. Visualizations and Quantifications of the water amounts in the membrane electrode assembly (MEA) as well as the gas diffusion layer and channel system via radiography and tomography are presented in this poster.

13 Capturing 3D Water Flow in Rooted Soil by Ultra-fast Neutron Tomography

Tötzke C, Kardjilov N, Manke I, Oswald SE

Neutron tomography is a unique non-invasive 3D tool to visualize plant root systems together with the soil water distribution in situ. So far, long acquisition times prevented imaging 3D water dynamics. We drastically reduced the acquisition to 10 s per entire tomogram! For the first time, we could track a water front ascending in a rooted soil column including the subsequent root water uptake.

14 Phase and Texture Evaluation in Dual-Phase Steel by Neutron Bragg-Edge Imaging

Tran VK, Woracek R, Penumadu D, Kardjilov N, Hilger A, Boin M, Markötter H, Tremsin A, Alrwashdeh SS, Al-Falahat AM, Manke I

The availability of suitable characterization techniques for polycrystalline materials is fundamental for the development of new materials, improving manufacturing processes and a better understanding of failure phenomena. The neutron based method “Bragg-edge tomography” is showcased for a TRIP steel that exhibits austenite to martensite transformation after tensile and torsional deformation.

15 First experimental tests of tensorial neutron tomography for quantitative measurements of magnetic vector fields

Hilger A, Kardjilov N, Manke I, Strobl M, Jericha E, Banhart J

Radiography and tomography with polarized neutrons allows for investigation of magnetic vector field distributions in 2D and 3D. We present quantitative 2D investigations and an approach for real 3D vector field (tensorial) tomography. Results from first experiments and from simulations are compared.

16 Influence of MEA design and gas distribution concepts on water distribution and transport inside PEMFCs using neutron imaging

Mohseninia A, Kartouzian D, Markötter H, Sulaiman S, Manke I, Kardjilov K, Scholta J

The effect of different membrane electrode assembly (MEA) designs and gas distribution concepts on water transport in Polymer electrolyte membrane fuel cell is investigated using neutron tomography and radiography. The results demonstrate that employing a relatively thick MEA and using the high resolution cold neutron radiation, unique in-situ information on the humidification inside the MEA can be obtained.

17 Analysis of the porosity of ordered and disordered mesoporous carbons by combining small-angle neutron scattering (SANS) with in-situ phyisorption

Badaczewski F, Felix B, Loeh MO, Pfaff T, Smarsly BM

Porosity of carbons was analyzed by evaluating their SANS patterns at different points of the deuterated para-xylene (DPX) physisorption isotherm. Pore accessibility, presence of voids & relation of porosity to disorder were investigated. Stepwise filling the pores with contrast matching DPX lead to an expected decrease in absolute scattering intensity. Quantitative SANS data analysis is planned.

18 SANS study of pyrite microestructure: the influence of oriented at-tachment on chemical reactivity

Gil-Lozano C, Losa-Adams E, Clemens D, Davila AF, Fairen AG, Gago-Duport L

In this series of experiments with the V16 instrument we have analyzed the scattering behavior from different pyrite microstructures as a way to establish relations between the crystal inhomogeneities and their different chemical reactivity.

Floor Plan of Poster Session – Science Day at BESSY II

Thursday, 14th of December

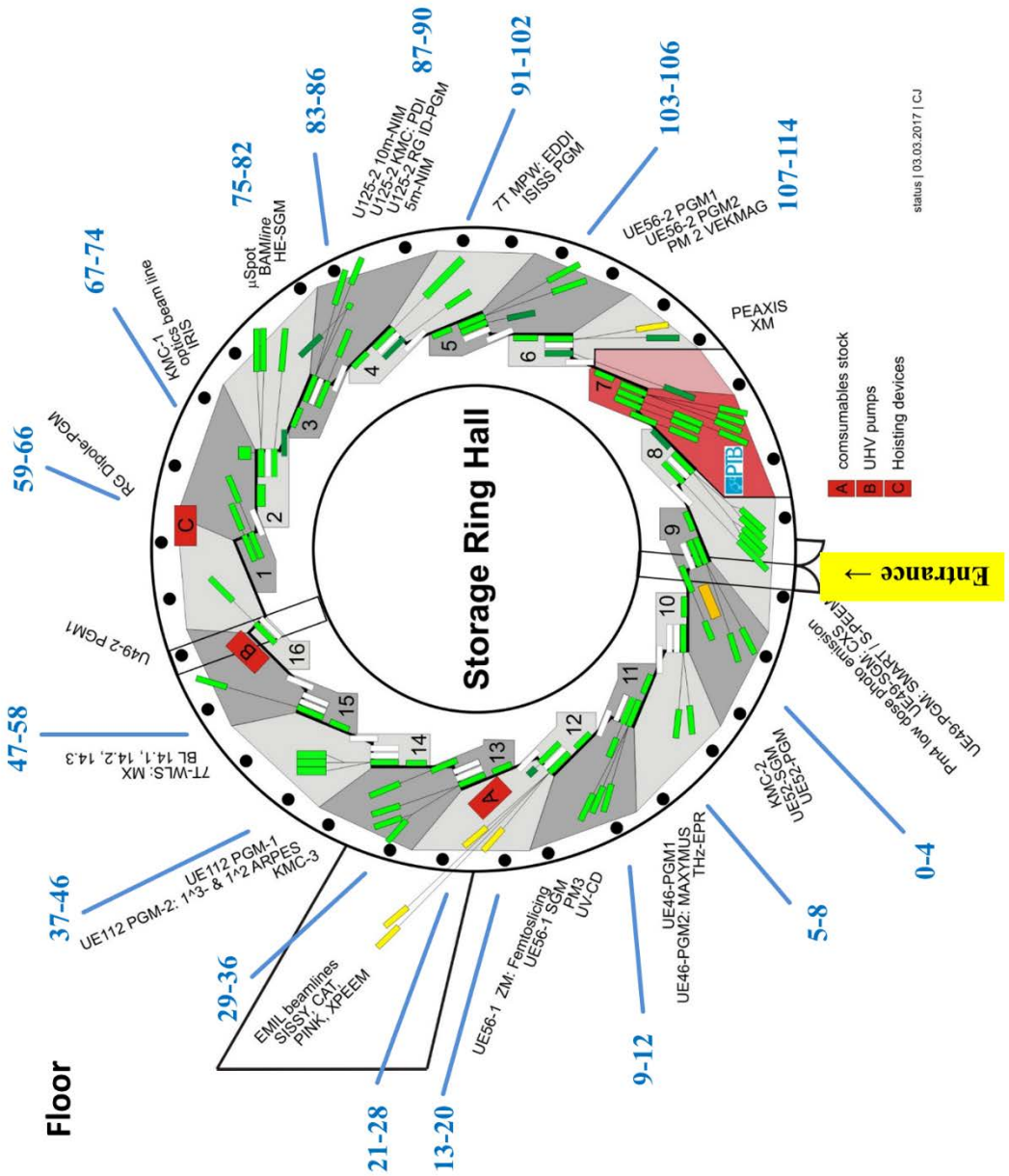

Floor Plan of Poster Session – Science Day at BESSY II

Thursday, 14th of December

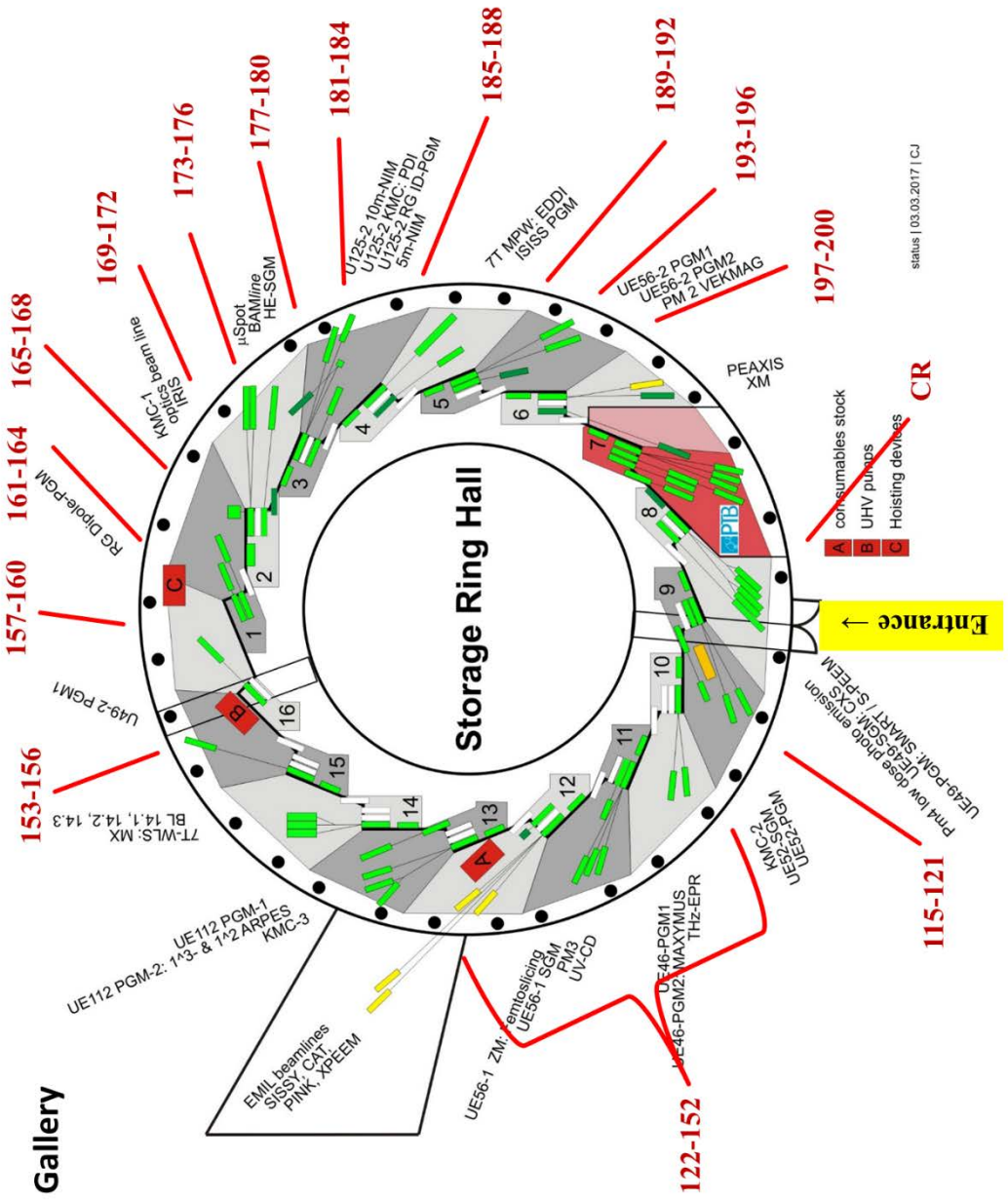

Vendor Exhibition

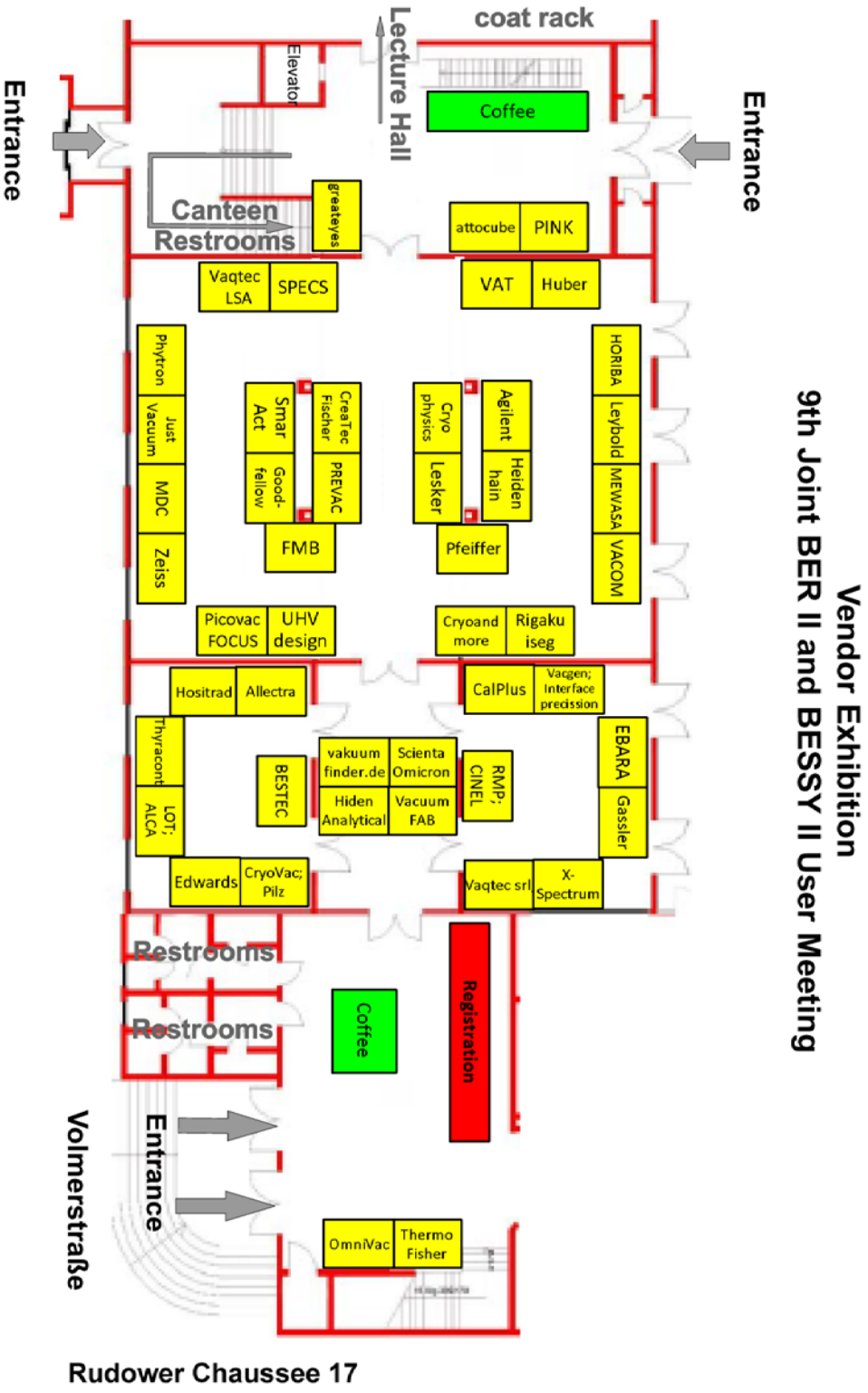

Vendor Logos

Vendor Addresses

Agilent
Lyoner Str. 20
60528 Frankfurt/M., Germany
+49 3514139617
www.agilent.com
johannes.schuricht@agilent.com

ALCA TECHNOLOGY SRL
Via Lago di Garda 130
SCHIO (VI), Italy
+39 3496096784
www.alcatechnology.com
andrea.lanaro@alcatechnology.com

Allectra GmbH
Traubeneichenstr. 62-66
16567 Mühlenbecker Land, Germany
+49 33056415980
www.allectra.com
b.luckscheiter@allectra.com

attocube systems aG
Königinstr. 11a
80539 München, Germany
+49 8928778090
www.attocube.com
julia.sekarev@attocube.com

BESTEC GmbH
Am Studio 2b
12489 Berlin, Germany
+49 3067099211
www.bestec.de
sabine.proll@bestec.de

CalPlus GmbH
Heerstr. 32
14052 Berlin, Germany
+49 4030395950
www.calplus.de
petra.hanold@calplus.de

Carl Zeiss SMT GmbH
Rudolf-Eber-Str. 2
73447 Oberkochen, Germany
+49 7364205971
www.zeiss.com/smt
norman.niewrzella@zeiss.com

CreaTec Fischer & Co. GmbH
Industriestrasse 9
74391 Erligheim, Germany
+49 714396700
www.createc.de
neumann@createc.de

Cryoandmore Budzylek GbR
Fuggerstraße 9a
41468 Neuss, Germany
+49 21316646339
www.cryoandmore.de
denise@cryoandmore.de

Cryophysics GmbH
Dolivostrasse 9
64293 Darmstadt, Germany
+49 615181570
www.cryophysics.de
info@cryophysics.de

Cryovac GmbH & Co KG
Heuserweg 14
53842 Troisdorf, Germany
+49 2241846730
www.cryovac.de
law@cryovac.de

Dr. Gassler Electron Devices
Liststraße 4
89079 Ulm, Germany
+49 73192608941
www.electron-devices.de
gerhard.gassler@electron-devices.de

EBARA Precision Machinery Europe GmbH
Am Promigberg 20
01108 Dresden, Germany
+49 1732641839
www.ebara-pm.eu
olossau@ebara-pm.eu

Edwards GmbH
Ammerthalstrasse 36
85551 Kirchheim, Germany
+49 1606672196
www.edwardsvacuum.com
juliane.garz@edwardsvacuum.com

FMB Feinwerk- und Messtechnik GmbH
Friedrich-Wöhler-Straße 2
12489 Berlin, Germany
+49 3067773057
www.fmb-berlin.de
j.jaehnigen@fmb-berlin.de

FOCUS GmbH
Neukirchner Strasse 2
65510 Huenstetten, Germany
+49 6126401431
www.focus-gmbh.com
d.pohlenz@focus-gmbh.com

Goodfellow
Am Edelspfad 4
61169 Friedberg, Germany
+49 8001000579
www.goodfellow.com
Hildyard@goodfellow.com

greateyes GmbH
Rudower Chaussee 29
12489 Berlin, Germany
+49 3063926237
www.greateyes.de
torsten.wende@greateyes.de

Handelsvertretung Technische Produkte
Brunnenstr. 36a
44623 Herne, Germany
+49 15752990009
www.vacgen.com
dietmar.hallfarth@vacgen.com

HEIDENHAIN
Dr. Johannes Heidenhain Str. 5
83301 Traunreut, Germany
+49 3054705240
www.heidenhain.de
lother@heidenhain.de

Hiden Analytical Vertr. Vacua GmbH
Niedmannweg 13
82431 Kochel am See, Germany
+49 885769301
www.hiden.de
roethlein@hiden.de

HORIBA Jobin Yvon GmbH
Neuhofstr. 9
64625 Bensheim, Germany
+49 6251847520
www.horiba.com/de/scientific
hans-erik.swoboda@horiba.com

Hositrad Deutschland
Lindnergasse 2
93047 Regensburg, Germany
+49 941 55827
www.hositrad.com
andre.kayser@hositrad.com

Huber Diffraktionstechnik GmbH & Co. KG
Sommerstr. 4
83253 Rimsting, Germany
+49 805168780
www.xhuber.com
sg@xhuber.com

Interface Precision Engineering
23-24 Brunel Road
St. Leonards-on-sea
East Sussex, TN38 9RT, United Kingdom
+44 1424850222
jamie.rhodes@interface-precision.com

Iseg Spezialelektronik GmbH
Bautzner Landstr. 23
01454 Radeberg, Germany
+49 351269960
www.iseg-hv.de
maik.donix@iseg-hv.de

JUST VACUUM GmbH
Daimlerstrasse 17
66849 Landstuhl, Germany
+49 6371927600
www.justvacuum.com
matthias.simon@justvacuum.com

Kurt J. Lesker Company
15/16 Burgess Road, Hastings
East Sussex TN35 4NR, United Kingdom
+44 1424458100
www.lesker.com
emilyw@lesker.com

Leybold GmbH
Industriestrasse 10 b
12099 Berlin, Germany
+49 15119772034
www.leybold.com
leander.schulz@leybold.com

LOT-QuantumDesign GmbH
Im Tiefen See 58
64293 Darmstadt, Germany
+49 61518806497
www.lot-qd.com
schreder@lot-qd.de

LSA GmbH Leischnig Automation
Aeusserer Hofring 11
09429 Wolkenstein, Germany
+49 373691720
www.lsa-gmbh.de
s.leischnig@lsa-gmbh.de

MDC Vacuum
Am Rotdorn 39
44577 Castrop-Rauxel, Germany
+49 2305947508
mdcvacuum.com
galthoff@mdcvacuum.de

MEWASA AG
Straubstrasse 11
7323 Wangs, Switzerland
+41 817204882
www.mewasa.ch
t.kuenzler@mewasa.ch

OmniVac
Hertelsbrunnenring 30
67657 Kaiserslautern, Germany
+49 6313110740
www.omnivac.de
h.ruppender@omnivac.de

Pfeiffer Vacuum GmbH
Berliner Str. 43
35614 Asslar, Germany
+49 934296103834
www.pfeiffer-vacuum.com
christiane.kempf@pfeiffer-vacuum.com

Phytron GmbH
Industriestr. 12
82194 Gröbenzell, Germany
+49 8142503163
www.phytron.de
b.mooshofer@phytron.de

picovac
Ziegekhüttenweg 30a
65232 Taunusstein, Germany
+49 61287993336
www.picovac.de
martin.oertel@picovac.de

Pilz-Optics
Enzianstrasse 29
73485 Unterschneidheim-Zöbingen, Germany
+49 79668039609
www.pilz-optics.de
info@pilz-optics.de

PINK GmbH Vakuumtechnik
Gyula-Horn-Straße 20
97877 Wertheim, Germany
+49 9342872142
www.pink-vak.de
npeichl@pink-vak.de

PREVAC
Raciborska 61
44-362 Rogow, Poland
+48 324592000
www.prevac.eu
j.kowalska@prevac.eu

Rigaku Innnovative Technologies Inc.
Indestrasse 109
52249 Eschweiler, Germany
+49 1729347323
www.rigakuoptics. com
paul.pennartz@rigaku.com

RMP Srl
Viale Enrico Ortolani 194
00125 Roma RM, Italy
+39 0652311797
www.rmpsrl.it
m.alessandroni@rmpsrl.it

Scienta Omicron GmbH
Limburger Str. 75
65232 Taunusstein, Germany
+49 6128987361
www.scientaomicron.com
andreas.frank@scientaomicron.com

SmarAct GmbH
Schütte-Lanz-Straße 9
26135 Oldenburg, Germany
+49 441800879942
www.smaract.com
ernzerhof@smaract.com

SPECS Surface Nano Analysis GmbH
Voltastr. 5
13355 Berlin, Germany
+49 304678249336
www.specs.com
Karen.Lueken@specs.com

STRUMENTI SCIENTIFICI CINEL SRL
Viale Dell'Artigianato 14
35010 Vigonza PD, Italy
+39 049725022
www.cinel.com
riccardo.signorato@cinel.com

Thermo Fisher Scientific
Zeppelinstrasse 7b
76185 Karlsruhe, Germany
+49 1795296548
www.alfa.com
norman.fischer@thermofisher.com

Thyracont Vacuum Instruments GmbH
Max-Emanuel-Straße 10
94036 Passau, Germany
+49 851959860
www.thyracont-vacuum.com
karin.schatzberger@thyracont.de

UHV Design Ltd
Judges House, Lewes Road
Laughton, East Sussex BN8 6BN, England
+44 1323811188
www.uhvdesign.com
p.ohara@uhvdesign.com

VACOM Vakuum Komponenten & Messtechnik GmbH
In den Brückenäckern 3
07751 Großlöbichau, Germany
+49 3641427525
www.vacom.de
Franziska.Straubel@vacom.de

Vacuum FAB Srl
Via Asilo 74
20010 Cornaredo (MI), Italy
+39 0290363318
www.vacuumfab.it
paola.beretta@vacuumfab.it

vakuumfinder.de c/o CompoNext GbR
Freiligrathstraße 35
07743 Jena, Germany
+49 3641274190
www.vakuumfinder.de
stine.heitmann@vakuumfinder.de

vaqtec srl
Corso Grosseto 437
10151 Torino, Italy
+39 0110968307
www.vaqtec.com
r.cometti@vaqtec.com

vaqtec-scientific
Thulestr. 18b
13189 Berlin, Germany
+49 3078713158
www.vaqtec-scientific.com
melzer@vaqtec-scientific.com

VAT Deutschland GmbH
Zur Wetterwarte 50, Haus 337/G
01109 Dresden, Germany
+49 1792527586
www.vatvalve.com/
f.petersen@vat.ch

X-Spectrum GmbH
Notkestr. 85
22607 Hamburg, Germany
+49 15731711472
www.x-spectrum.de
vladislav.minukhov@x-spectrum.de

List of Participants

Akhmetova	Irina	irina.akhmetova@bam.de
Al-Falahat	Alaa	alaa.al-falahat@helmholtz-berlin.de
Allenspach	Stephan	stephan.allenspach@psi.ch
Allibon	John	allibon@ill.fr
Al-Temimy	Ameer	ameer.al-temimy@helmholtz-berlin.de
Amrhein	Tim	tim@adrhinum.de
Anselmo	Ana Sofia	ana.anselmo@helmholtz-berlin.de
Arlt	Tobias	arlt@tu-berlin.de
Arora	Ashima	ashima.arora@helmholtz-berlin.de
Arruda	Lucas	l.arruda@fu-berlin.de
Atak	Kaan	kaan.atak@helmholtz-berlin.de
Baczmanski	Andrzej	andrzej.baczmanski@fis.agh.edu.pl
Badaczewski	Felix	felix.badaczewski@gmail.com
Banchenko	Sofia	sofia.banchenko@charite.de
Bär	Marcus	marcus.baer@helmholtz-berlin.de
Barciszewski	Jakub	agent007@man.poznan.pl
Barinka	Cyril	cyril.barinka@ibt.cas.cz
Bergmann	Arno	arno.bergmann@helmholtz-berlin.de
Berrod	Quentin	quentin.berrod@cea.fr
Bidermane	Ieva	ieva.bidermane@helmholtz-berlin.de
Bischoff	Tobias	tobias.bischoff@physik.tu-berlin.de
Bobowski	Kamil	kamil.bobowski@fu-berlin.de
Bock	Tobias	tobias.bock@mdc-berlin.de
Bommer	Martin	martin.bommer@mdc-berlin.de
Born	Artur	artur.born@helmholtz-berlin.de
Brandt	Astrid	brandt@helmholtz-berlin.de
Breternitz	Joachim	joachim.breternitz@helmholtz-berlin.de
Brzhezinskaya	Maria	maria.brzhezinskaya@helmholtz-berlin.de
Buchner	Franziska	franziska.buchner@helmholtz-berlin.de
Bülow	Christine	christine.buelow@helmholtz-berlin.de
Buzanich	Günter	g.buzanich@lla.de
Bykova	Iuliia	bykova@is.mpg.de
Bzheumikhova	Karina	karina.bzheumikhova.ext@ptb.de
Cabeza	Sandra	cabeza@ill.eu
Cao	Dawei	dawei.cao@helmholtz-berlin.de
Chellappan	Rajesh Kumar	rajesh.k.chellappan@ntnu.no
Cheng	Zongzhe	cheng@pdi-berlin.de
Cherkashinin	Gennady	cherk@surface.tu-darmstadt.de
Chernev	Petko	petko.chernev@fu-berlin.de
Chmielus	Markus	chmielus@pitt.edu
Choudhury	Sneha	sneha.choudhury@helmholtz-berlin.de
Christensen	Niels Bech	nbch@fysik.dtu.dk

Ciftyurek	Engin	engin.ciftyuerek@uni-duesseldorf.de
Dambrauskas	Gerardas	gerardas.dambrauskas@lig-nanowise.com
Darowski	Nora	darowski@helmholtz-berlin.de
De Bortoli	Francesca	f.debortoli@fu-berlin.de
de Vasconcelos Emim	Eduardo	eduardo.emim@gmail.com
Decker	Regis	regis.decker@helmholtz-berlin.de
Dedkov	Yuriy	yuriy.dedkov@icloud.com
Deng	Xiujie	xiujie.deng@helmholtz-berlin.de
Dixneit	Jonny	jonny.dixneit@bam.de
Dong	Kang	kang.dong@helmholtz-berlin.de
Donskyi	Ievgen	idonskyi@gmail.com
Dubourdieu	Catherine	catherine.dubourdieu@helmholtz-berlin.de
Dudzik	Esther	dudzik@helmholtz-berlin.de
Efimov	Vadim	efimovvv2006@mail.ru
Ekimova	Maria	ekimova@mbi-berlin.de
Emmerling	Franziska	franziska.emmerling@bam.de
Ershad	Afarin	st140680@stud.uni-stuttgart.de
Faelber	Katja	katja.faelber@mdc-berlin.de
Falk	Florian	florian.falk@bam.de
Felix	Roberto	roberto.felix_duarte@helmholtz-berlin.de
Fernandez Herrero	Analía	analia.fernandez.herrero@ptb.de
Fingerle	Mathias	mfingerle@surface.tu-darmstadt.de
Föhlisch	Alexander	grunewald@helmholtz-berlin.de
Fondell	Mattis	mattis.fondell@helmholtz-berlin.de
Förschner	Felix	felix.foerschner@uni-konstanz.de
Förster	Ronald	foerster@helmholtz-berlin.de
Franz	Alexandra	alexandra.franz@helmholtz-berlin.de
Franz	Martin	martin.franz@physik.tu-berlin.de
Friese	Carmen	carmen.friese@bam.de
Fuhrich	Alexander	fuhrich@fhi-berlin.mpg.de
Gago-Duport	Luis	duport@uvigo.es
Garcia-Diez	Raul	raul.garcia_diez@helmholtz-berlin.de
Gast	Heike	gast@helmholtz-berlin.de
Gaupp	Andreas	andreas.gaupp@helmholtz-berlin.de
Gelen	Ismet	ismet.gelen@fu-berlin.de
Genzel	Christoph	genzel@helmholtz-berlin.de
Gericke	Eike	eike.gericke@helmholtz-berlin.de
Gerlach	Martin	martin.gerlach@helmholtz-berlin.de
Ghazanfari	Mohammad Reza	ghazanfari.mr@gmail.com
Giangrisostomi	Erika	erika.giangrisostom@helmholtz-berlin.de
Giovanni	Ligorio	giovanni.ligorio@hu-berlin.de
Gleich	Markus	gleich@physik.fu-berlin.de
Goerigk	Guenter	guenter.goerigk@helmholtz-berlin.de
Gollwitzer	Christian	christian.gollwitzer@bam.de
Golnak	Ronny	ronny.golnak@helmholtz-berlin.de

Goslawski	Paul	paul.goslawski@helmholtz-berlin.de
Gottwald	Alexander	alexander.gottwald@ptb.de
Grunewald	Christian	christian.grunewald@bam.de
Grüninger	Peter	peter.grueninger@uni-tuebingen.de
Grzimek	Veronika	veronika.grzimek@helmholtz-berlin.de
Guhl	Conrad	cguhl@surface.tu-darmstadt.de
Guilherme Buzanich	Ana	ana.buzanich@bam.de
Gurieva	Galina	galina.gurieva@helmholtz-berlin.de
Guttmann	Peter	peter.guttmann@helmholtz-berlin.de
Habicht	Klaus	habicht@helmholtz-berlin.de
Hackl	Johanna	j.hackl@fz-juelich.de
Haebel	Catharina	catharina.haebel@helmholtz-berlin.de
Haferkamp	Sebastian	sebastian.haferkamp@bam.de
Hanke	Michael	hanke@pdi-berlin.de
Härk	Eneli	eneli.haerk@helmholtz-berlin.de
Hartmann	Claudia	claudia.hartmann@helmholtz-berlin.de
Haumann	Michael	michael.haumann@fu-berlin.de
Hauss	Thomas	hauss@helmholtz-berlin.de
Hävecker	Michael	mh@fhi-berlin.mpg.de
Heinemann	Udo	heinemann@mdc-berlin.de
Heinze	Leonie	l.heinze@tu-braunschweig.de
Hellmig	Michael	michael.hellmig@helmholtz-berlin.de
Hendel	Stefan	stefan.hendel@helmholtz-berlin.de
Hergenhahn	Uwe	uwe.hergenhahn@iom-leipzig.de
Hermanns	Anja	anja.hermanns@bam.de
Hesse	Ronald	rhesse@uni-leipzig.de
Hilger	Andre	hilger@helmholtz-berlin.de
Hoell	Armin	hoell@helmholtz-berlin.de
Hoffmann	Jens-Uwe	hoffmann-j@helmholtz-berlin.de
Hofmann	Tommy	tommy.hofmann@helmholtz-berlin.de
Hofmann	Stephan	sh315@cam.ac.uk
Holfelder	Ina	ina.holfelder@ptb.de
Hönicke	Philipp	philipp.hoenicke@ptb.de
Huang	Yongheng	yhhuang@zedat.fu-berlin.de
Huesges	Zita	zita.huesges@helmholtz-berlin.de
Huhtinen	Hannu	hannu.huhtinen@utu.fi
Huschmann	Franziska	franziska.huschmann@helmholtz-berlin.de
Ilina	Yulia	julia.ilina@gmail.com
Ince	Utku Ulas	utku.ince@helmholtz-berlin.de
Jankowiak	Andreas	andreas.jankowiak@helmholtz-berlin.de
Janowitz	Christoph	janowitz@physik.hu-berlin.de
Jansing	Christine	c.jansing@fh-muenster.de
Jeoung	Jae-Hun	jae-hun.jeoung@hu-berlin.de
Jia	Junqiao	jqjia@zedat.fu-berlin.de
Jung	Christian	christian.jung@helmholtz-berlin.de

Jungwirth	Sebastian	jungwirth@physik.hu-berlin.de
Kascakova	Barbora	barbora.karaffova@gmail.com
Kabelitz	Anke	anke.kabelitz@bam.de
Kakiuchi	Takuhiro	kakiuchi.takuhiro.mc@ehime-u.ac.jp
Karpinski	Dzmitry	dmitry.karpinsky@gmail.com
Kaser	Hendrik	hendrik.kaser@ptb.de
Kastner	Alexandra	alexandra.kastner@helmholtz-berlin.de
Kayser	Yves	yves.kayser@ptb.de
Keiderling	Uwe	keiderling@helmholtz-berlin.de
Kent	Benjamin	ben.kent@helmholtz-berlin.de
Keskinbora	Kahraman	keskinbora@is.mpg.de
Kiefer	Klaus	klaus.kiefer@helmholtz-berlin.de
Kipgen	Lalminthang	kipgen@zedat.fu-berlin.de
Kjærvik	Marit	maritkjarvik@gmail.com
Klaus	Manuela	klaus@helmholtz-berlin.de
Klein	Roman	roman.klein@ptb.de
Klemke	Bastian	bastian.klemke@helmholtz-berlin.de
Klingan	Katharina	katharina.klingan@fu-berlin.de
Kolbe	Michael	michael.kolbe@ptb.de
Kolenko	Petr	petr.kolenko@ibt.cas.cz
Kontopou	Vasiliki-Eirini	vasikont9@pme.duth.gr
Kraus	Werner	w.kraus@bam.de
Krumrey	Michael	michael.krumrey@ptb.de
Kubella	Paul	paul.kubella@fu-berlin.de
Kubin	Markus	markus.kubin@helmholtz-berlin.de
Kuch	Wolfgang	kuch@physik.fu-berlin.de
Kudlinzki	Denis	d.kudlinzki@dkfz.de
Kulla	Hannes	hannes.kulla@bam.de
Kumberg	Ivar	i.kumberg@fu-berlin.de
Kuzkova	Nataliia	nataliia.kuzkova@helmholtz-berlin.de
Kwiatkowski	Dennis	dennis.kwiatkowski@charite.de
Laihem	Karim	karim.laihem@helmholtz-berlin.de
Lake	Bella	bella.lake@helmholtz-berlin.de
Laquai	Rene	rene.laquai@bam.de
Lau	Tobias	tobias.lau@helmholtz-berlin.de
Lauermann	Iver	iver.lauermann@helmholtz-berlin.de
Lebedev	Mikhail	mleb@triat.ioffe.ru
Lee	Jooseop	jl3536@cornell.edu
Legut	Dominik	dominik.legut@vsb.cz
Leitner	Torsten	leitner@helmholtz-berlin.de
Li	Chenghao	chenghao.li@mpikg.mpg.de
Li	Ji	ji.li@helmholtz-berlin.de
Liang	Yanqin	yqliang@zedat.fu-berlin.de
Lindblad	Rebecka	rebecka.lindblad@sljus.lu.se
Linhard	Verena	vlinhard@nmr.uni-frankfurt.de

Lippitz	Andreas	andreas.lippitz@bam.de
Liu	Ying	liuychch@ustc.edu.cn
Loderer	Christoph	christoph.loderer@tu-dresden.de
Loos	Stefan	stefan.loos@fu-berlin.de
Losa Adams	Elisabeth	elosa@uvigo.es
Lubeck	Janin	janin.lubeck@ptb.de
Luo	Chen	chen.luo@ur.de
Maciej	Vincent D.	vincent.maciej@fu-berlin.de
MacQueen	Rowan	rowan.macqueen@helmholtz-berlin.de
Magari	Francesca	magari@staff.uni-marburg.de
Mahler	Willy	mahler@fhi-berlin.mpg.de
Makarova	Anna	aa.makarova@yandex.com
Malecki	Piotr	piotr.malecki@helmholtz-berlin.de
Malliaras	George	gm603@cam.ac.uk
Manzoor	Alina	alina.manzoor@fu-berlin.de
Marbina	Stonia	stonia.marbina@fu-berlin.de
Markelz	Amdrea	amarkelz@buffalo.edu
Markötter	Henning	henning.markoetter@helmholtz-berlin.de
Martins	Berta	berta.martins@hu-berlin.de
Mayer	Thomas	mayerth@surface.tu-darmstadt.de
Mebarka	Gherib	m.gherib@epst-annaba.dz
Mebs	Stefan	stefan.mebs@fu-berlin.de
Medjanik	Kateryna	medyanyk@uni-mainz.de
Melo	Arthur	arthur.melo@mdc-berlin.de
Meng	Siqin	siqin.meng@helmholtz-berlin.de
Menneken	Martina	martina.menneken@bam.de
Mertins	Hans-Christoph	mertins@fh-muenster.de
Mesilov	Vitaly	mesilov@imp.uran.ru
Michalchuk	Adam	adam.michalchuk@ed.ac.uk
Mishra	Aum Niranjana	n.mishra@mailbox.tu-berlin.de
Moberg	Robert	robert.moberg@romoscientific.se
Mohammadi	Mohammad Reza	reza.mohammadi@fu-berlin.de
Muller	Yves	yves.muller@fau.de
Müller	Bernd R.	bernd.mueller@bam.de
Muziol	Tadeusz	tmuziol@chem.umk.pl
Nefedov	Alexei	alexei.nefedov@kit.edu
Nekipelov	Sergey	nekipelovsv@mail.ru
Nibbering	Erik T. J.	nibberin@mbi-berlin.de
Nickel	Fabian	fabian.nickel@fu-berlin.de
Ning	De	de.ning@helmholtz-berlin.de
Niskanen	Johannes	johannes.niskanen@helmholtz-berlin.de
Novakova	Zora	zora.novakova@ibt.cas.cz
Oelsner	Andreas	oelsner@surface-concept.de
Ogor	Oskar	oskar.ogor@ptb.de
Osenberg	Markus	markus.osenberg@helmholtz-berlin.de

Ovsyannikov	Ruslan	ovsyannikov@helmholtz-berlin.de
Palau	Anna	palau@icmab.es
Palmer	Benjamin	benjamin.palmer@weizmann.ac.il
Palm	Rasmus	rasmus.palm@ut.ee
Papp	Christian	christian.papp@fau.de
Parlak	Umut	u.parlak@fz-juelich.de
Pasquini	Chiara	chiara.pasquini@fu-berlin.de
Penghui	Yang	penghui.yang@helmholtz-berlin.de
Peredkov	Sergey	sergey.peredkov@cec.mpg.de
Peschel	Gina	peschel@fhi-berlin.mpg.de
Petit	Tristan	tristan.petit@helmholtz-berlin.de
Pfaff	Torben	torben.pfaff@phys.chemie.uni-giessen.de
Pflüger	Mika	mika.pflueger@ptb.de
Pinto	Haroldo	haroldo@sc.usp.br
Portnichenko	Pavlo	pavlo.portnichenko@tu-dresden.de
Prieto	Mauricio	prieto@fhi-berlin.mpg.de
Prokes	Karel	prokes@helmholtz-berlin.de
Prokhnenko	Oleksandr	prokhnenko@helmholtz-berlin.de
Puskar	Ljiljana	ljiljana.puskar@helmholtz-berlin.de
Radtke	Martin	martin.radtke@bam.de
Radu	Ilie	radu@mbi-berlin.de
Radu	Abrudan	radu-marius.abrudan@helmholtz-berlin.de
Raheem	Azhr	azhr.raheem@helmholtz-berlin.de
Rainer	Fink	rainer.fink@fau.de
Raja Thulasimani	Monika	monika.raja_thulasimani@helmholtz-berlin.de
Rander	Torbjörn	torbjorn.rander@gmail.com
Raoux	Simone	simone.raoux@helmholtz-berlin.de
Rech	Bernd	bernd.rech@helmholtz-berlin.de
Reehuis	Manfred	reehuis@helmholtz-berlin.de
Rehbein	Stefan	rehbein@helmholtz-berlin.de
Reichardt	Gerd	gerd.reichardt@helmholtz-berlin.de
Reichmann	Felix	reichmann@ihp-microelectronics.com
Reinholz	Uwe	uwe.reinholz@bam.de
Ren	Jian	jian.ren@helmholtz-berlin.de
Richter	Mathias	mathias.richter@ptb.de
Riesemeier	Heinrich	heinrich.riesemeier@bam.de
Ritter	Eglof	eglof.ritter@hu-berlin.de
Ronneburg	Arne	arne.ronneburg@helmholtz-berlin.de
Roth	Christina	christina.roth@fu-berlin.de
Rouabeh	Wafa	wafarouabeh@uni-koblenz.de
Röwer	Karine	karine.sparta@helmholtz-berlin.de
Rupp	Axel	rupp-a@helmholtz-berlin.de
Russina	Margarita	margarita.russina@helmholtz-berlin.de
Ryll	Hanjo	hanjo.ryll@helmholtz-berlin.de
Saloaro	Minnamari	minnamari.saloaro@utu.fi

Sauer	Katrein	katrein.sauer@charite.de
Schade	Ulrich	ulrich.schade@helmholtz-berlin.de
Scharf	Oliver	oliver.scharf@helmut-fischer.de
Schavkan	Alexander	alexander.schavkan@ptb.de
Scherb	Tobias	tobias.scherb@helmholtz-berlin.de
Schiwietz	Gregor	schiwietz@helmholtz-berlin.de
Schlebrowski	Torben	schlebrowski@uni-koblenz.de
Schlegel	Moritz-C.	schlegel.moritz@bam.de
Schmidbauer	Martin	martin.schmidbauer@ikz-berlin.de
Schmidt	Ingo	ingo.schmidt@mpikg.mpg.de
Schmidt	Andrea	schmidt.andrea@charite.de
Schmitz	Detlef	schmitz@helmholtz-berlin.de
Schmitz-Antoniak	Carolin	c.schmitz-antoniak@fz-juelich.de
Schmuckermaier	Lukas	lukas.schmuckermaier@helmholtz-berlin.de
Schneider	Gerd	gerd.schneider@helmholtz-berlin.de
Schneidewind	Astrid	astrid.schneidewind@frm2.tum.de
Scholze	Frank	frank.scholze@ptb.de
Schön	Daniela	daniela.schoen@helmholtz-berlin.de
Schorr	Susan	susan.schorr@helmholtz-berlin.de
Schulz	Christian	schulz-c@helmholtz-berlin.de
Schumacher	Gerhard	schumacher@helmholtz-berlin.de
Schüssler-Langeheine	Christian	christian.schuessler@helmholtz-berlin.de
Schütz	Gisela	schuetz@is.mpg.de
Schwarzkopf	Jutta	jutta.schwarzkopf@ikz-berlin.de
Schwefel	David	david.schwefel@charite.de
Seidel	Robert	robert.seidel@helmholtz-berlin.de
Seidlhofer	Beatrix	beatrix-kamelia.seidlhofer@helmholtz-berlin.de
Serrano Munoz	Itziar	itziar.serrano-munoz@bam.de
Shabadi	Vikas	vikas@incienta.com
Shaker	Maryam	maryam.shaker@helmholtz-berlin.de
Shams	S. Fatemeh	sfs.academic@gmail.com
Sikolenko	Vadim	vadim.sikolenko@jinr.ru
Silvi	Luca	luca.silvi@helmholtz-berlin.de
Smekhova	Alevtina	a.smekhova@fz-juelich.de
Spodaryk	Mariana	mariana.spodaryk@epfl.ch
Sreekantan Nair Lalithambika	Sreeju	sreeju.sreekantan@helmholtz-berlin.de
Staier	Florian	florian.staier@helmholtz-berlin.de
Staude	Andreas	andreas.staude@fei.com
Steffien	Michael	michael.steffien@helmholtz-berlin.de
Steigert	Alexander	alexander.steigert@helmholtz-berlin.de
Steinhauer	Miriam	miriam.steinhauer@dlr.de
Strasser	Peter	pstrasser@tu-berlin.de
Stroh	Julia	julia.stroh@bam.de
Strunskus	Thomas	ts@tf.uni-kiel.de
Süllow	Stefan	s.suellow@tu-bs.de

Sun	Fu	fu.sun@helmholtz-berlin.de
Surowka	Artur	asurowka@agh.edu.pl
Svechkina	Nataliya	n.svechkina@fz-juelich.de
Szabó	Eszter	szabo.eszter1@med.semmelweis-univ.hu
Tesch	Marc	marc.tesch@helmholtz-berlin.de
Thiede	Tobias	tobias.thiede@bam.de
Timm	Martin	martin.timm@helmholtz-berlin.de
Többens	Daniel	daniel.toebbens@helmholtz-berlin.de
Tovar	Michael	tovar@helmholtz-berlin.de
Tymen	Simon	simon.tymen@uni-jena.de
Ulm	Gerhard	gerhard.ulm@ptb.de
Unger	Wolfgang	wolfgang.unger@bam.de
Van De Krol	Roel	roel.vandekrol@helmholtz-berlin.de
Vetterlein	Matthias	vito@physik.tu-berlin.de
Viefhaus	Jens	jens.viefhaus@helmholtz-berlin.de
Viktor	Sivkov	svn@dm.komisc.ru
Vogel	Uwe	uwe.vogel@helmholtz-berlin.de
Vollmer	Antje	antje.vollmer@helmholtz-berlin.de
Vyalikh	Denis	denis.vyalikh@tu-dresden.de
Wagermaier	Wolfgang	wolfgang.wagermaier@mpikg.mpg.de
Wählisch	Andre	andre.waehlisch@ptb.de
Wallacher	Dirk	dirk.wallacher@helmholtz-berlin.de
Wang	Weijia	weijia.wang@kit.edu
Wang	Qiankun	qiankun@physik.hu-berlin.de
Wansleben	Malte	malte.wansleben@ptb.de
Wegner	Berthold	berthold.wegner@helmholtz-berlin.de
Weigand	Markus	mweigand@is.mpg.de
Weiss	Manfred	msweiss@helmholtz-berlin.de
Weller	Miriam	weller@atom.uni-frankfurt.de
Wells	Justin	justin.wells@ntnu.no
Wendt	Robert	robert.wendt@helmholtz-berlin.de
Wernet	Philippe	wernet@helmholtz-berlin.de
Werwein	Anton	anton.werwein@uni-leipzig.de
Weyand	Michael	michael.weyand@uni-bayreuth.de
Wiese	Karl	karl.wiese@ptb.de
Wilk	Piotr	piotrek.wilk@helmholtz-berlin.de
Wilkinson	Iain	iain.wilkinson@helmholtz-berlin.de
Wilpert	Thomas	wilpert@helmholtz-berlin.de
Wimpory	Robert	robert.wimpory@helmholtz-berlin.de
Witte	Steffen	steffen.witte@bam.de
Wolfgang	Klesse	klesse@ihp-microelectronics.com
Wollgarten	Markus	wollgarten@helmholtz-berlin.de
Wolter	Bettina	bettina.wolter@helmholtz-berlin.de
Wurzler	Nina	nina.wurzler@bam.de
Xi	Lifei	lifei.xi@helmholtz-berlin.de

Xiao	Jie	jie.xiao@helmholtz-berlin.de
Xiao	Ting	ting.xiao@helmholtz-berlin.de
Zabel	Hartmut	hartmut.zabel@rub.de
Zamudio-Bayer	Vicente	vicente.zamudio-bayer@physik.uni-freiburg.de
Zech	Claudia	claudia.zech@ptb.de
Zhang	Yufeng	yufengzhang@xmu.edu.cn
Zivanovic	Vesna	vesna.zivanovic@hu-berlin.de

Procedures for electing members of the HZB User Committee

The user representatives for the HZB User Committee are elected online by eligible users **via the HZB access portal GATE**:

https://www.helmholtz-berlin.de/user/gate/index_en.html

The voting period for the User Committee 2018 is
02. December 2017 [00:01] – **15. December 2017** [23:59]

Eligible users are defined as users of HZB's large-scale facilities, BER II and BESSY II, who have been actively registered on the HZB access portal GATE as a proposer, co-proposer or user during the three years immediately preceding the election.

All eligible users are informed in advance by email by the User Committee election Committee. In order to be able to vote, the users must be registered in GATE.

List of candidates

Allegretti, Francesco	Technische Universität München, Germany	Physicist Methods: PES, XPD, NEXAFS, XSW, Resonant Auger-Raman Spectroscopy, STM, TPD Areas of interest: organic and oxide thin films, surface-supported low-dimensional nanostructures, determination of adsorbate and surface structure **Photons**
Kovacevic, Eva	GREMI - Université d'Orléans, France	Physicist Methods: NEXAFS, XPS, FTIR Areas of interest: Plasma, thin films, nanostructures, carbon, polymers **Photons**

Procedures for electing members of the HZB User Committee are organized and supervised by an independent election committee consisting of one member of the HZB User Committee, one representative of HZB User Coordination and one representative of the Scientific Director's Office at HZB. The election committee processes the proposals and nominates the final candidates for election.

The members of the current election committee are:

Carolin Schmitz-Antoniak	Forschungszentrum Jülich	Member of the User Commitee
Olaf Schwarzkopf	HZB	Representative of the Scientific Director's Office
Astrid Brandt	HZB	Representative of the HZB User Coordination

Friends of Helmholtz-Zentrum Berlin e.V.

The purpose of the Association of Friends of Helmholtz-Zentrum Berlin includes the support of the development of science and research, especially by the support of scientific activities at BESSY II. The association is a link between HZB and the general public and it shall develop the cooperation between HZB, its friends and sponsors and other national and international institutions. In particular, it is dedicated to support young scientists.

Main activities of the association include the annual bestowals of science awards. In memory of the former scientific director of BESSY, who died in September 1988, the association awards annually the Ernst-Eckhard-Koch-Prize. This prize is given for outstanding Ph.D. theses completed during the current or past year in the field of research with synchrotron radiation and performed at either BESSY II or HASYLAB (Hamburg) as the main places of activities of Ernst-Eckhard Koch. Furthermore, the association bestows the Innovation-Award on Synchrotron Radiation since 2001, which is announced Europe wide for an outstanding technical achievement or experimental method that promises to extend the frontiers of research with synchrotron radiation.

All natural or juristic persons may become member of the association. The regular annual membership fee amounts to 10 € for undergraduate and graduate students, 40 € for other natural persons and, as a rule, 150 € for juristic persons. In its work, the association depends also on donations which can also be addressed with a specific purpose, such as "Ernst-Eckhard-Koch-Prize" (Account-No.: 414 44 40 at the Deutsche Bank AG, BLZ 100 700 00). Fees and donations are enjoying tax privileges.

If somebody else feels associated with Helmholtz-Zentrum Berlin and its circle of friends we kindly ask him to support our activities by becoming a member.

The Board of the Association

An den Vorstand
Freundeskreis Helmholtz-Zentrum Berlin e.V.
Albert-Einstein Straße 15
12489 Berlin
Germany

Tel.: +49-30-8062 - 12901
Fax.: +49-30-8062 - 12920
e-mail: freundeskreis@helmholtz-berlin.de
Internet: http://www.helmholtz-berlin.de/freundeskreis

Mitgliedschaft

Hiermit beantrage ich die Aufnahme in den Verein Freundeskreis Helmholtz-Zentrum Berlin e.V.

Membership

Herewith I apply for admission to the Association Friends of Helmholtz-Centre Berlin

Angaben zur Person / personal data	
	Anrede: / salutation: Nachname: / last name: Vorname: / first name:
	Geburtsdatum: /date of birth: (DD-MM-YYYY) Herkunftsland:/Staatsangehörigkeit: /nationality
	Titel: / title: Berufsbezeichnung: / profession:
Institution / institution	
Name: / name:	
Abteilung: / department:	
Straße: / street:	
PLZ: / zip: Ort: / city: district:	
Land: / country:	
Telefon: / phone: Fax: / fax:	
Homepage: / e-mail: homepage of institution:	

Die jährlichen Mitgliedsbeiträge betragen zur Zeit für natürliche Personen EUR 40,-, für juristische Personen EUR 150,-, EUR 100,- oder EUR 50,-, für Studenten EUR 10,-. / The regular annual membership fees amount to EUR 40,- for natural persons, EUR 150,–/100,-/50,- for legal entities, EUR 10,- for students.

Art der Person: / Character of person: natural person _____ legal entity _____
Mitgliedsbeitrag : / Membership fees: Euro _____

Im Rahmen freiwilliger Höherstufung/ voluntary upgrading: Euro _____

Datum: / date: Unterschrift: / signature:

This page is intentionally left blank for your notes.

This page is intentionally left blank for your notes.

This page is intentionally left blank for your notes.

Helmholtz-Zentrum Berlin
Lise-Meitner Campus
Wannsee

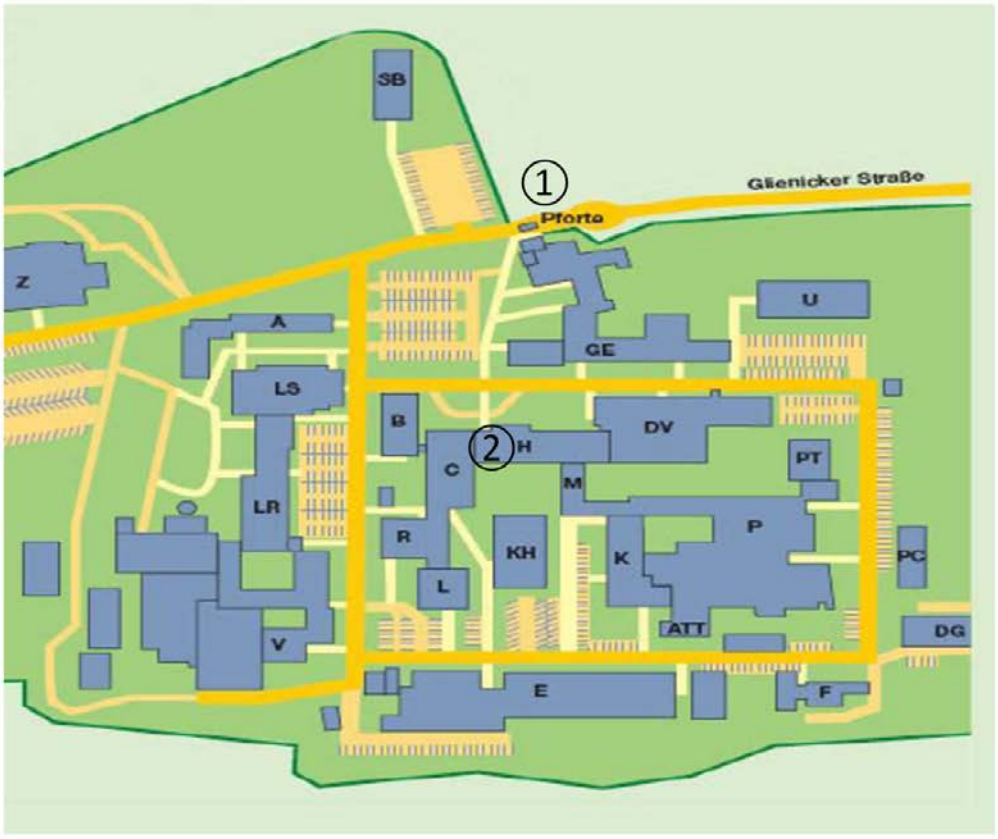

① Main entrance
② Lecture building (H): LMC-Foyer
Cafe Jahn
Lecture Hall

BER II
Hahn-Meitner-Platz 1
14109 Berlin

tel +49 (0)30 8062-42304
fax +49 (0)30 8062-42523
neutrons@helmholtz-berlin.de

Helmholtz-Zentrum Berlin
Wilhelm Conrad Röntgen Campus
Adlershof

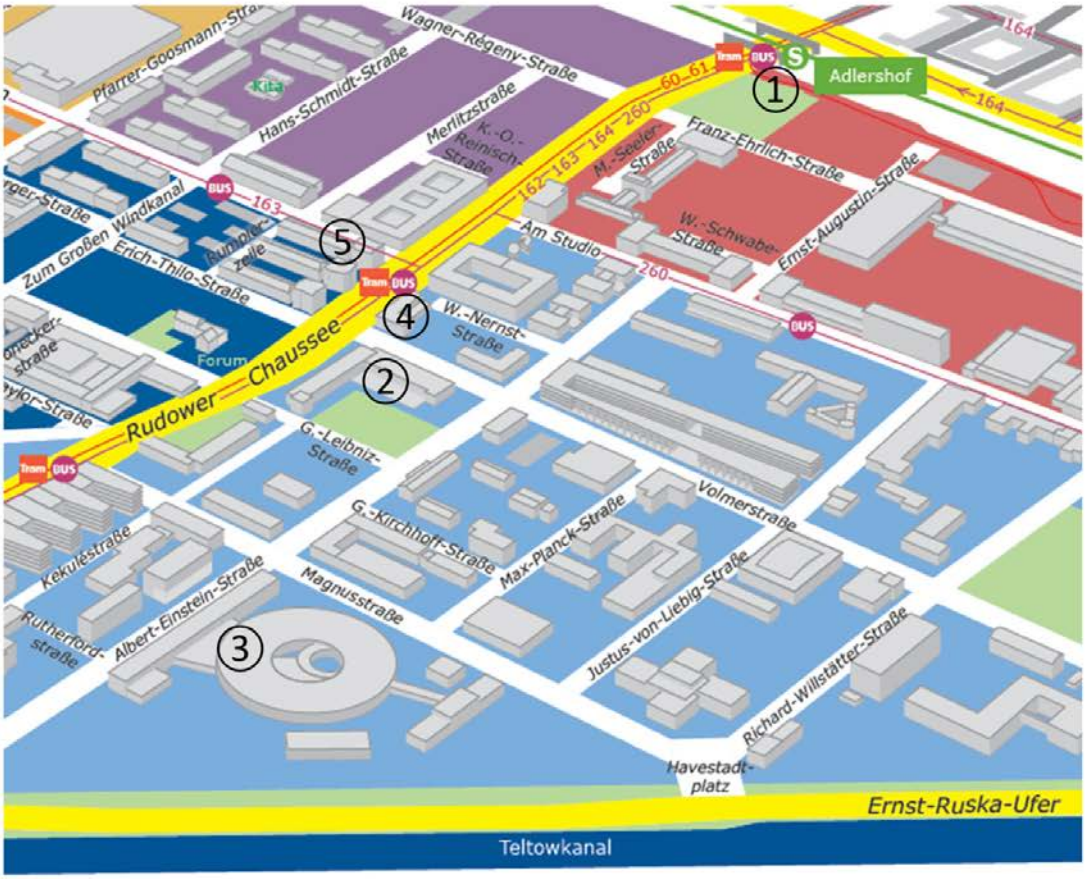

① Train Station Adlershof
② Wista centre: Registration
Bunsen Auditory
Vendor Exhibition
③ BESSY II Storage Ring Hall: Poster Session

Hotels:
④ Dorint
⑤ Airporthotel

BESSY II
Albert-Einstein-Str. 15
12489 Berlin

tel +49 (0)30 8062-12931
fax +49 (0)30 8062-14746
photons@helmholtz-berlin.de

HZB Helmholtz Zentrum Berlin

Next deadline for submission:

1st March 2018

Call for Proposals 2018/II

HZB kindly invites you to submit proposals for the next allocation period from August 2018 to February 2019 for BESSY II and BER II.

Beamtime applications may only be submitted via the General Access Tool GATE:

http://hz-b.de/gate

For guidance in writing a proposal, please refer to the online guide for beamtime application:

http://hz-b.de/beamguide

http://hz-b.de/proposals

HZB-Usermeeting on Twitter:
#um17HZB

Follow us: **@HZBde**